Charles University in Prague

Faculty of Mathematics and Physics

DOCTORAL THESIS

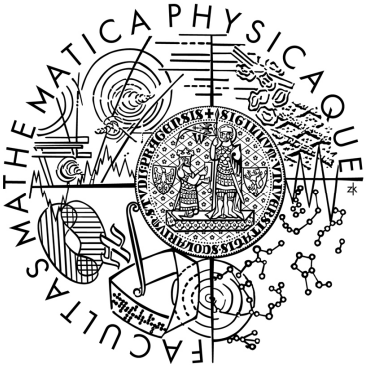

Evgeny Karpushkin

Polymer hydrogels: heterogeneous structure and deformation behavior

Institute of Macromolecular Chemistry
Academy of Sciences of the Czech Republic

Supervisor: Miroslava Dušková-Smrčková PhD

Study program: Physics
Specialization: F4 – Biophysics, chemical and polymer physics

Prague 2012

Univerzita Karlova v Praze
Matematicko-fyzikální fakulta

DISERTAČNÍ PRÁCE

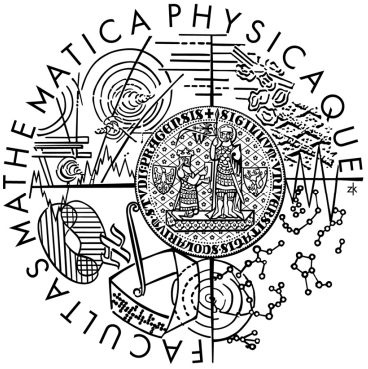

Evgeny Karpushkin

Makromolekulární hydrogely: heterogenní struktura a deformační chování

Ústav makromolekulární chemie

Akademie věd České republiky, v.v.i.

Vedoucí disertační práce: Miroslava Dušková-Smrčková Ing. Dr.

Studijní program: Fyzika
Studijní obor: F4 - Biofyzika, chemická a makromolekulární fyzika

Praha 2012

Acknowledgments

It is my great pleasure to begin my Thesis with expressing my sincere gratitude to many people who have helped me and inspired me during my work. Without them this work could be hardly possible.

Firstly, I would like to thank my supervisor Dr. Miroslava Dušková-Smrčková and my consultant Prof. Karel Dušek. They inspired the research that constituted this Thesis and continuously supported my interest in the field of hydrogels morphology and mechanical properties in course of fruitful discussions. Their instructions on writing and presenting research results cannot be overestimated, as well as their constant desire to share the scientific experience.

I have appreciated the opportunity to carry out my research in the Institute of Macromolecular Chemistry, AS CR, and I am grateful to its Management for everyday financial and administrative support.

Many of my colleagues have contributed to this research. In particular, I would like to acknowledge Torsten Remmler (from Malvern) for numerous instructive trainings in practical rheometry; Dr. Miroslav Šlouf (from IMC) and his Department od Morphology and Rheology of Polymer Materials for microscopy studies of hydrogels; Dr. Adriana Šturcová (from IMC) for IR measurements; Dr. Antonín Sikora (from IMC) for DSC measurements, data processing and interpretation; and Dr. Andrey Bogomolov (from J&M Analytik) for ideas on chemometrics application.

Last but not least, I thank my family and friends who were supporting me during my PhD study. Here is not enough space to name everybody in person, but I never forget any piece of inspiration and friendly environment they have created.

I declare that I carried out this doctoral thesis independently, and only with the cited sources, literature and other professional sources.

I understand that my work relates to the rights and obligations under the Act No. 121/2000 Coll., the Copyright Act, as amended, in particular the fact that the Charles University in Prague has the right to conclude a license agreement on the use of this work as a school work pursuant to Section 60 paragraph 1 of the Copyright Act.

In…..... date..... Evgeny Karpushkin

Název práce: Makromolekulární hydrogely: heterogenní struktura a deformační chování
Autor: Evgeny Karpushkin
Katedra / Ústav: Katedra makromolekulární fyziky MFF UK
Vedoucí disertační práce: Miroslava Dušková-Smrčková Ing. Dr., Ústav makromolekulární chemie AV ČR, Heyrovského náměstí 2, 162 06 Praha 6

Abstrakt: Morfologie, botnání a dynamicko-mechanické vlastnosti syntetických hydrogelů o různé morfologické struktuře byly studovány s cílem nalézt vztah mezi strukturou sítě, architekturou porozity a mechanickou odezvou. Modelová řada syntetických hydrogelů byla připravena radikálovou polymerizací 2-hydroxethylmethakrylátu se síťovadlem za přítomnosti vody a jiných aditiv tak, aby se v průběhu síťování uplatnil jev fázové separace a tím došlo k vytvoření modelových gelů o různé morfologii. Z mechanické odezvy rovnovážně zbotnalých vzorků vyplývá, že frekvenční průběh hlavního relaxačního přechodu nezávisí na uspořádání a typu porů a do malé koncentrace síťovadla (1 mol% na monomery) ani na struktuře sítě. Odezva v nízkém oboru frekvencí (<10-2) závisí značně jak na struktuře polymerní sítě, tak na morfologické stavbě zbotnalého hydrogelu. Mírně sesíťované gely vykazovaly vyšší mechanické ztráty v oblasti kaučukového plata, což je připsáno přeskupování asociovaných hydrofobních domén polymerních řetězců. U gelů o částicové struktuře s komunikujícími póry byl vždy pozorován vzrůst ztrátové tamgenty při nízkých frekvencích. U gelů, v jejichž struktuře je patrná porozita, ale póry nejsou vzájemně komunikující, nebyl takový vzrůst ztrátového úhlu pozorován.
Klíčová slova: hydrogel, fázová separace, morfologie, botnání, mechanické vlastnosti

Title: Polymer hydrogels: heterogeneous structure and deformation behavior
Author: Evgeny Karpushkin
Department: Department of Macromolecular Physics, Faculty of Mathematics and Physics, Charles University in Prague
Supervisor: Miroslava Dušková-Smrčková Ing. Dr., Institute of Macromolecular Chemistry AS CR, Heyrovského náměstí 2, 162 06 Prague 6

Abstract: Model series of crosslinked poly(2-hydroxyethyl methacrylate) hydrogels differing in morphology were prepared by polymerization-induced phase separation. Morphology, swelling and dynamic mechanical properties in broad frequency range of the model gels were tested. The vitrification of gels was found sensitive to microstructure of polymer network and to solvent content and to polymer-solvent interaction, but not to the macroscopic morphology of the gel. The low-frequency mechanical response was found sensitive to both polymer network properties and hydrogel morphology. Lightly crosslinked hydrogels showed relatively high mechanical losses in the rubbery plateau region, due to physical association of chains. Fused-particles type hydrogels revealed a weak secondary relaxation at low frequency, ascribed to motion of the dangling particles aggregates. These aggregates, elastically inactive, along with inhomogeneous stress field arisen in porous material, were responsible for underestimation of equilibrium shear modulus of the matrix.
Keywords: hydrogel, phase separation, morphology, swelling, mechanical properties

Contents

Introduction

The history of 2-hydroxyethyl methacrylate (HEMA) and its copolymers studies has counted more than half a century so far. The work of Czechoslovak group of Otto Wichterle (started in 1951) has led to recognition of mechanically strong, swellable in water and other physiological media and optically transparent polyHEMA hydrogels as a valuable biomaterial for soft contact lens production, ophthalmic surgery and dentistry.

During HEMA polymerization in presence of inert diluent not miscible with polyHEMA, phase separation occurs resulting in heterogeneous, non-transparent hydrogels. Due to improved transport of nutrients and metabolism products, and possibility of living cells to accommodate inside the voids filled with the swelling medium, such porous polyHEMA gels are excellent candidates for tissue engineering applications.

Intensive studies on animals have revealed that encapsulation, cell ingrowth, neovascularization and calcification strongly depend on the overall polyHEMA overall porosity, pores average size and connectivity. Moreover, mechanical properties of porous material matrix may affect the cells behavior within a scaffold. Thus, effective application of hydrogels as biomaterials requires precise control of their morphology and mechanical properties. Realization of this comprises several pieces of knowledge:

- control of final material porosity by preparation procedure;
- influence of preparation conditions on material matrix properties;
- influence of material porosity and matrix properties on the material utilitarian characteristics.

Even though basic principles of preparation-morphology and preparation-mechanical properties relationships have been formulated in the early poly HEMA studies, at that time it was not possible to characterize extremely soft, highly porous hydrogel due to insufficient technology development. The first commercial ESEM instrument to study swollen samples was introduced in 1988, and further important improvements were introduced even in late 1990s. Controlled-stress rheometers enabling characterization low-modulus materials appeared in 1990s.

In author's experience, properties of gels produced by polymerization accompanied by phase separation are sensitive to even small changes in the preparation procedure, including the nature and amount of initiator, or temperature. This is especially so in case of macroporous final products.

Rheological testing of soft materials in proper conditions (no slippage of uncompressed sample) is not trivial. To author's knowledge, it has not been mentioned in literature for macroporous hydrogels. At the same time, such protocol is required to avoid useless replications of measurements in different laboratories.

Despite numerous studies on polyHEMA hydrogels, the systematic studies on samples of varying morphology are quite limited, and in the best link the preparation conditions with morphology or one of the utilitarian properties. Thus, direct study of relationships between morphology of hydrogels prepared in varied conditions, and their mechanical properties has been lacking till now. This work has been done in order to fill in this gap.

1 Theoretical part

1.1 HEMA-based hydrogels

Hydrogels form a group of materials, properties of which place them at the edge between solid and liquid materials. Like solids, they usually hold a defined shape and thus can be applied in construction of scaffolds, supports, functional surfaces, artificial tissues or substitutes (especially in ophthalmology). On the other hand, being swollen in liquid aqueous medium, hydrogels are soft and permeable to low-molecular species, which opens for them fields of biomaterials, responsive soft machines, chromatography solid phases, sorbents for concentration of solutes or controlled release of drugs, etc.

According to the recent IUPAC recommendation [**1**], hydrogel is a "non-fluid colloidal or polymeric network that is expanded throughout its whole volume by water". In turn, network is a "highly ramified structure in which essentially each constitutional unit is connected to each other constitutional unit and to a macroscopic phase boundary by many paths throughout the structure".

2-hydroxyethyl methacrylate HEMA is a common monomer for preparation of synthetic hydrogels. This is due to its good availability and low price, simplicity in use, high biocompatibility of polyHEMA and low toxicity of both monomer and polymer, and large variety of prepared hydrogel properties.

HEMA and its polymers were first reported in a patent [**2**] in 1938. In the next two decades, HEMA was episodically mentioned in the patent literature in connection with novel synthetic pathways or with its potential use as a comonomer for polymeric compositions.

The history of polyHEMA as a biomaterial started in 1950s when Wichterle and Lím [**3**] synthesized hydrogels based on HEMA copolymers with ethylene dimethacrylate (EDMA) designed for medical applications. After their biocompatibility was proved [**4**], these hydrogels were widely applied as materials for soft contact lenses. Commercial success of such lenses stimulated further interest in hydrogels, and eventually led to the development of responsive soft materials that upon exposure to an external stimulus could abruptly change size, or even shape [**5**]. Further successful applications of polyHEMA hydrogels include intraocular lens [**6**, **7**] and dental materials [**8**].

First polyHEMA hydrogels applied as biomaterials were homogeneous and optically transparent. However, already during early polyHEMA research [**2**, **3**] it was evidenced that at certain conditions porous polyHEMA hydrogels could be prepared. Highly depending on the pores fraction [**9**], such materials showed great potential in cell cultivating and tissue engineering, as they allowed cells attachment, growth and proliferation.

The *in vivo* evaluation of tissue reaction in the animal models was reported by Czechoslovak researchers [**10, 11**]: cellular invasion, encapsulation, vascularization and salts deposition were followed after implantation in rats, rabbits, pigs and mice. The first study to show the influence of polyHEMA hydrogels porosity on their behavior as implanted materials was reported in [**9**]. At higher porosity, fibrous capsule was narrower and zone of cell ingrowth and vascularization was broader. Also, porosity was the major factor governing cellular invasion and deposition of calcium salts in the implants [**12**]. Macroporous polyHEMA hydrogels were successfully probed (in animal models) as implants for bone formation [**13, 14**], in brain surgery [**15**], and as membranes for artificial pancreas [**16, 17**].

Due to numerous potential applications of macroporous polyHEMA hydrogels, they are extremely attractive research objects. Even fundamental study of polyHEMA properties not only adds new knowledge about basic theoretical questions of polymer gels behavior, but brings important practical information.

1.2 Remarks on terminology

In the referenced literature, various expressions are used for description of hydrogels internal structure. For instance, according to visual appearance they may be called transparent (or clear), semi-transparent (or opaque, translucent), and non-transparent (white). As far as the phase structure is considered, hydrogels are termed homogeneous (or single-phase) and heterogeneous (or phase-separated, multi-phase). For hydrogels containing only part of swelling medium solvating the polymer chains, while part of the solvent is expelled to a distinct phase (porous gels) further accurate definitions are used. According to the IUPAC, macroporous polymers are those that have pores in the range of 50 nm to 1 μm [**1**], while microporous gels are those with even smaller pores. Materials with pore sizes more than 1 μm are sometimes called supermacroporous, but as the border between these types of materials is very diffuse,

both names supermacroporous and macroporous may be used as synonyms to describe systems with pores larger than micrometer range. Often, especially in papers related to biomaterials, macroporous gels are called sponges.

In the scientific literature, some of these classifications are mixed, and terms "clear" and "homogeneous", or "porous" and "non-transparent" are used as synonyms, which may be only partially correct depending on the objects in question. Throughout this work, in the Theoretical part section, the terminology offered by authors of cited papers was used, where it did not cause misunderstanding. An exception was made for term "sponge", in our opinion this is not reasonable use of scientific slang. Spongy gels were referred to as macroporous in the theoretical part of this work.

In the Results and discussion section of this work the following simplified classification was used to refer to different types of hydrogels. Those called "homogeneous gels" were fully transparent with no heterogeneities detectable either visually, by light or electron microscopy. Other (non-transparent) gels revealed several types of morphology under scanning electron microscope (SEM). Non-transparent swollen gels that only revealed a single phase in SEM (that is, the heterogeneities were below electron microscopy resolution) were referred to as "intermediate". Gels showing micrometer-range partially connected droplets of swelling medium surrounded by walls of swollen polymer, were assigned to gels of "interlocking, bicontinuous" morphology. The group of non-transparent gels with communicating pores surrounding well-defined fused spherical particles of swollen polymer constituted a category of "fused particles type" or "particulate gels".

1.3 Swelling of hydrogels

Hydrogels swell in aqueous media to an equilibrium state (limitedly). The amount of swelling medium a material needs to absorb to be classified as a hydrogel is not precisely defined (no mention in the IUPAC definition [**1**]), but generally if a material has absorbed 10% water or more, and is not soluble, it can be classified as a hydrogel [**18**]. The swollen equilibrated state of a hydrogel is a balance between the osmotic forces that cause water to enter the hydrophilic polymer and the cohesive forces exerted by the polymer chains in resisting expansion.

The swelling ability of a material can be expressed by different values. They are equivalent, and can be recalculated, provided that the polymer and swelling medium densities are known. Often used expressions are: amount of water absorbed per weight of dry polymer material (Eq. 1.1), amount of water absorbed per weight of swollen gel (Eq. 1.2), and weight (Eq. 1.3a) or volume (Eq. 1.3b) change upon swelling from dry state:

$$\mathrm{WC} = \frac{m_\mathrm{s} - m_\mathrm{d}}{m_\mathrm{d}} \tag{1.1}$$

$$\mathrm{WC} = \frac{m_\mathrm{s} - m_\mathrm{d}}{m_\mathrm{s}} \tag{1.2}$$

$$Q_\mathrm{w} = \frac{m_\mathrm{s}}{m_\mathrm{d}} \tag{1.3a}$$

$$Q_\mathrm{V} = \frac{V_\mathrm{s}}{V_\mathrm{d}} \tag{1.3b}$$

with m_s, weight of a swollen sample, m_d, dry polymer weight, V_s, volume of a swollen sample, and V_d, dry polymer volume.

More hydrophilic a polymer is, higher is its hydrogel equilibrium water content (EWC). Also, hydration can be controlled through crosslink density – more crosslinking for a given polymer system results in lower EWC.

To derive EWC of the material, variations of the Flory-Huggins theory for polymer solutions are often applied. It is a mathematical model of polymer-solvent mixing thermodynamics accounting for dissimilarity in molecular sizes to adapt the usual expression for the entropy of mixing. The result is an equation for the Gibbs free energy change ΔG_m for mixing a polymer with a solvent. Despite of simplifying assumptions, Flory-Huggins scheme is very useful for interpreting experiments.
The basic result of the theory is ([**19**, **20**]) as follows:

$$\Delta G_\mathrm{m} = RT(n_1 \ln \phi_1 + n_2 \ln \phi_2 + n_1 \phi_2 \chi_{12}). \tag{1.4}$$

Here n and ϕ are number of moles and volume fraction of solvent (index 1) and polymer (index 2). The polymer-solvent interaction parameter χ_{12} is defined as

$$\chi_{12} = z\Delta w/kT \tag{1.5}$$

with z standing for the coordinate number in the model lattice, Δw – energy difference between polymer-solvent contact and mean of polymer-polymer and solvent-solvent contacts. χ_{12} depends on the nature of both solvent and polymer, and is the only material-specific parameter in the Flory-Huggins model.

Application of the Flory-Huggins model to polymer networks requires an additional term to describe network elasticity arising from its crosslinked nature. The following result allows calculation of EWC in terms of solvent volume fraction [**21**]:

$$\frac{\Delta\mu_1}{RT} = 0 = [\ln(1-\phi_2) + \phi_2 + \chi_{12}\phi_2^2] + \frac{\phi_2^{1/3}}{m_c} \quad (1.6)$$

There are facts proving that water in hydrogels consists of "bound" and "free" fractions [**22-24**]. When dry polymer is placed in water, the hydrophilic groups along polymer chains are hydrated first: water will form hydration spheres around these groups, it is called *bound water*. It is tightly held in the hydrogel matrix through hydrogen bonding. As the hydrogel continues to hydrate, additional absorbed water is referred to as *unbound* or *free water*. Filling the voids and pores of the hydrogel, it is less structured and more mobile. These types of water were observed experimentally with DSC [**25**] and NMR [**26**, **27**].

However, not all scientists support the free and bound water theory. For example, as determined by pulsed gradient NMR, all water in polyHEMA hydrogels diffused as a homogeneous phase [**28**]. Also, in [**29**] extremely close to equilibrium conditions DSC measurements did not reveal thermodynamically different states of water, and multiple melting peaks observed for hydrogels water in rapid DSC scans were ascribed to metastable states; same was concluded in [**30**].

In equilibrium, homogeneous polyHEMA gels uptake up to 40-42 wt% of water [**31**]. PolyHEMA hydrogels swelling ability is only slightly dependent on temperature [**31, 32**], and decreases with increasing crosslink density [**33**]. Thermodynamic quality (including introduction of low-molecular weight salts) of the medium can alter the swelling of polyHEMA [**34**], this is especially important for biomedical applications, when a gel-based device is placed at physiological conditions. A defined correlation was found between the polyHEMA network mesh size and its swelling ability [**33**]. When polyHEMA preparation is carried out in presence of diluent which is a poor solvent for the polymer, the swelling of final product is sensitive to amount of the diluent. When it exceeds certain critical value, porous hydrogels are formed, and the apparent swelling degree is increased [**35**]. This phenomenon will be addressed in detail in Section 1.5.

1.4 Benefits of polyHEMA hydrogels porosity

Swollen macroporous hydrogels offer interesting possibilities in biotechnology and medicine due to their heterogeneous structure. The polymer nature, pore size, size distribution, and connectivity are factors that strongly influence the materials properties and possibilities for applications.

Broad spectrum of macroporous hydrogel monoliths for *chromatographic* devices can be attributed to several properties related to the macroporous structure [**36**]. There are normally no dead-end pores in the monoliths, and mass transfer between the stationary and the mobile phase via convection is fast. This is beneficial for purification of large molecules of proteins, polynucleotides, or viruses. Another consequence of the monolithic structure is high porosity. The internal porosity of polyHEMA-based porous particles is normally up to 70% [**37**], while the external porosity (voids between particles) in packed beds is up to 40%; then the bed collapses. The monoliths, on the other hand, exhibit external porosity up to 90% [**38**].

Macroporous hydrogels are suitable as matrices for *cell separation* [**39**] and for *cell culture* [**40**] applications due to the combination of elastic polymeric network and interconnected porous structure capable of absorbing and keeping large amount of biologic fluids inside the pores as well as ensuring non-hindered mass transport of nutrients and metabolic products.

In *tissue engineering* applications, high porosity and pore size provide space for cell accommodation and migration, and enable the exchange of nutrients between the scaffold and the environment. For better recognition of gels by cells, they may be modified with bioactive molecules [**41**]. PolyHEMA and HEMA copolymer hydrogels has been tested for using in a variety of artificial tissue applications.

The porous and elastic nature of hydrogels is close to native cartilage. The water content in macroporous hydrogels is about 80–95%, which is similar to that of natural cartilage tissue. Cartilage, as a predominately avascular, aneural, and alymphatic tissue with a limited ability of self-repair, is an ideal system for tissue engineering. Mechanically stable 3-dimensional scaffolds have shown a great promise for cartilage tissue engineering [**42-44**].

For bone tissue replacement, a scaffold must possess an interconnected porous structure with pore size of 200–900 μm [**45**]. Surface properties are also important: rough surface imprisons the fibrin matrix better than a smooth one, and

hence facilitate the migration of osteogenic cells [**46**]. *In vitro* the scaffolds should have sufficient strength to withstand the hydrostatic pressure and maintain porous morphology; *in vivo* mechanical strength should be close to natural bone. Macroporous polyHEMA hydrogels were successfully probed (in animal models) as implants for bone formation [**13, 14**]

The use of porous hydrogels to assist tissue repair in central nervous system, axonal regeneration in the brain and the spinal cord was intensively investigated. Extremely soft macroporous hydrogels successfully mimic the mechanical characteristics of natural tissues. Additionally, oriented pores produced by various template techniques may additionally promote guided cell growth [**47**].

For peripheral nerve repair, hydrogels based on crosslinked polyHEMA and poly(N-2-hydroxypropyl methacrylamide) were implanted into the rat cortex, and showed that astrocytes and NF160-positive axons grew similarly into both types of hydrogels. No cell types other than astrocytes were found in the polyHEMA hydrogels [**48**].

Macroporous scaffolds can be applied alone or in combination with different growth factors or cellular components for spinal cord repair and regeneration. As an example, in [**49**] a polyHEMA hydrogel scaffold of well-defined geometry was created and modified with laminin-derived peptides that enhanced cell adhesion and neurite outgrowth. Scaffolds were designed to have numerous longitudinally oriented channels with an average channel diameter of about 200 μm to ultimately promote fasciculation of regenerating cables, and a compressive modulus of 192 kPa to match the modulus of the soft nerve tissue. Such peptide-modified scaffolds enhanced neural cell adhesion and guided neurite outgrowth of primary chick dorsal root ganglia neurons relative to non-modified controls. It was concluded that a combination of well-defined chemical and physical stimuli developed in that work provided a means for guided regeneration both *in vitro* and *in vivo*.

Several temporary liver assist devices were developed based on macroporous hydrogels, including polyHEMA hydrogels [**50, 51**]

Probably, the first study demonstrating the influence of polyHEMA gels porosity on their behavior as implanted materials was reported in [**9**]. Hydrogels synthesized with increasing amounts of water (50-90 wt%) crosslinked with 2 wt% of EDMA were implanted in rats and sampled at 30, 60 and 90 days after implantation. The polymers prepared with 50 and 60 wt% water behaved like

homogeneous hydrogels (only encapsulation occurred), but those obtained with 70, 80 and 90 wt% water were penetrated by cells and blood vessels. At higher porosity, the fibrous capsule was narrower and the zone of cell ingrowth and vascularization enlarged; no significant calcium salt deposition was noticed. Similar experiments with macroporous HEMA copolymers containing ionic comonomers confirmed these findings [**52**]. In a more detailed study [**12**], the phenomenon of calcification was investigated. It was found that variation of porosity, controlled by water amount in polymerizing mixture, was the major factor governing cellular invasion and deposition of calcium salts in the implants.

Detailed studies revealed dependence of specific tissues regeneration on the support porosity [**53**]. The diameter of cells dictated the minimum suitable pore size. Depending on the application, pore size must be carefully controlled. Experiments revealed optimum pore size of 5 μm for neovascularization, 5–15 μm for fibroblast ingrowth, close to 20 μm for the ingrowth of hepatocytes, 20–125 μm for regeneration of adult mammalian skin, 40–100 μm for osteoid ingrowth and 100–350 μm for regeneration of bone **[54]**. Fibrovascular tissues required pores of >500 μm for rapid vascularization and survival of transplanted cells [**55**].

Continuity of pores is also important: mass transport and cell migration were inhibited if the pores were not interconnected even if the matrix porosity was high [**56**]. Cells located more than approximately 200 μm from a blood supply were either metabolically inactive or necrotic due to low oxygenation [**57**].

A further concern is change in pores structure over time *in vivo*. Even if matrix does not degrade, effective pore size may be reduced by *in vivo* events (invasion of fibrous tissue into the pores, nonspecific adsorption of proteins onto material) [**57**].

Thus, for majority of macroporous hydrogels applications, porosity characteristics (average size, volume fraction, connectivity, etc.) are important, in addition to other functional characteristics (mechanical properties, presence of functional comonomers, etc.). It is clear that developing well-controlled procedures to produce macroporous materials with desired morphology is desired.

1.5 Methods for porous polyHEMA hydrogels fabrication

Common methods for preparation of porous gels include: polymerization in presence of diluent which is a non-solvent for formed polymer (phase separation during polymerization), crosslinking polymerization in presence of washable solid substances (salts, sugars, organic fibers), cryogelation (at temperatures below freeze point of a solvent, which serves as a porogen), polymerization in presence of gas-releasing components.

Each of these methods has advantages and drawbacks. The relative importance of them depends on the particular task, and possibly it is impossible to choose the ultimately best method of pores generation.

Using polyHEMA gels as a model, in [**58**] a comparison of several routes to prepare porous materials was made: morphology, overall porosity and pores connectivity were checked for prepared samples. Results of the study are summarized in Tab. 1.1. Gaseous porogen approach allowed for almost no control of morphology, and the overall porosity was low. Fiber-based gels showed good properties, but procedure was complicated, and it should be developed separately for each new comonomers mixture composition.

The methods proved to be most convenient were phase separation polymerization and polymerization in the presence of soluble solid porogen. With the latter method it was easier to fine-tune the pores size and distribution, but overall complexity of this procedure makes polymerization-induced phase separation one of the preferred methods for HEMA-based hydrogels preparation.

Table 1.1 *Comparison of porous gels production methods related to typical properties of final products (from [**58**]).*

Method	Preparation	Reproduci-bility	Overall porosity	Adjustability of pores size	Distribution of pores size
Phase separation	very easy	good	20-100%	narrow	broad
Washable porogen	easy	excellent	68-97%	any >5 μm	narrow
Gas release	usually easy	poor	0-20%	narrow	very broad
Fiber spinning	complicated	good	100%	wide	broad

Polymerization-induced phase separation

During crosslinking copolymerization in presence of inert diluent, the latter plays an important role in the design of the final material morphology. At low crosslinker contents and in the presence of solvating diluent, it remains in the gel throughout the reaction so that an expanded, non-porous network is obtained. Permanent heterogeneities and/or pores in the network appear if the diluent separates out of the gel phase during polymerization. HEMA polymerization in presence of more than 40 wt% of water is a well-known example, many other common monomers behave in the same way: (N-(2-hydroxypropyl)methacrylamide in acetone [**59**], methyl methacrylate in heptane [**60**]).

Phase separation during crosslinking can be induced either by increasing the crosslinker concentration (ν-induced syneresis) or by decreasing the solvating power of the diluent (χ-induced syneresis, [**35, 61**]). In both cases, the growing polymer network cannot absorb all solvent available in the reaction system (i.e. equilibrium degree of swelling of the network is less than its degree of dilution). Thus, the system collapses to form reaction particles within the separated continuous liquid phase. As the reaction proceeds, new microparticles are continuously generated due to the successive separation of the growing polymer. The agglomeration of the microspheres results in the formation of a heterogeneous gel consisting of continuous phases of a gel and a diluent.

It was proved experimentally that no crosslinks were necessary for a limited swelling of polyHEMA in water and phase separation to occur [**35**]. A fundamental study of phase separation during HEMA polymerization in presence of aqueous solutions of low-molecular-weight compounds was offered in ([**62**]) with uncrosslinked polyHEMA of various molecular weights as a model.

Microsyneresis and macrosyneresis are both usually operative in crosslinking polymerization. Microsyneresis is separation of diluent as droplets inside the gel phase to give dispersion. It is a non-equilibrium process caused by the existence of regions differing in segment and crosslinking density (local incompatibility), and by a slow relaxation of the network. Macrosyneresis includes the decrease of swelling due to the weakening of thermodynamic polymer-diluent interaction. It results in the formation of distinct diluent and gel phases. Microsyneresis usually impacts much on hydrogel structure, since polymerization is faster than gel relaxation, and thermodynamically unstable disperse structure is fixed by crosslinks. A theoretical

treatment [**61**] suggested a greater complexity of the process, in which various factors, such as interaction parameter χ, molar volumes of components, content of diluent in the mixture, and concentration of crosslinking agent all affect phase separation during copolymerization. A variety of morphologies induced by phase separation is schematically shown in Fig. 1.1.

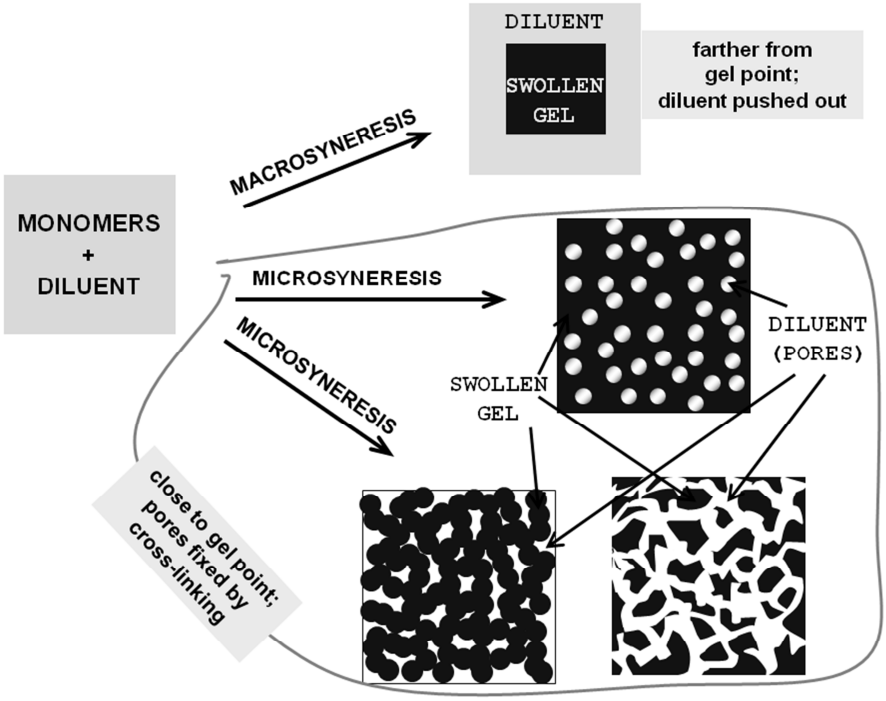

Figure 1.1 *Syneresis during polymerization as a mean to produce porous crosslinked polymers.*

Relationship between formation conditions and structure of macroporous networks was studied in [**35, 61**, **63-65]**. The main factors determining the macroporosity of polymer networks were crosslinker concentration, type and amount of diluent, along with temperature and type of initiator.

Among first reports on preparation of hydrogels under varied conditions were [**9**] and [**12**]. Two parameters varied were water and crosslinker concentrations, the first being the major factor to influence hydrogel morphology. Even though in 1970s modern ESEM methods were not yet developed [**66**], structure of polyHEMA hydrogels was examined microscopically, and morphology type diagrams were collected (an example [**12**] is shown in Fig. 1.2).

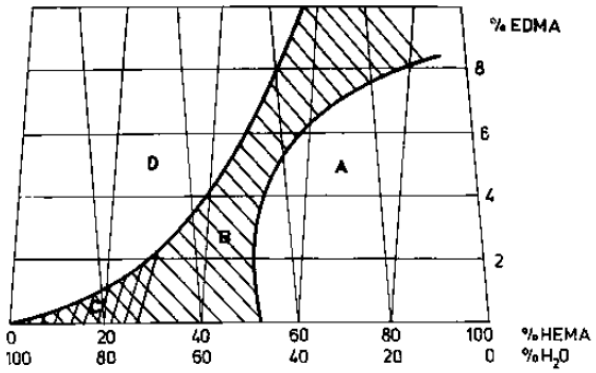

Fig. 1. Regions of formation of homogeneous (*A*), microporous (*B*) and macroporous (*C*) poly(glycol monomethacrylate)

Figure 1.2 *Diagram of final hydrogel morphologies as a function of polymerized mixture of HEMA, EDMA and water composition. From [**12**].*

Similar behavior was revealed in other studies [**67-69**]. Water concentration above which heterogeneous polyHEMA hydrogels were produced was slightly variously reported to be around 45 wt%, whereas at water concentration above 70-75 wt% macroporous samples were formed. The only measurable and effective porosity in heterogeneous hydrogels was found to be due to the large spaces between polymer particles. It was estimated [**10**] that for particles as large as 2-5 μm, the channel-like pores could attain 40-80 μm.

With development of modern microscopy methods, the influence of preparation conditions on the polyHEMA hydrogels morphology was studies in more detail. In [**65**] it was found that increase of water concentration led to appearance of isolated pores, which at higher dilution formed interconnected voids between collated swollen polymer particles (Fig. 1.3).

At constant dilution (80 wt% of water) corresponding to macroporous hydrogel morphology, increase of the crosslinker concentration led to to higher porosity (Fig. 1.4). Changes of the overall porosity were mainly due to decreasing size of polymer particles at higher crosslinker concentration, while void spacing and average diameters of pore openings were not affected by crosslinker content. In the presence of larger amounts of water (90 wt%) unfavorable water-polymer interactions dominated, and the effect of crosslinker was negligible.

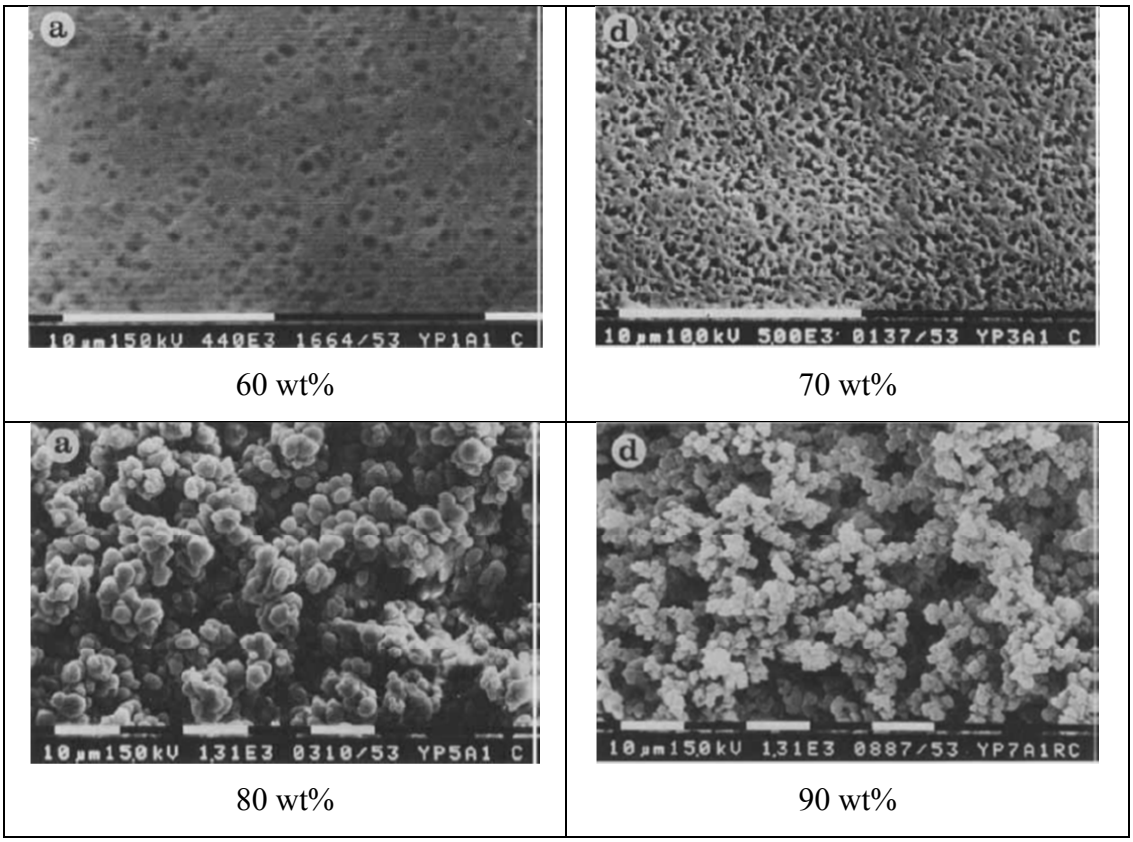

Figure 1.3 *Morphology of polyHEMA hydrogels prepared at various dilutions in water. Concentration of crosslinker EDMA was 0.5 wt%. Weight fraction of water is shown under corresponding pictures. From [**65**].*

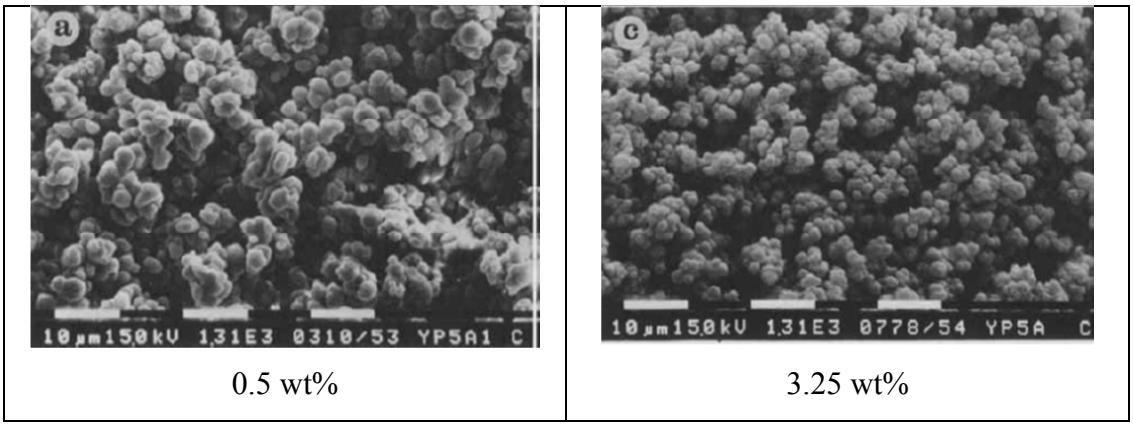

Figure 1.4 *Morphology of polyHEMA hydrogels prepared at various concentrations of crosslinker EDMA with 80 wt% of water as a diluent. Weight fraction of the crosslinker is shown under corresponding pictures. From [**65**].*

Increase of crosslinker concentration can cause macroporous hydrogels formation at lower concentration of diluent. As an example, morphologies of polyHEMA hydrogels prepared at 60 wt% of water are shown in Fig. 1.5.

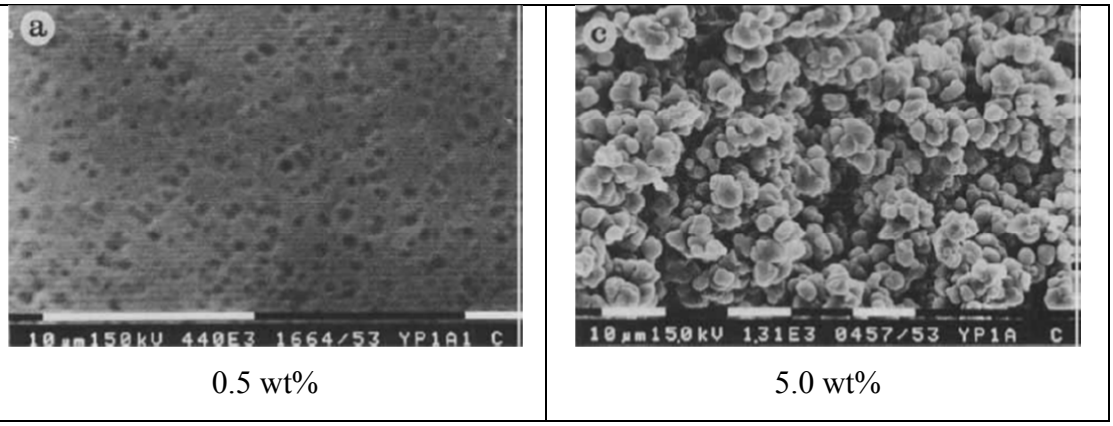

0.5 wt% | 5.0 wt%

Figure 1.5 *Morphology of polyHEMA hydrogels prepared at various concentrations of crosslinker EDMA with 60 wt% of water as a diluent. Weight fraction of the crosslinker is shown under corresponding pictures. From [**65**].*

The hydrophilicity of crosslinker also altered the extent of phase separation at a given mixture composition (Fig. 1.6): 1,6-hexamethylene dimethacrylate HDMA induced more pronounced phase separation than did more hydrophilic EDMA.

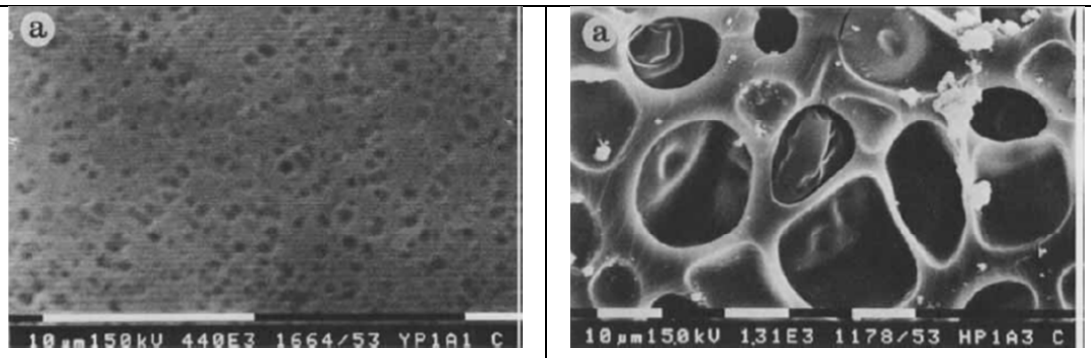

EDMA | HDMA

Figure 1.6 *Morphology of polyHEMA hydrogels prepared with 60 wt% of water and 0.5 wt% of crosslinker EDMA or HDMA (latter is less hydrophilic). The crosslinker type is shown under corresponding pictures. From [**65**].*

Besides factors mentioned above, solvating power (thermodynamic quality) of the diluent is important. It can be modulated by addition of certain inorganic salts [**34**]. In particular, sodium chloride aqueous solutions are poorer solvents for polyHEMA than water. In [**70**], addition of sodium chloride significantly enhanced phase separation during HEMA polymerization. With 60 vol% of diluent final hydrogel was non-porous in case of water, but with 0.3 M NaCl macropores were revealed by SEM, and at 0.7 M NaCl they became interconnected (Fig. 1.7).

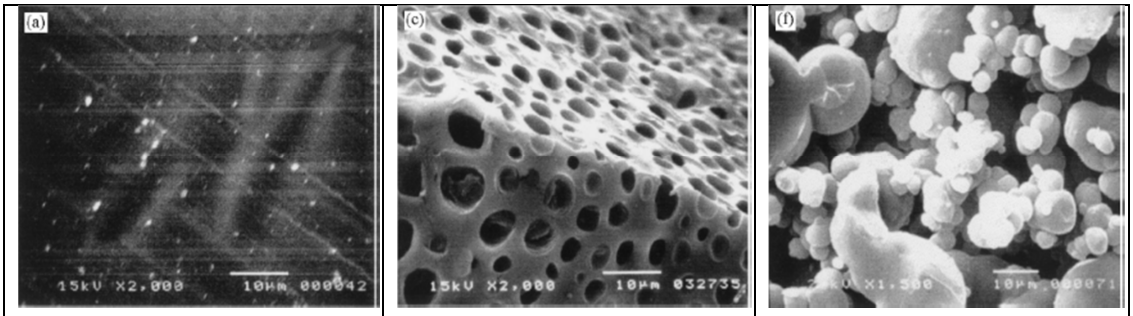

0 M	0.3 M	0.7M

Figure 1.7 *Morphology of polyHEMA hydrogels prepared with 60 vol% of the diluent (aqueous NaCl of varied concentration) and 0.6 mol% of crosslinker EDMA. Concentration of NaCl in the diluent is shown under corresponding pictures. From [**70**].*

The initiator effect studied in [**65**] was evident only at lower concentrations of water: at 60% water and 5.0% EDMA increasing of initiator concentration led to progressive phase separation. This was either due to number of growing radicals and kinetic chain length, or because initiator (mixture of $(NH_4)_2S_2O_8$ + $Na_2S_2O_5$) used decreased the solvating power of diluent. For 70% water and above no effect of initiator on porosity was observed.

In [**71**] a hydrophilic and less reactive crosslinker was used: DVG (divinyl glycol, or 1,5-hexadiene-3,4-diol). Crosslinking with DVG led to stratification (macroscopic inhomogeneity, especially at sample surface), likely due to phase separation before network gelation because of low reactivity of DVG allyl groups. Stratified samples did not reveal porosity suitable for biomedical usage. The stratified layer (up to about 250 μm from the sample base) had a cellular structure, with droplets of water entrapped in a polymer matrix (Fig. 1.8). At 250-600 μm from the sample base, cellular regions became interspersed with domains consisted of

polymer droplets within a continuous water phase. At more than 600 μm from the sample base, there was a significant increase in the volume occupied by water.

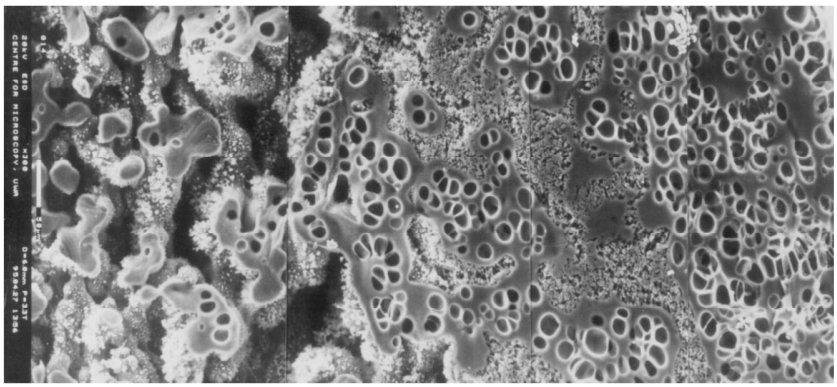

Sample top surface ⟶

Figure 1.8 *Composite micrograph of polyHEMA sample prepared with 75 wt% of water and 1 wt% of DVG. From [**71**].*

Stratification was less pronounced at high dilution, but these gels were mechanically too weak. Two possible solutions of the problem were suggested: using either more active initiating system or hydrophilic crosslinker with active methacrylate groups. This was investigated in [**72**]. PolyHEMA macroscopic hydrogels were prepared with 5 chemically different crosslinkers (hydrophobic vinylic EDMA and BDMA; hydrophobic allylic HD, hydrophilic vinylic BHDMA, and hydrophilic allylic DVG), other conditions being the same, and phase separation onset was evaluated.

In case of vinylic compounds (EDMA, BDMA and BHDMA), with more crosslinker used phase separation occurred faster. At the same concentration hydrophobic BDMA promoted faster phase separation than its hydrophilic homologue BHDMA. However, at higher concentrations, all vinylic crosslinkers showed similar onset of phase separation time, likely because of efficiency loss (cyclization reactions).

Hydrophobic allylic agent HD induced, at low concentrations, a delay in phase separation, as compared to the vinylic agents. This indicated lower crosslinking efficiency of HD, due to lower reactivity of allylic groups. Hydrophilic allylic agent DVG induced an erratic range of phase separation onset times, generally

longer than those induced by other crosslinkers. This might be related to both better miscibility and lower reactivity of DVG.

The onset of phase separation correlated well with size of polymer droplets in macroporous hydrogels: the longer it took for phase separation to occur, the larger the size of resulting polymer droplets. Crosslinker concentration being the same, droplet size and phase separation time followed the row: DVG>HD≈BHDMA>BDMA.

To conclude, variation of diluent composition and concentration, and/or crosslinker concentration and type provide vast opportunities in designing hydrogels of variable porosity and morphology using method of phase separation during polymerization. This method can be used even for preparation of functional materials, with HEMA being only a minor comonomer. For instance, in [**73**] macroporous hydrogels of functional polypeptides were prepared. Pores in the material appeared due to phase separation of monomers mixture induced by presence of 10-20 wt% HEMA with respect to solids. An example of final hydrogel morphology is shown in Fig. 1.9.

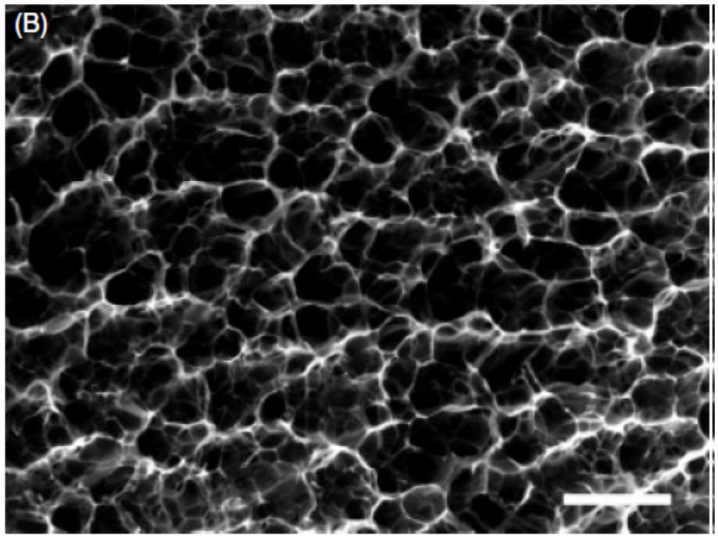

Figure 1.9 *Morphology of polypeptide hydrogel prepared with 80 wt% of water, 18 wt% of methacrylated polypeptide and 2 wt% of HEMA. Scale bar is 50 mm. From [73].*

Porogen leaching techniques

With porogen technology, polymer is prepared around a crystalline matrix which is leached from the material after polymerization. This method was introduced in [**74**], and numerous variations of the procedure for production of porous hydrophilic materials were developed later.

In [**75**] water-soluble sugars were used for preparation of polyHEMA membranes: HEMA and EDMA (1 wt%) were copolymerized in presence of 15 wt% of 40 μm sized sucrose or lactose. 10-25 μm pores were detected in the prepared membranes. Major advantage of the technique was independent control of mixture composition and pores size. Also, construction of asymmetrical membranes (with dense non-porous layer for extra mechanical support) could be achieved.

Preparation of macroporous polyHEMA using crystalline NaCl as a washable porogen was developed by Pradný [**76-77**]. NaCl particles size was 0.03 mm, 0.03-0.05 mm, or 0.05-0.09 mm. Increasing of NaCl fraction in the mixture led to higher pores connectivity at the price of poorer mechanical properties. An example of final hydrogel morphology achieved after NaCl washing out is shown in Fig. 1.10.

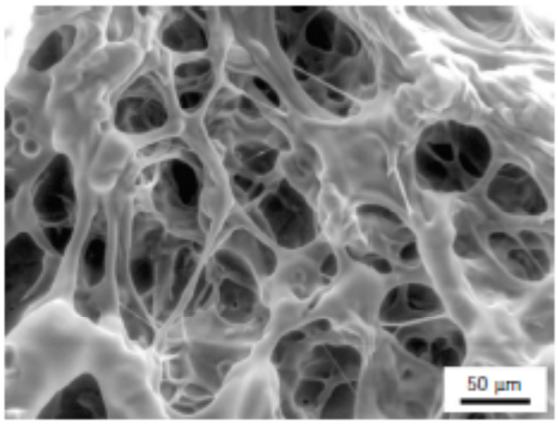

Figure 1.10 *Morphology of a polyHEMA-based hydrogel prepared with NaCl (0.05–0.09 mm) as porogen. From [**76**].*

Washable porogen is not necessarily water-soluble. For example, in [**47, 78**], poly(ε-caprolactone) fibers served as a template for polymerization. Then fibers were extracted from the product with suitable solvent (acetone or 2-aminoethanol). Such procedure enabled preparation of scaffolds with properly oriented asymmetrical pores (Fig. 1.11). Pores diameter was determined by fibers geometry.

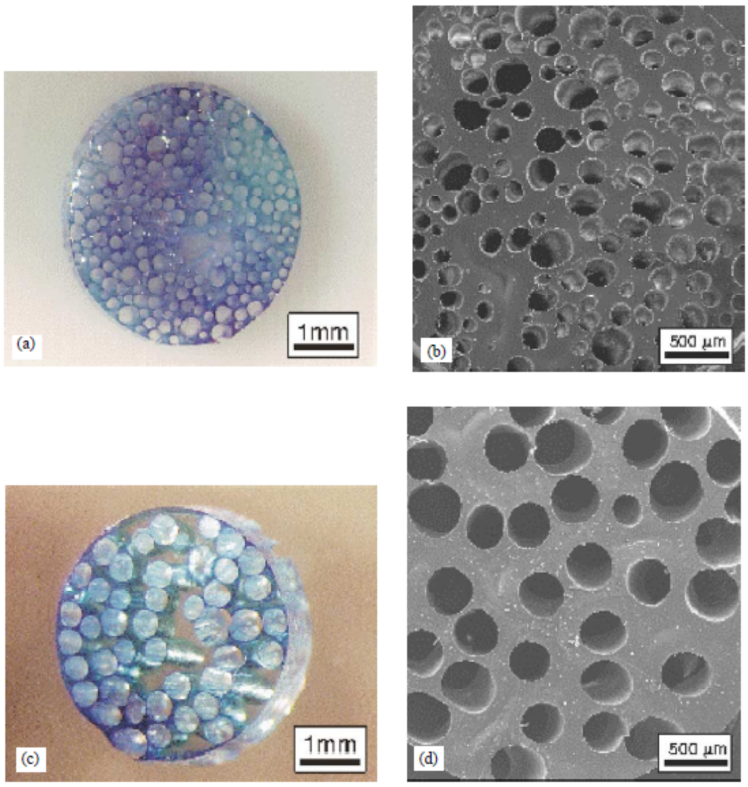

Figure 1.11 *Examples of polyHEMA materials with oriented pores. From [**47**].*

Combination of porogen leaching and phase separation may lead to interesting double porous structures (Fig. 1.12, [**79**]). In such cases giant pores formation is caused by porogen, and smaller pores in the surrounding continuous matrix appear due to phase separation process.

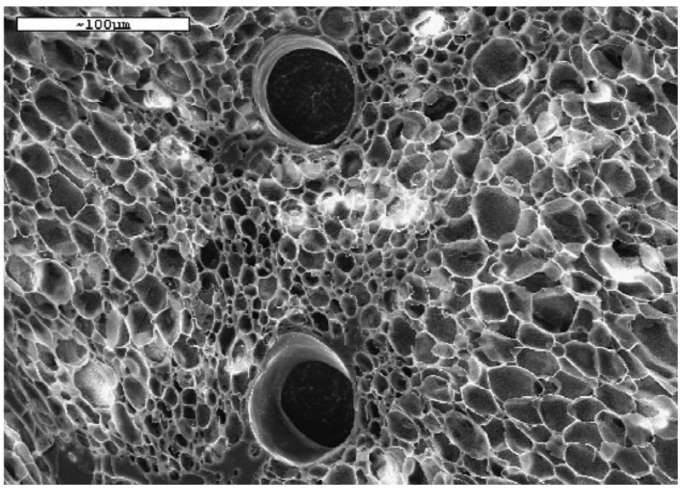

Figure 1.12 *Example of porous polyHEMA-based material with double porosity. From [**79**].*

Cryogelation

Cryogelation at subzero temperatures [**80**] enables production of macroporous samples via polymerization of the hydrophilic monomers or crosslinking of polymers in aqueous medium. Most of water is frozen and performs like porogen while the dissolved substances (monomers or polymers) are concentrated in unfrozen regions providing solutes with sufficient molecular or segmental mobility for reactions to perform. Within some range of negative temperatures chemical reactions performed in unfrozen liquid microphase are faster compared to bulk solution [**81**].

Applications of cryogelation to HEMA-based systems are presented in [**82, 83**]. After melting of the ice crystals, a system of large interconnected pores was formed. The resulting materials had porosity up to 90%, with pores of 10–200 μm. They could withstand compressive deformations down to 20% of their original volume without being destroyed [**84**]. The morphology of pores was determined by freezing rate, final temperature, initial concentration of monomers, content of crosslinker, and presence of nucleation agents [**81, 85, 86**]. Thus, to obtain a reproducible freezing pattern, careful control of conditions was required.

***

Analysis of routes to prepare macroporous polyHEMA hydrogels leads to conclusion that the polymerization-induced phase separation method offers probably the most flexibility in the final product morphology combined with the ease of procedure. Moreover, this approach can potentially by used *in situ* for construction of injectable gel formulations. Thus, phase separation method was selected for preparation of macroporous hydrogels in this work.

1.6 Mechanical properties of hydrogels: common considerations

For majority of applications, mechanical properties of hydrogel are of extreme importance. If a material serves as a scaffold for tissue replacement or as a chromatography column filler, hydrogel requires certain mechanical integrity. It was shown in studies of cell growth that substrate modulus can efficiently determine the behavior of cells attached to the surface; a recent example is provided in [**87**]. The general principle of proper mechanical properties for tissue construction selection is described in [**88**]. Briefly, *in vivo* stress/strain histories need to be measured for a

variety of activities both in normal and for (sub)failure conditions. These data provide mechanical thresholds for tissue repairs/replacements to hold. The set of mechanical properties must be further selected and prioritized, as the mechanical properties of the designs are not expected to completely duplicate the properties of the native tissues. Then, the effects of physical factors on cellular activity must be determined in engineered tissues. Thus, successful design of a tissue presumes accurate and thorough testing of both natural tissue and an artificial tissue candidates.

Nevertheless, in many application-oriented studies, for low-cost and rapid measurements, simple instruments are used. Several types of forces can be applied simultaneously during such tests, for example, cutting implies both shear and compression. Even though results are reproducible, they are not related to fundamental rheological properties of a material (stresses and strains applied are not defined). To compare data from different laboratories, it is essential to follow all conditions (sample size, magnitude of force or deformation, device design, speed of the probe, and others).

To my knowledge, there are no documented protocols completely describing shear testing of soft non-flowing solids (swollen polymer gels). ASTM standards are limited to descriptions of solutions and pastes studies (inks [**89**] or melts [**90**]). One of the best descriptions of rheological testing of gels is available in [**91**]. As discussed there, two precautions are critical for correct food gels rheometry: sample steady state and testing in the linear viscoelastic range. At the same time deformation amplitude should be high enough to provide reasonable signal-to-noise ratio.

Further complication not mentioned in that protocol, neither in other available standards, is the test gap size estimation. Fig. 1.13 illustrates what "gap size" means in rotational rheometry tests.

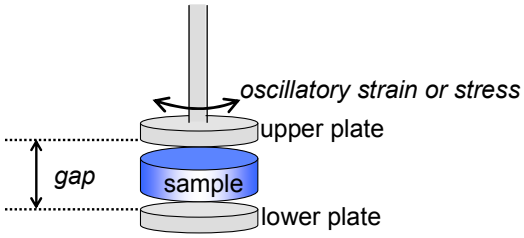

Figure 1.13 *Gap during measurement with plate-plate geometry of rotational rheometer.*

If the sample flows, its proper loading is quite easy. On the other hand, from a hard material, the sample can be manufactured precisely with required dimensions. But for soft non-flowing gel (besides prepared directly inside the rheometer cell), the correct measurement gap should be trialed experimentally. Probably, because of the complications of gap estimation and consequent uncertainties in the data, tensile [**92-94**] and compression stress-strain measurements [**92**], [**93**] are currently more popular than shear tests in case of gels. On the other hand, due to construction of measurement instruments, shear testing is easier to be carried out in physiological surrounding (e.g., swollen state, presence of certain substances, normal force loading), and, when properly organized, it provides valuable information. Based on these considerations, the shear testing was selected as a primary technique for hydrogel mechanical properties characterization, and care was taken to achieve relevant and reproducible results.

1.7 Background of shear rheometry

Mechanical properties of a material define the relation between the force acting on a sample, and deformation of a sample caused by this force. Stress is acting force divided by the area over which it is applied, and strain is deformation relative to initial dimension. Stress is usually denoted as σ in equations, and strain is γ. Both stress and strain are in general tensors.

Two basic models of rheological behavior of materials are ideal elastic solid body and ideal viscous liquid.

Purely elastic bodies at relatively low (linear) deformations obey a simple law

$$\sigma = G\gamma \tag{1.7}$$

with G (Pa) being shear modulus (it reflects material resistance to the acting force). At higher deformation G may be not constant, and differential equation holds:

$$G = \frac{d\sigma}{d\gamma}. \tag{1.8}$$

For purely viscous fluids resistance of fluid to flow is characterized by the viscosity coefficient η. Newtonian liquid viscosity is constant over a range of shear rates, and Newton's law is fulfilled:

$$\sigma = \eta \frac{d\gamma}{dt} = \eta\dot{\gamma}. \tag{1.9}$$

If viscosity is rate-dependent, the same equation is used in differential form:

$$\eta = \frac{d\sigma}{d\dot{\gamma}}. \tag{1.10}$$

Properties of real polymer materials are in between the ideal cases, and may be described by combination of these models. In particular, for a hydrogel its liquid-like properties originate from the fact that the major constituent is water, and the solid-like behavior is due to the network which prevents the system from flowing. Practically all hydrogels are viscoelastic. Thus, dynamic testing methods (relaxation or oscillation experiments) are to be used for characterization of polymer hydrogels.

1.7.1 Stress relaxation

During stress relaxation test, a constant strain is applied to the sample, and the stress caused by that deformation is recorded. An ideal elastic material responds with a constant stress (proportional to strain), an ideal viscous material responds with a constant zero stress. A viscoelastic material shows a decreasing stress over time (Fig. 1.14) in the form of an exponential decay (stress relaxation) $\sigma = \sigma_0 e^{-t/\tau}$.

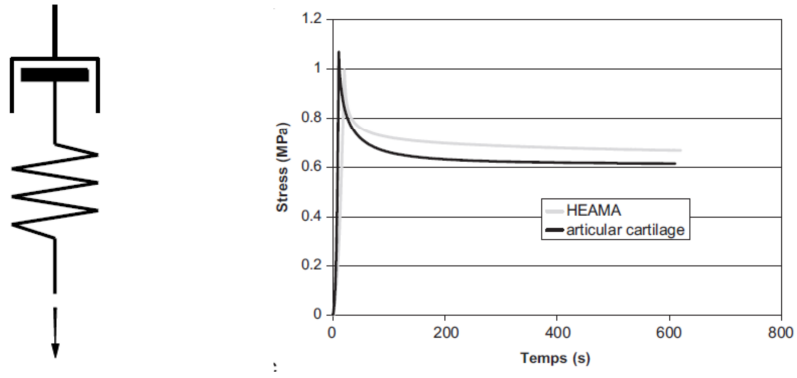

Figure 1.14 *Left: Maxwell model of a viscoelastic body ([**95**]); right: stress relaxation tests of polyHEMA construct and a natural articular cartilage ([**96**]).*

The Maxwell model (consecutive spring and dashpot) illustrates stress relaxation (Fig. 1.14). In response to a sudden deformation, the spring is immediately extended, and applies a force on the dashpot. As the spring recoils, the force decreases, thus, the rate of dashpot also decreases, leading to the exponential decay of the relaxing stress.

The relaxation time τ of liquids is small (~10^{-3} s for water). Solid elastic materials have very large relaxation time constants. Viscoelastic hydrogels have relaxation times in between, in the range of $\tau = 10^{-1}$ to 10^{6} s.

If a material stress relaxation cannot be described by a single exponential decay term, a generalized form of the Maxwell model is used (*n* Maxwell elements in parallel, each element having its own set of constants). If a permanent residual stress remains indefinitely, one of the equation terms is a constant: $\sigma = \sum_{i=1}^{n} \sigma_{0,i} e^{-t/\tau_i} + \sigma_e$. Model parameters are determined by fitting methods.

1.7.2 Creep

In creep test, strain response over time is observed under a constant applied stress. Simple creep behavior can be described mathematically by the Kelvin model made up of spring and dashpot in parallel (Fig. 1.15). When stress is applied to a sample and held constant over time, the strain increases, but the rate of increase diminishes over time in the form of an exponential decay. In the Kelvin model the dashpot controls the rate of the spring elongation.

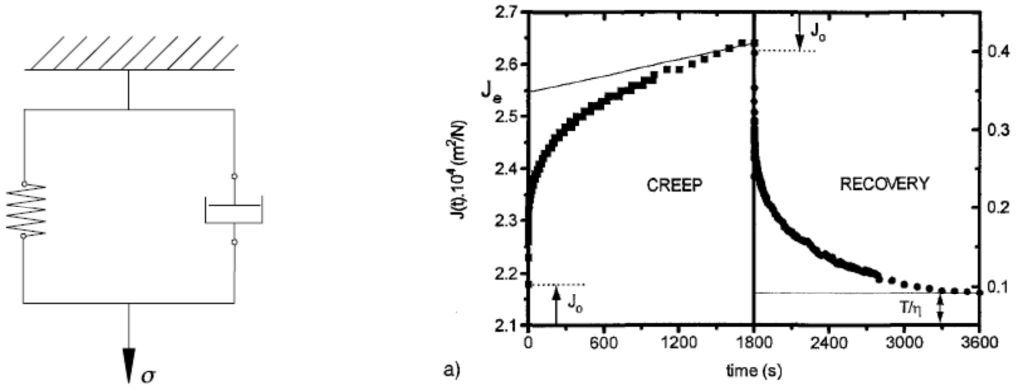

Figure 1.15 *Left: Kelvin model of a viscoelastic body (from [**95**]); right: example of shear creep testing of gelatin (from [**97**]).*

1.7.3 Oscillation

In oscillating mode, viscous and elastic properties of a material can be measured simultaneously. At appropriate oscillation amplitude, the material can be subjected to an oscillating shear stress without breakage of its molecular structure. In the case of a sinusoidal oscillation, the deformation is:

$$\gamma = \gamma_0 \sin(\omega t). \tag{1.11}$$

For an ideal viscous material, the shear stress follows the shear deformation with a phase shift of 90°, whereas an elastic material has a phase shift of 0°. Real materials show a phase shift in between 0 and 90°. The stress and deformation signals shape for these ideal cases is schematically shown in Fig. 1.16.

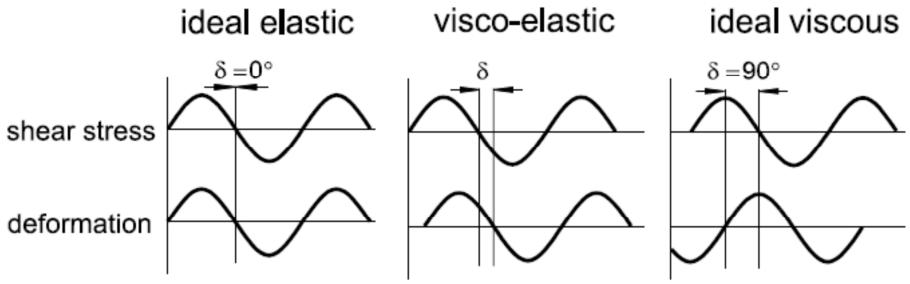

Figure 1.16 *Forced oscillations test of ideal elastic, ideal viscous, and viscoelastic bodies (from [**95**])*

With the complex shear modulus G^*, both viscous and elastic properties of a material can be characterized by measuring the phase shift δ:

$$G^* = G' + iG'' \tag{1.12}$$

with G' for the elastic, and G'' for the viscous component. The phase shift is

$$\tan \delta = \frac{G''}{G'}. \tag{1.13}$$

Frequency sweep (oscillation test at different frequencies) gives elastic and viscous properties over a range of time scales.

An interesting variation of dynamic test is a free oscillation technique described in [**98**] (experiment) and [**99**] (theory). For some soft materials under special conditions, creep growth and creep recovery curves are not purely exponential, but are superimposed with damped oscillations. From their frequency and decrement it is possible to calculate G', G'' and phase angle δ at the frequency of oscillations. If system inertia can be changed, these properties are monitored over a range of frequencies ([**97**]). The interest in this method which is sophisticated and time-taking is that sometimes it is possible to achieve higher frequencies of free oscillations than are available in frequency sweep tests.

1.8 Mechanical properties of swollen gels

Properties of water-swollen crosslinked polyHEMA are controlled by both transient (physical) and permanent (covalent) interactions. Physical hydrophobic interactions viewed as association of stickers (methacrylate moieties) assisted by changes in the iceberg structure of water play an important role in dynamic and static properties of the hydrogels: they are strong enough not to allow chemically uncrosslinked polyHEMA to dissolve in water but only to swell.

Discrimination of permanent and transient networks by examining the storage and loss moduli in the low-frequency region was discussed by Kavanagh and Ross-Murphy [**100**]. The interplay between covalent bonds and attractive physical interactions is not enough clear: the chemical crosslinks can suppress the formation of physical bonds hindering the alignment of chains. Alternatively, increasing number of chemical crosslinks can enhance the weaker, non-specific interactions by increasing the probability of pairing of interacting sites.

1.8.1 Homogeneous gels

Detailed systematic studies of homogeneous polyHEMA hydrogels swelling and equilibrium deformational behavior [**101**] revealed that it in all cases the actual crosslink density was lower than calculated that from polymerization feed composition. This was ascribed to two major factors: diffusional and steric limitations decreasing the reactivity of the second vinyl group of crosslinker molecule incorporated into a growing polymer chain, and side reaction of cyclization. Crosslinking efficiency was dependent on the nature of the crosslinker: with 20 wt% of water at preparation, crosslinking efficiency of EDMA was 84%, and for DEGDMA and trimethyleneglycol dimethacrylate it was 43% only. The crosslinking efficiency was dependent on the reaction mixture dilution; results for the system HEMA-DEGDMA are summarized in the Tab. 1.2.

Table 1.2 *Efficiency of crosslinking and polymerization yield in HEMA-EDMA system as functions of initial dilution (from **[101]**).*

Water concentration in the mixture, %	Crosslinking efficiency, %	Cyclization, %	Unreacted vimyl groups, %
0	70	0	30
10	55	23	22
20	43	41	16
30	31	60	9
40	26	70	4

In case of polyHEMA networks swollen in di(ethylene glycol) to various swelling degrees ([**102**], [**103**]), an indication of a low-frequency secondary relaxation was found and ascribed to presence of entanglements. With increasing swelling of the gel, the secondary maximum was weakened and even disappeared.

The level of crosslinking by physical interactions depends on the solvent nature: while water is a relatively poor solvent, many other are better, for instance diethylene glycol used in [**102**, **103**], in which hydrophobic interactions do not exist. Concerning aqueous solutions, ionic salting-in additives [**34**] or urea [**104**] minimize the attractive interactions between hydrophobic moieties of polyHEMA and only the effect of covalent crosslinks should be seen. On contrary, additives decreasing the degree of swelling should strengthen attraction between segments.

The effect of crosslink density and dilution at preparation on mechanical properties of homogeneous polyHEMA hydrogels was studied in detail for optimization of contact lenses manufacture. These early findings on polyHEMA gels are summarized in a review [**105**].

In the main transition region, for lightly crosslinked networks, the shapes of the retardation spectra of dry polyHEMA and of the same sample swollen with diethylene glycol to polymer volume fractions of 0.606 and 0.495 were similar; on the other hand, more swollen polyHEMA showed considerably broadened distribution of retardation times. The creep measurements revealed secondary mechanism of entanglements over long time scale. At high degree of swelling the contributions of both mechanisms were difficult to differentiate.

Investigation of the effect of the crosslinker concentration on the shape of the main transition region of polyHEMA swollen with diethylene glycol (polymer volume fraction 0.34) showed that the sample with a higher network density yielded spectra of greater symmetry; on the other hand, the sample having a low degree of crosslinking exhibited a broad distribution of retardation times.

In the rubbery region, the effect of the crosslinker concentration upon the viscoelastic behavior of the homogeneous polyHEMA networks (concentration of crosslinker EDMA was $2.058 \cdot 10^{-4}$-$8.55 \cdot 10^{-2}$ mole/cm^3) swollen with diethylene glycol was investigated. While networks with the EMDA concentration above $0.5 \cdot 10^{-4}$ mole/cm^{-3} attained equilibrium almost immediately, the compliance of networks having a lower crosslink density went on increasing even after 20 hours at 35 °C. In the time interval of 300 to 10000 s, an additional creep effect was observed for all studied samples – as sudden increase in the slope of the dependence of creep compliance with time. With increasing of either degree of swelling, or crosslinker concentration, the characteristic time of the secondary creep increased. It was

assumed that this effect was connected with the heterogeneity of the network and the presence of the hydrogen bonds in the polyHEMA samples.

The effect of the concentration of the crosslinker upon equilibrium characteristics of the polyHEMA gels was investigated for samples swollen with water to equilibrium. Concentration of elastically active network chains determined experimentally was linear with the concentration of the crosslinker at preparation. The slope of the dependence was less than 1. General reasons for this were suggested: incomplete incorporation of the crosslinker molecules into the network; and formation cycles which did not act as effective crosslinks. On the other hand, trapped entanglements which played a role similar to that of the crosslinks raised the physical degree of crosslinking. From the results it followed that in polyHEMA entanglements exhibited an effect which was in part permanent and in part labile.

The influence of crosslinker type on mechanical properties of homogeneous polyHEMA hydrogels was studied in [**92**]. PolyHEMA hydrogels were prepared in the presence of 30 wt% water with different crosslinkers: divinylic (EDMA, BDMA, HDMA) and diallylic (DVG and HD), over a crosslinker-to-monomer ratio between 0.1 and 5 mol%. The hydrogels were characterized in terms of equilibrium swelling, tensile properties, and in compression.

Two patterns were observed for equilibrium swelling EWC versus crosslinker concentration. For polyHEMA crosslinked with allylic compounds (DVG, HD), EWC remained constant over the studied range. In case of dimethacrylate crosslinkers (EDMA, BDMA, HDMA), EWC decreased with decreasing concentration of crosslinker.

Type and amount of crosslinking agents had little effect on ultimate tensile stress (UTS) at <1 mol% of crosslinker. More crosslinked samples revealed two different trends. For gels crosslinked with dimethacrylates, UTS increased with crosslinker concentration, whereas for allylic crosslinker, its ratio did not affect UTS.

The insensitivity of EWC and tensile properties to concentration of DVG and HD was due to the lower reactivity of these crosslinking agents. Indeed, low crosslinking efficiency was confirmed in [**92**]: a ratio of observed and theoretical crosslink densities was 0.013 for DVG and 0.336 for EDMA.

1.8.2 Porous gels

For the porous polyHEMA gels, the situation is more complicated: the topological structure of the matrix gel is not known, and often a working hypothesis is used that it is the same as that formed at dilution at which the gel is homogeneous. This may be questionable especially for macroporous gels and needs verification or rejection. Moreover, for porous polyHEMA hydrogels, their properties depend both on the interactions in the matrix, and the pores volume and geometry.

Majority of studies of porous gels mechanical properties were limited to simple indication of equilibrium modulus decrease as a sign of phase separation. For example, in [**106**] hydrogels based on poly(N,N-diethylacrylamide) were prepared at various temperatures around critical mixing temperature. With developing porous structure, elastic modulus measured in compression decreased to 1-5 kPa from 50 kPa typical of homogeneous samples. Similar observation was made in [**107**] where series of copolymer hydrogels based on N-isopropylacrylamide and poly(ethylene glycol) monomethyl ether acrylate were prepared with porogen poly(ethylene glycol) of various M_W. As pores size increased from ten to hundreds of micrometers, *G*' decreased from 94 to 7 kPa.

In a more detailed study [**82**] a series of polyHEMA gels and HEMA/N,N-dimethylacrylamide (DMAA) copolymers were prepared via cryogelation and conventional polymerization. Porosity was found to be 94-97% for cryogel, and all the pores were interconnected. As monomer concentration increased, pores in cryogels became smaller, but overall porosity increased. Morphology of conventional hydrogels was not directly studied, but from the preparation conditions a porous structure might be presumed.

For cryogels, the effect of initial dilution on mechanical modulus was less pronounced than for conventional hydrogels. For example, at HEMA/DMAA = 4:1, in the range of initial monomers concentration of 6-20 wt%, the equilibrium modulus measured in compression increased from 4-7 to 25 kPa for cryogels, and from 5 to 300 kPa for conventional gels. Also, conventional gels were found to be more fragile (compression at break 25-55%, versus 86-98% for cryogels).

Although there were only few detailed investigations on macroporous hydrogels dynamic (viscoelastic) mechanical properties, some studies cited above as well as older ones ([**67**], [**105**]) clearly revealed poor mechanical properties of

heterogeneous hydrogels as a limitation for their biomedical applications. To be readily invaded with cells, a gel should contain interconnected pores larger than 10 μm. Strength of such gels is usually not sufficient to provide mechanical integrity.

A usual way to improve mechanical properties of homogeneous hydrogels is incorporation of a suitable co-monomer (methyl methacrylate, cyclohexyl methacrylate and *t*-butylcyclohexyl methacrylate are often used). Even in small proportion, they dramatically improve mechanical integrity at the cost of lower swelling [**108**]. This approach, however, is seriously limited in that phase separation often occurs far before gelation, and microparticles are formed instead of bulk samples before acceptable properties are achieved.

For macroporous polyHEMA hydrogels this approach was tested in [**94**]. Addition of up to 5 wt% of strengthening comonomer (4-*t*-butyl-2-hydroxycyclohexyl methacrylate) led to decrease of the ultimate tensile strength, and even with 5 mol% of the comonomer it did not reach that of the homopolymer. This clearly indicated that the approach to improve mechanical properties developed for homogeneous hydrogels might not be relevant for phase-separated materials.

Another way to modulate mechanical properties of porous polyHEMA hydrogels was evaluated in [**109**]: increase of the crosslinker hydrophilicity. Macroporous hydrogels were prepared (at 80 wt% of water) by copolymerization of HEMA with 1,5-hexadiene-3,4-diol, 2-hydroxytrimethylene dimethacrylate or 2,3-dihydroxytetramethylene dimethacrylate. Two initiating systems were used: SMBS/APS or more active APS/TEMED, and the hydrogels properties were compared with that for hydrogels prepared with a common crosslinker EDMA. Tensile properties were considerably improved by changing EDMA to more hydrophilic crosslinkers with SMBS/APS initiator (Tab. 1.3).

The effect was assigned to more even distribution of the crosslinker within network (due to higher reactivity, close to that of HEMA) and, thus, delayed phase separation and more regular porosity. Supporting this, hydrogels prepared with different crosslinkers and APS/TEMED initiator did not differ much in mechanical properties, as in case of faster polymerization morphology of the hydrogel was affected more by its overall rate rather than conversion at phase separation point.

Besides hydrophilicity, reactivity of a crosslinker affected mechanical properties of hydrogel. In [**93**], EDMA and 1,5-hexadiene-3,4-diol DVG (more hydrophilic but less reactive) were compared. Due to DVG lower reactivity, effective

crosslink density was almost independent of its concentration at preparation. Sol fraction increased with DVG concentration, being constant and generally lower with EDMA concentration (0.5-5.0 wt%). Elongation at break was higher DVG-crosslinked hydrogels, and constant with DVG concentration, while in case of EDMA it decreased with crosslinker concentration. Finally, *E* modulus was higher (and increasing with concentration) for EDMA-crosslinked hydrogels, and almost independent of DVG concentration.

Table 1.3 *Mechanical properties of polyHEMA macroporous hydrogels prepared at initial dilution of 80 wt% water with different crosslinkers – 0.1 mol% (from [**109**]).*

Crosslinker	Energy to break, N/mm	Elongation at break, %	Modulus, kPa
EDMA	**5.90±0.33**	**483±77**	**3.78±0.32**
1,5-hexadiene-3,4-diol (divinyl glycol)	6.54±0.86	513±23	6.31±1.98
2-hydroxytrimethylene dimethacrylate	7.86±0.2	605±23	5.17±2.89
2,3-dihydroxytetramethylene dimethacrylate	8.10±0.56	604±52	3.92±1.07

In [**72**] studies of macroporous hydrogels morphology, ultimate mechanical properties and swelling behavior were reported. Macroporous polyHEMA gels were produced with 80 wt% of water as diluent, using active APS/TEMED system as initiator to eliminate the effect of crosslinker reactivity. The following crosslinkers were used at concentrations from 0.1 to 2 mol%: hydrophobic vinylic EDMA and BDMA; hydrophobic allylic HD, hydrophilic vinylic BHDMA, and hydrophilic allylic DVG. Some anomalous values and relatively large scatter of results during tensile strength measurements reflected the intrinsic inhomogeneity of the samples and non-uniformity of their internal morphology. Their low strength, and problems associated with the clamping in the grips of the instrument could also contribute to the quality of results.

The peak stress (reflection of ultimate strength) was almost insensitive to nature and concentration of the crosslinking agents, being very low (10-30 kPa). The measurements of energy to break (representing toughness) led to more definite conclusions. In each series of vinylic agents, there was a clear trend of decreasing toughness as the concentration of the crosslinker increased, which correlated well with decrease of elongation. In the series of allylic crosslinking agents, both energy

to break and elongation were relatively constant and much higher than for vinyl-crosslinked hydrogels. This invariance was also attributed to the narrow range of effective crosslink density (lower crosslinking efficiency) of allylic agents.

In the series of hydrogels crosslinked with vinylic compounds, the modulus of elasticity showed an expected increase with the concentration of crosslinking agents. The moduli of materials crosslinked with allylic compounds were relatively constant over the concentration range investigated.

Correlation between the size of spheroidal droplets of polymer in macroporous hydrogels and the nature of crosslinking agents was investigated. The droplet size followed the order DVG>HD ≈ BHDMA>BDMA, similar to the row of the time taken for the onset of phase separation. Thus, the later was phase separation, the larger the size of resulting polymer droplets.

As compared with the results of similar investigations [**92**], the effect of crosslinking agents on the properties of homogeneous polyHEMA hydrogels was more definite. This might be due to the higher dilution of the polymerization mixture for the macroporous hydrogels formation which overshadowed the influence of the crosslinking agents, as well as to structural inhomogeneities in the resulting macroporous gels, which induced erratic values for some properties.

***

Major part of studies on mechanical properties of swollen hydrogels and effects of preparation conditions reported so far were devoted to homogeneous materials. At the same time, systematic studies of mechanical properties of macroporous materials are quite limited, due to experimental complications. At most, the measurements include ultimate tensile properties and equilibrium modulus determination. Even for such measurements, due to non-linearity of compression stress-strain curves, relatively low modulus, and inhomogeneity of the materials, it is often impossible to get information on mechanical properties of porous materials in well-defined conditions. This complication is expected to be overcome in this work by measuring mechanical properties in shear mode taking advantage of sensitive instrument, Bohlin HR Nano rheometer, designed for measurement of low torques. The hydrogel sample could be fully immersed in the swelling medium during measurement, making it possible long measurements even at elevated temperature.

2 Aims and scope

The ultimate goal of this work is to understand the structure formation in phase separating hydrogels and the influence of morphology type (homogeneous, phase-separated, macroporous) on the material mechanical properties. Precautions has been taken to measure mechanical properties in a way that they are relevant to intact samples; and to study both mechanical properties and morphology for the samples prepared under same preparation conditions.

The main problems addressed in the work are:

1. Effect of polyHEMA preparation conditions on final mechanical properties of hydrogels (suppressing/promoting phase separation by change of crosslinker concentration, diluent concentration, diluent quality).
2. Extracting structural information from mechanical spectra, in particular:
   a. diversification between homogeneous, macroporous and intermediate gels by means of shear rheometry, elucidation of the most important measurable variables;
   b. elucidation of matrix structure in phase-separated gels by means of shear rheometry and supplementary techniques;
   c. elucidation of intermediate gels (phase-separated with structure below microscopy resolution) structure by means of shear rheometry and supplementary techniques;
   d. elucidation of the chemical and physical crosslinks role in determining mechanical properties of swollen networks.
3. Development and verification of the procedure to measure rheological properties of swollen hydrogels (homogeneous and macroporous) in shear, in the state close to intact (non-deformed).

In scope of these aims, the results are presented and discussed as follows:

In Section 4.1 preparation of hydrogels is described. The results are presented proving that preparation of polyHEMA gels using the chosen procedure leads to full conversion of monomers, and that the possible effects of mixing time are eliminated.

In Section 4.2 results of microscopy studies of prepared gels are presented. The influence of preparation conditions on final gels morphology is discussed.

In Section 4.3 the swelling ability of the polyHEMA networks is discussed in connection with the morphology of samples and the swelling medium.

Section 4.4 contains discussion of mechanical properties of polyHEMA hydrogels with respect to their internal structure. In particular, effects of network structure on the vitrification (α-relaxation) of swollen polyHEMA gels are shown, and the identity of heterogeneous hydrogels matrix and homogeneous hydrogels is concluded; the role of physical interactions and interconnected pores in determining the mechanical properties of polyHEMA materials is discussed; the secondary (low-frequency) relaxation observed for particulate gels is explained.

Discussion on some experimental techniques is given in the Attachments (Section 10). In Section 10.1 procedures to find proper conditions to measure shear properties of swollen hydrogel samples are presented. It is proved that in such manner intact material properties independent of measurement conditions can be determined. In Section 10.2 the time-temperature superposition is described as a suitable method to extend the range of measurable frequencies, and evidences of superimposed properties identity with the result of direct measurement are provided. In Section 10.3, creep measurement results are presented in support of data obtained in forced oscillation tests. In Section 10.4, details of multivariate analysis procedure and algorithm are described, and examples of its application to analysis of the experimental data are given.

3 Experimental part

3.1 Chemicals

Monomers: 2-hydroxyethyl methacrylate HEMA (Rohm) and di(ethylene glycol) dimethacrylate DEGDMA (Aldrich) were used as received. HEMA contained 0.07% DEGDMA (bifunctional crosslinker) and 0.44% of di(ethylene glycol) monomethacrylate (according to results of gas chromatography).

Initiators: ammonium persulfate (Fluka) and N,N,N',N'-tetramethylethylenediamine TEMED (Helicon) were used as received.

Diluents: distilled water, aqueous sodium chloride (Aldrich, 0.05 to 0.7 mol/L), aqueous magnesium perchlorate (Aldrich, 0.05 to 1.0 mol/L).

Swelling media: distilled water, aqueous NaCl (Aldrich, 3 mol/L), DMSO (Aldrich).

3.2 Preparation of samples

3.2.1 Synthesis of HEMA/DEGDMA hydrogels.

2-hydroxyethyl methacrylate (HEMA) and di(ethylene glycol) dimethacrylate (DEGDMA) were copolymerized in the presence of various amounts of diluent (water or aqueous salt) using ammonium persulfate (APS) as initiator, and N,N,N',N'-tetramethylethylenediamine (TEMED) as promoter. APS was first mixed with the diluent, HEMA and DEGDMA were added, and the solution was stirred for 5 min (the solutions were always clear at this point, proving full miscibility of components). Then, the sample was bubbled with nitrogen for 5 min, TEMED was added, and the mixture was quickly poured between two glass plates separated with 3 mm silicone rubber sealing. The sample lost its fluidity after 5 to 15 minutes indicating the crosslinked structure formation. The reaction was carried out overnight at room temperature to ensure complete conversion.

After the polymerization the sample was washed several times with an excess of distilled water (at least 5 washes, 24 hours each), and if necessary, re-swollen in a different medium via gradual solvent exchange. Then, a disk (20 mm in diameter) was cut to be used in the rheology tests. The rest of the sample was used for swelling, morphology and calorimetry studies.

The parameters varied within tested series were: diluent concentration (40 to 80 wt%); DEGDMA amount with respect to HEMA (0.1 to 5.0 mol%); diluent type (water, aqueous salt); and swelling medium (water, DMSO, aqueous salt). APS to monomers ratio was 0.75 wt% for all samples.

The initial water content is expressed either in wt%, (IWC)

$$\mathrm{IWC} = \frac{m_\mathrm{w}}{m_\mathrm{w}+m_\mathrm{p}} \times 100\% \tag{3.1}$$

or as volume fraction of polymerizable material during polymerization

$$\phi_2^0 = \frac{m_\mathrm{p}/\rho_\mathrm{p}}{m_\mathrm{w}/\rho_\mathrm{w}+m_\mathrm{p}/\rho_\mathrm{p}} \tag{3.2}$$

where m_p is the mass of the polymer or polymerizable components and m_w is the mass of water. The density of dry polymer was used in calculations instead of monomer density to account for contraction of the monomer during polymerization.

The crosslinker concentration CC, is expressed in molar percent of crosslinker in its mixture with HEMA

$$\mathrm{CC} = \frac{moles_\mathrm{crosslinker}}{moles_\mathrm{crosslinker}+moles_\mathrm{HEMA}} \tag{3.3}$$

3.2.2 Coding of samples

The samples prepared with water as diluent and then swollen in water are coded as follows: **40/1.0**, where the first number (40) is the initial water concentration (IWC) in wt%, and the second (1.0) stands for the crosslinker-to-monomers ratio (CC) in mol%.

For samples prepared with aqueous salt as diluent, the type and concentration of salt is indicated in brackets before the sample code: **(NaCl-0.1M)40/1.0**. For samples re-swollen in solvent other than water before the measurement, the type of swelling medium is indicated in brackets after the sample code: **40/1.0(DMSO)**.

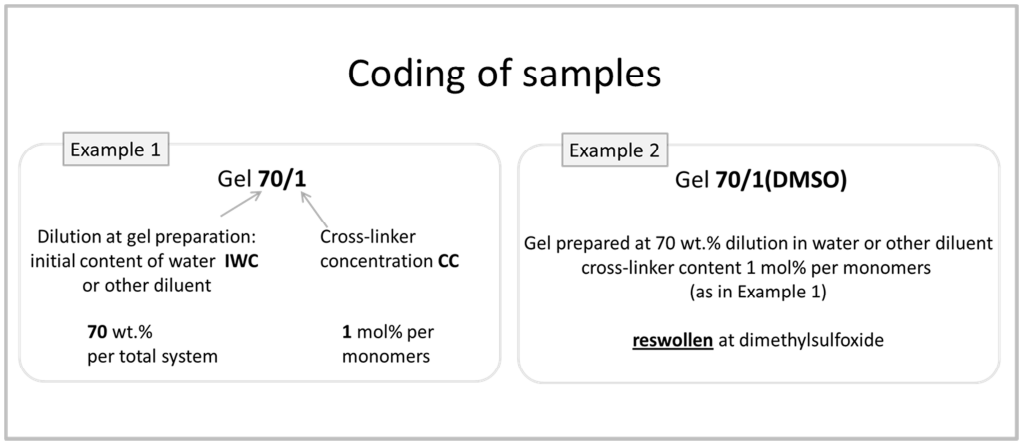

Scheme 3-1 *Coding of gel samples*.

3.3 Rheometry

3.3.1 Techniques

Rheological measurements were performed using Bohlin Gemini HR Nano rotational stress-strain rheometer [**110**]. It offers ultra-low torque measurements (10nNm to 200mNm) and thus enables the rheological characterization of weakly structured materials such as swollen hydrogels. This top of the range research instrument incorporates a high resolution air bearing of the rotor, that can be driven with very small torques (10nNm) providing precise reading of position (stress control mode) or vice versa, the position of the rotor when rotating or oscillating is precisely controlled to cause small strains and corresponding stresses are measured (strain control mode).

All measurements were run with plate-plate geometry on swollen samples immersed in water during the test using a special solvent dish. Samples were conditioned at a pre-set temperature (Fig. 3.1). The presence of water did not influence the measured values (additional friction of rotating part was negligible). The swollen disk diameter was always 20 mm, measuring gap was varied between 1.00 and 3.05 mm depending on the sample dimensions. However, measuring gap did not correspond exactly to the sample thickness as reaching the *no slippage* between sample and measuring geometry condition demanded certain small compression of the soft gel sample. The value of compression is found qualitatively and precisely from the measuring system response. Details of measuring gap determination are given in Section 10.1. To our knowledge, the procedure to find correct gap in shear rheometry of soft gels was not documented in literature, so we developed original method. The correct gap influences the absolute values of moduli significantly. If the gap size is set with even 2% deviation from the right position (50 μm for the sample of 3 mm thickness), the deviation of measured modulus and loss factor from the correct values can be up to 25%.

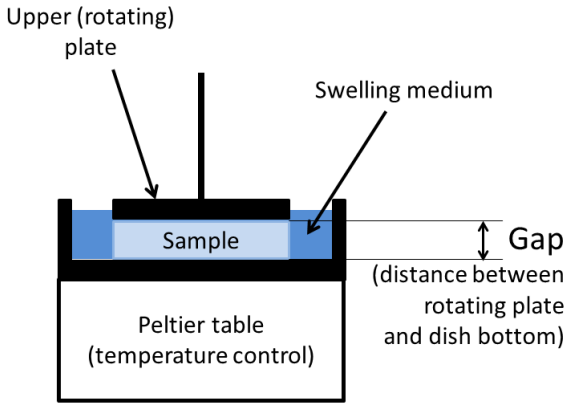

Figure 3.1 *Loading of hydrogel sample for rheometry measurement.*

The amplitude sweep forced oscillations tests were performed in the strain-control mode in the range of strains between 10^{-5} and 1, the oscillation frequency being 1 Hz. This test served as pre-measurement to find correct value of applied deformation not to depart from linear viscoelasticity region of materials.

The frequency sweep forced oscillations tests were performed with all swollen gels in the stress-control mode. Frequency range was typically between 0.05 and 15-80 Hz. The upper limit of frequencies was limited by resonance of the sample and rotating part of the rheometer system. The resonance frequency depended on the sample stiffness as already documented in the literature [**111**].

Normal force versus normal deformation measurements were performed by manually changing the gap value and recording the normal force value when it came to equilibrium.

High-frequency mechanical oscillations. A unique Piezoelectric Rotary Vibrator (PRV) [**112**] attachment was used to directly measure hydrogels behavior in the high-frequency oscillations range: 10-2000 Hz, in these tests sample thickness could be only around 0.5 mm, and the sample disk diameter was 40 mm. Due to the sample stiffness and thus its thickness limitation, the method was not well suitable for highly porous samples.

Creep tests were performed in the range of shear stresses of 1 to 5000 Pa, the response signal, displacement, was recorded for up to 3600 s. The recovery curve at 0 Pa shear stress was then recorded to prove absence of permanent deformation (either due to flow or sample slippage).

3.3.2 Precautions

All measurements were performed consecutively at least twice while ensuring complete sample relaxation after loading, changing gap or temperature, and between the measurements.

The stress value in the frequency sweep test was auto-adjusted so that the "target strain" laid within the limits of linear viscoelasticity as determined from the amplitude sweep test (see sample measurement in the Fig. 3.2).

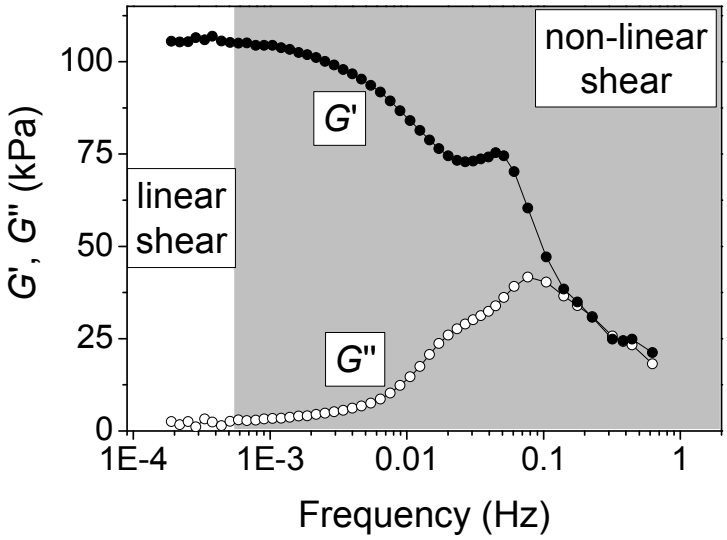

Figure 3.2 *Amplitude sweep test as a mean to find the range of linear viscoelastic behavior (gel 50/1 measured at 85 °C).*

Gap (or gap size) is spacing between the bottom and the top plates of the rheometer during measurement (Fig. 3.1). To our knowledge, the procedure to find correct gap for shear rheometry of macroporous gels was not documented in literature, so we developed our own approach to it. It is described in Section 10.1.

3.4 Morphology studies

Morphology of the hydrogels was studied both in the swollen state (light microscopy LM or environmental scanning electron microscopy, ESEM) and in the frozen state (cryo low-vacuum scanning electron microscopy; cryoLVSEM).

SEM was performed with Quanta 200 FEG microscope (FEI, Czech Republic) was used, equipped with a Peltier cooling stage and secondary electrons detector working in low-vacuum conditions (LFD detector). For cryoLVSEM

morphology studies, a small piece of wet sample was flash-frozen in a liquid nitrogen, fixed with ice onto the pre-cooled stage (-10 °C) of the SEM microscope, the top frozen layer was cut off and the fresh, and frozen, cut surface was observed at cryo low-vacuum conditions (T = -10 °C; p = 100 Pa; LFD detector). For ESEM, a hydrogel sample was trimmed with a blade, transferred to a table conditioned at 2 ºC, and scanned at this temperature. The water vapor pressure in the chamber was adjusted so that a thin water layer at sample surface existed.

LM studies of the samples in their natural state were performed with Leica DM 6000 M (Leica, Germany) microscope. The microscope was equipped with large working distance objectives with extended depth of focus and possibility of bright field and dark field imaging in both transmitted and reflected light. The samples were submerged in water during the whole sample preparation procedure: The bulk piece of hydrogel was cut with a sharp blade to obtain as thin wedge shaped specimen as possible. The slice with a droplet of water was placed between the support and cover glasses and observed in the light microscope.

3.5 Equilibrium water content

The equilibrium weight content of water, EWC, was determined gravimetrically by weighing the samples in their equilibrium swollen state (m_{sw}) and after drying to constant weight under vacuum at 100 °C (m_d). The equilibrium swelling degree was expressed either as weight fraction of water in the swollen sample after extraction of sol fraction:

$$\mathrm{EWC} = \frac{m_{sw} - m_d}{m_{sw}} \tag{3.4}$$

or as the equilibrium volume content of water, EVC,

$$\mathrm{EVC} = 1 - \phi_2 = \frac{(m_{sw} - m_d)/\rho_w}{m_d/\rho_p + (m_{sw} - m_d)/\rho_w} \tag{3.5}$$

where ρ_w and ρ_p are, respectively, the partial specific gravities of water and the polymer in the swollen sample.

The equilibrium swelling of networks in medium other than water was expressed similar to Eq. 3.4, as weight of swelling medium in the swollen sample per 1 g of swollen gel.

3.6 DSC

Differential scanning calorimetry (DSC) measurements were performed with the Perkin-Elmer 8500 DSC calorimeter. Samples of about 5 mg were closed in

aluminum sample pans, and the system was flushed with dry helium during the DSC scan. The temperature scale was calibrated according to the melting points of cyclohexane and indium. The power output scale was calibrated with indium. Measurements in the standard DSC mode performed with constant heating rate 1 °C/min at heating and cooling runs.

Cooling of a swollen gel causes its de-swelling and following transition into glassy state. The glass transition of swollen polyHEMA gels is situated in temperature range of water phase transition. This practically eliminates founding of glass transition by a standard DSC scan. The de-swelling of hydrogel is relatively slow process. During a standard DSC measurement water driven out from gel does not follow equilibrium path due to fast change of temperature. To reach the equilibrium content of water in gel, the sample first was cooled to under-cooled state at -10 °C and kept at this temperature for 5 hours. Then it was cooled to -50 °C at cooling rate -10 °C/min. After 5 min at this temperature the sample was heated in Step Scan® regime with the step of 1 °C and heating rate 1 °C/min to 30 °C.

3.7 IR

Infrared spectra were acquired with a Nexus Nicolet 870 FTIR spectrometer purged with dry air and equipped with a liquid nitrogen cooled MCT (mercury cadmium telluride) detector. Spectra of solution and hydrogel samples were acquired using the Golden Gate single reflection ATR (attenuated total reflectance) cell (Specac) equipped with a diamond internal reflection element. When an initial mixture sample was transferred onto the diamond crystal, the spectrum was obtained without applying any force and without covering the sample. When a hydrogel sample was placed onto the crystal area, a force was applied to the sample using the pressure arm of the ATR accessory. The spectra were recorded with a resolution of 4 cm^{-1}; 256 scans were averaged per spectrum. After subtraction of the spectrum of atmosphere, baselines were corrected (linear baseline correction) and an advanced ATR correction was applied. A spectrum of water at 28 °C was subtracted from the corrected hydrogel spectra and the corrected initial mixture spectrum to obtain better visualization of the C=C band at around 1630 cm^{-1}. The spectra were normalized using the integrated intensity of the C=O band at around 1700 cm^{-1}.

3.8 Accuracy

Gels preparation. Monomers, initiators and diluent were dosed using the laboratory balance, accuracy of weighing was ±0.5% of the calculated feed. Thus, the sample composition 40/1 means that the gel was prepared with 40.0±0.2 wt% of water and 1.00±0.01 mol% of the crosslinker, with respect to the monomers. For all the experiments reported in this work, the same batches of HEMA and DEGDMA were used.

Accuracy of experimentally determined values was verified by reproducing of measurement using an independently prepared piece of gel of the same composition.

Equilibrium swelling degree. Content of the swelling medium in the homogeneous, intermediate and interlocking gels was reproduced with the relative accuracy of ±3%. For particulate gels, which were extremely soft, and part of the swelling medium could be inevitably pushed out when blotting the surface, the estimated relative accuracy was within ±7% of the averaged value. The validity of swelling data was also confirmed by differential thermal analysis of selected water-swollen samples.

Shear moduli. The major source of errors in determining the elastic shear modulus of homogeneous, intermediate and interlocking samples was incorrect placement of the specimen (off-center of the rotating plate). From the replicated measurement the accuracy of measured G' was found to be ±5% of the averaged value. For particulate samples, finding the correct measurement gap was more complicated, this resulted in determined G' accuracy within ±10%.

Accuracy of the viscous shear modulus measurement depended largely on G''/G' ratio. With $G''/G'>0.05$ typically the accuracy of G'' measurement was close to that of G'.

Loss factor $\tan\delta = G''/G'$ was typically determined with accuracy of ±3% of the averaged value. As elastic and viscous shear moduli were similarly affected by the off-center position of the specimen, and this source of errors was partially eliminated in loss factor calculation. However, low values of $\tan\delta$ could not be determined with sufficient accuracy. According to the rheometer specification, loss factor in the range of $0.01 < \tan\delta < 0.05$ could be subjected to significant error, values below 0.01 should be treated as zero.

4 Results and discussion

As a core of this work, model series of differently structured hydrogels was prepared to understand the relationship between the heterogeneous gel structure and its mechanical properties. Hydrogels with various porosities comprising samples with communicating pores (swollen polymer particles fused together and surrounded by swelling medium) and/or non-communicating pores (droplets of swelling medium enclosed in the swollen polymer matrix) were prepared by polymerization-induced phase separation in presence of inert diluent. When the polymerizing system reaches certain conversion at which the activity of diluent equals one, the condition for coexistence of pure diluent with swollen polymer is fulfilled, and the diluent can separate into a new phase. The phase separation can take place either before or after the gel point and, thus, leads to various morphologies depending on system composition, thermodynamic quality of components and also reaction rate (Fig. 1.1).

The microsyneresis in 2-hydroxyethyl methacrylate (HEMA)/water system (a well-known process, see details in Section 1.5, p. 12) in this work served as a tool for reproducible preparation of various gels morphologies, see examples in Fig. 4.1. In this figure, picture A represents a non-porous gel; B shows isolated droplets of swelling medium, created by diluent exclusion during polymerization, in the continuous swollen polymer matrix. Such droplets can increase in number and percolate to form long channels and larger voids (C). When the critical fraction of such channels is exceeded, they interconnect forming bicontinuous structures (D). Another type of porous samples is represented by those consisting of swollen polymer particles, fused together (E).

The morphology of gels was characterized by light and/or scanning electron microscopy under varying conditions, their swelling was determined gravimetrically. The main target of this work, mechanical responses of differently structured gels in their swollen state, were investigated in detail by means of shear rheometry in linear viscoelastic region at a range of frequencies or relaxation times. The recent findings [**113**] brought the idea that dynamic mechanical responses of hydrogels could serve as a method to find whether the swollen material contains connected pores. This work, therefore, has been an attempt, basing on the critical amount of collected experimental data, to answer this question and present the general rules linking the soft material structure with its dynamic mechanical behavior.

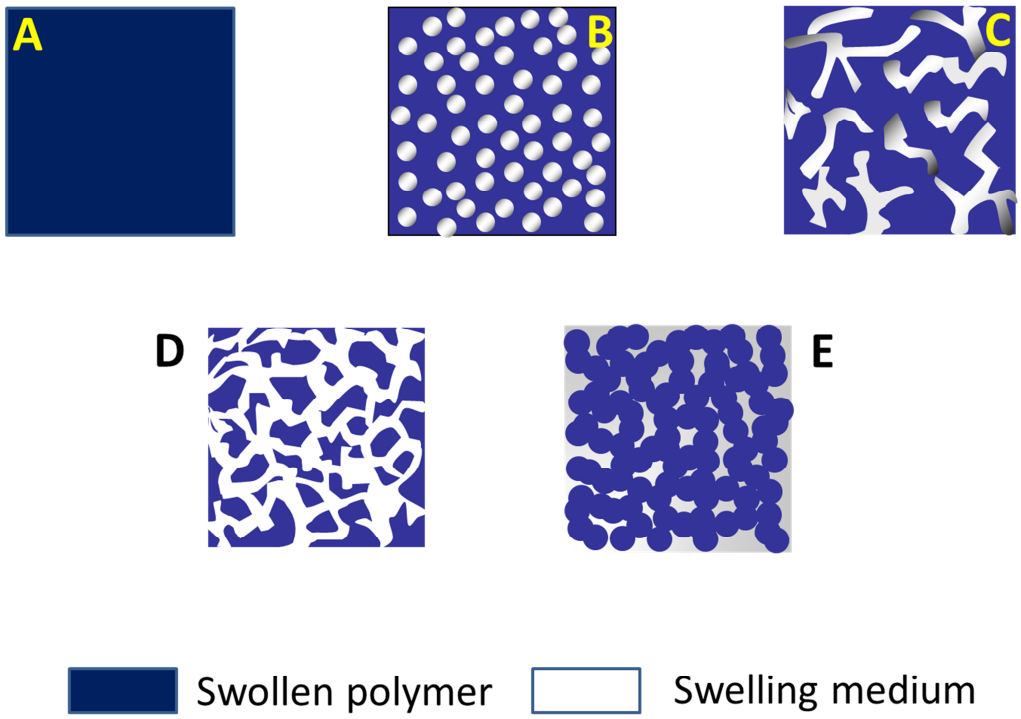

Figure 4.1 *Porosity types of samples prepared and studied in this work (see text).*

4.1 Hydrogels preparation

Monomer/crosslinker/water mixtures miscibility. The miscibility of the reacting systems that is represented by the tertiary mixture **monomer/crosslinker/diluent** (*2-hydroxyethyl methacrylate (HEMA) / di(ethylene glycol) dimethacrylate (DEGDMA) / water*) was examined prior their use in model gelling mixtures. If the starting mixture would be immiscible or only partially miscible and thus unstable, some poorly defined and irreproducible effects could alter the final gel morphology. Such effects would be caused by the reactants mixing time, components addition order, intensity and type of stirring, presence or formation of surface active agents. In our study, the intention was to obtain various morphologies by defined and reproducible way – by the reaction-induced phase separation, therefore only homogeneous and fully miscible starting mixtures for gel preparation were chosen.

The range of miscibility of HEMA/DEGDMA/water mixture was determined by visual assessment of mixtures opacity. To do so, a mixture of HEMA and water was titrated with DEGDMA till turbidity lasting for at least 10 minutes was detected. In Fig. 4.2, to the left of the experimental curve, there is an area of compositions at

which the HEMA/DEGDMA/water system is fully miscible. All gels studied in this work were prepared from such initially homogeneous mixtures.

When the diluent other than water was used (aqueous solution of NaCl or $Mg(ClO_4)_2$), the situation was further complicated. For such mixtures, miscibility of 4-component mixtures (HEMA/DEGDMA/water/additive) was checked to ensure that polymerization started in the initially homogeneous solution.

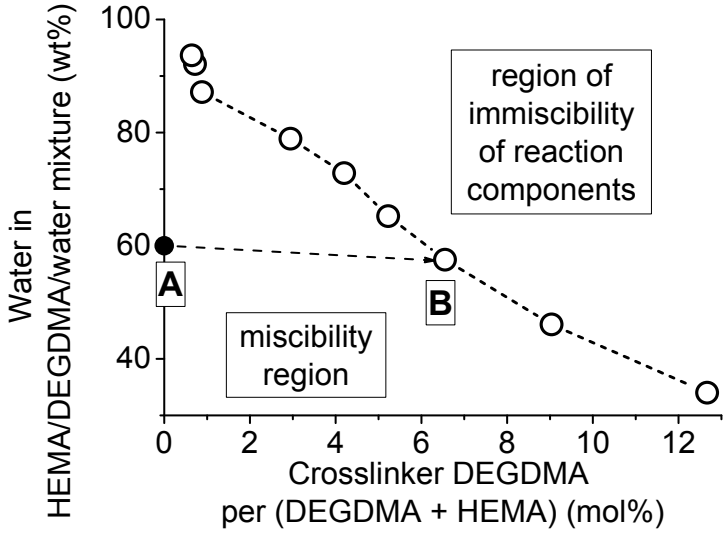

Figure 4.2 *Miscibility of HEMA-DEGDMA-water mixtures (without initiator) at 25 °C. Point A shows a starting mixture of HEMA and water. As the addition of DEGDMA decreased water concentration, the actual water concentration at the cloud point (point B) was recalculated.*

Gelation and phase separation during polymerization course. During crosslinking polymerization, the initially low viscous mixtures lose fluidity at certain reaction time, corresponding to gel point, i.e. or critical gel conversion. Depending on the mixture composition, the phase separation can also occur at some point, corresponding to critical phase separation conversion. All samples were in the rubbery state during polymerization (non-glassy).

Gelation times (determined as time at which the sample loses fluidity during polymerization at room temperature) and phase separation times (appearance of visually noticeable turbidity, cloud point) for gels prepared with water as diluent are collected in Figs. 4.3 and 4.4.

Although the time of fluidity loss (Fig 4.3a) is only an approximation of gelation time, it revealed some important trends. It sharply decreased with adding more crosslinker in the range of 0-2 mol% of DEGDMA, whereas in the range 2-5

mol% of DEGDMA its effect on the gel point time is minor. At initial water content IWC=40-60 wt%, amount of water had only negligible effect on the gel point time, further increase of water concentration at preparation noticeably delayed the gelation.

The cloud point time (Fig 4.3b) decreased with dilution at IWC = 40-60 wt% of water at preparation, and at constant dilution more crosslinker DEGDMA added accelerated phase separation. With 70-80 wt% of water at preparation, phase separation occurred very fast, and crosslinker effect was negligible.

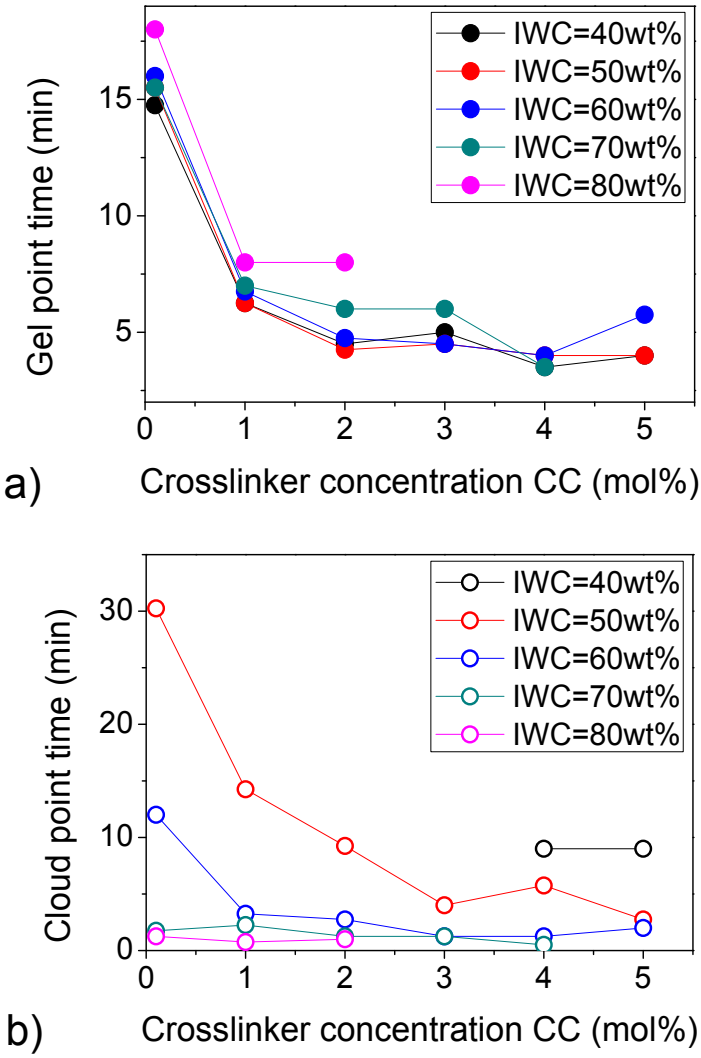

Figure 4.3 *Gelation time (a) and phase separation time (b) determined during polymerization of HEMA/DEGDMA/water mixtures.*

Comparison of the gel point time and phase separation time for mixtures of the same compositions showed that at relatively low dilution (40 wt% of water at preparation) and crosslinker concentration (<5 mol% of DEGDMA) phase separation did not occur till polymerization was over (Fig. 4.4a). Increase of initial dilution (to

IWC = 50 wt% of water at preparation) and/or crosslinker concentration led to phase separation observed after or close to the gel point (Fig. 4.4a), more diluent and/or crosslinker led to even earlier phase separation, before formation of the bulk gel (Fig. 4.4b). These interplays between gel and phase separation times led to diverse morphological effects.

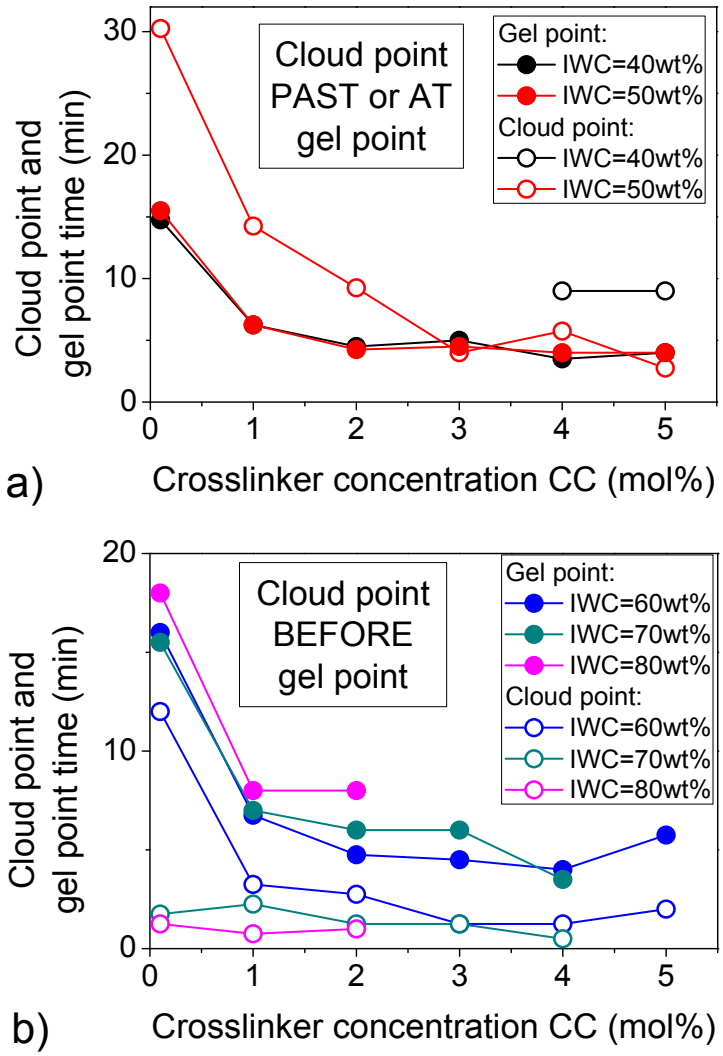

Figure 4.4 *Gelation time and phase separation time determined during polymerization of HEMA/DEGDMA/water mixtures. Initial water content: (a) 40-50 wt%, (b) 60-80 wt%.*

Reaction rate of polymerization. The gels were prepared using chain polymerization initiated by reducing-oxidizing system (ammonium persulfate, initiator and N,N,N',N'-tetramethylethylenediamine, promoter, enabling initiation with a reasonable rate at room temperature). To estimate reaction time needed to

reach complete monomers conversion in all experiments, the reaction rate was measured for the system that showed the slowest gel point time (Fig. 4.3a) – a mixture containing 80 wt% of water and 20 wt% of monomers, 0.1 mol% of them being crosslinker DEGDMA – i.e. 80/0.1 sample. Conversion of C=C bonds of the monomers was followed with IR ATR technique, Fig. 4.5.

From comparison of the initial and final spectra, it followed that polymerization induced a shift of the monomers C=O bands to lower wavenumber, and to complete disappearance of the C=C bands (both C=O and C=C bands of HEMA and DEGDMA were not distinguishable). For the 80/0.1 mixture, the C=C bonds conversion reached nearly 100% within 40 minutes. As the preparation procedure used in this work involved overnight polymerization, it was assumed that full conversion of monomers was reached for all the samples studied. This was directly confirmed by IR ATR studies of several representative final gels – in none of them C=C band was found.

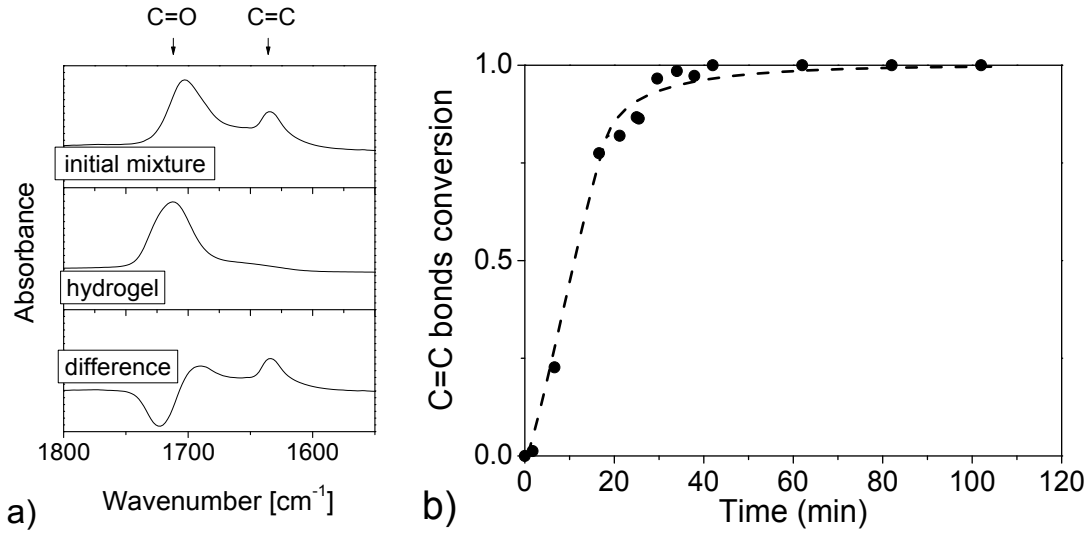

Figure 4.5 *IR spectra of HEMA/DEGDMA/water mixture, final swollen hydrogel, and their difference spectra (a). Conversion of C=C bonds in time followed by IR (b). Sample composition was 80/0.1.*

Extraction of sol. The completeness of reaction and extent of network development in these systems can be seen from the sol fraction. Results of solids extraction with water revealed (Fig. 4.6) that only at highest dilution part of solids from the final gel could be extracted (7-8 wt%) whereas for other compositions no more than 3 wt% of the solids were extracted. Because sol content is a function of

conversion, and reaches zero at full conversion, it was concluded, that with acceptable accuracy the composition of polymer corresponded to composition of monomers mixture, and the attained conversion was reasonably high. This also meant that approximately all crosslinker was incorporated into the gel.

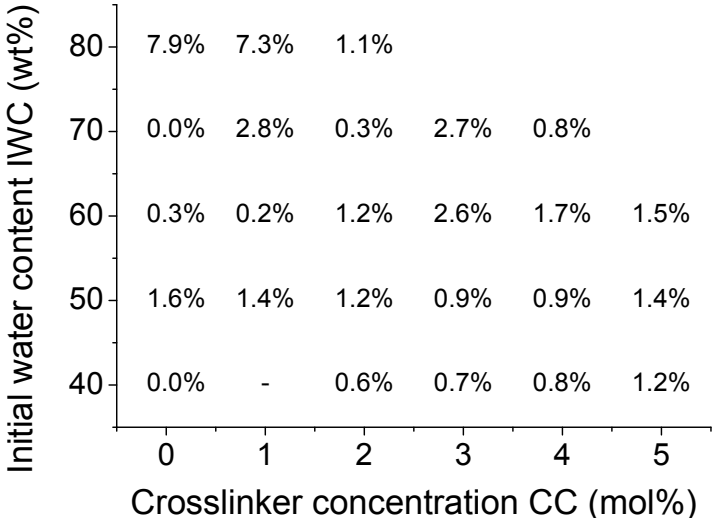

Figure 4.6 *Sol fraction in the hydrogels prepared from HEMA/DEGDMA/water mixtures, determined by extraction with water.*

It can be summarized that the preparation procedure used in this work allowed for complete conversion of the monomers during polymerization. That the initial mixtures were always clear, suggested that the phase separation started only due to polymerization, and possible pre-polymerization effects were eliminated.

4.2 Hydrogels morphology

The morphology of gels in swollen state was studied by means of scanning electron microscopy and light microscopy (LM). The low-vacuum cryoSEM method (SEM) and environmental scanning electron microscopy (ESEM) were used in parallel. Typically, SEM gave higher-quality pictures with more details (SEM can achieve resolution of about 0.4-20 nm in the ideal observation conditions), but the sample was flash frozen in liquid nitrogen prior to taking scan at -10 °C, which might led to artifacts in gels due to solvent crystallization. During ESEM procedure, the swollen sample was not deeply frozen – it was kept at 2 °C at observation state – and thus its structure could be detected with higher fidelity, at the cost of lower resolution. However, the result from ESEM imaging depended on observation conditions, namely water vapor saturation above the sample that was controlled by reducing the pressure (see these effects in Fig 4.9).

The great advantage of light microscopy is the possibility to observe samples in their native swollen state without any temperature treatment. Thus, the images from LM can help to unequivocally decide whether some structures seen in SEM/ESEM scans are present in the sample from.

Diluent and crosslinker concentration effects. The content (and type) of diluent at preparation and crosslinker concentration were the factors to alter the gel morphology. After gelation, the sol fraction and low-molecular weight species were extracted with water, and samples were swollen typically in water to equilibrium.

Water-swollen gels differ in appearance which suggests varying morphology. With results from approximately 100 samples prepared at different conditions, it was possible to divide the studied hydrogels into several groups showing characteristic morphology types, and create maps of morphologies, like the one for hydrogels prepared with water as diluent shown in Fig. 4.7.

Typical morphology types of polyHEMA hydrogels observed in this work are as follows. Those hereafter called **"homogeneous gels**" were fully transparent with no heterogeneities detectable either visually, by light or electron microscopy. If the gel was not optically clear, it contained heterogeneities on the order of visible light wavelength (~100 nm). In electron microscope, non-transparent gels revealed several types of morphology. Non-transparent swollen gels that only revealed a single phase in SEM or ESEM (that is, the heterogeneities were below electron microscopy

resolution) are referred to as **"intermediate"**[1]. Of the gels with heterogeneities visualized by ESEM or SEM, those showing relatively large (micrometer-range) partially connected droplets of swelling medium surrounded by walls of swollen polymer, were assigned to gels of "**interlocking, bicontinuous"** morphology. The group of non-transparent gels with communicating pores surrounding well-defined fused spherical particles of swollen polymer constituted a category of "**fused particles type**" or "**particulate gels**".

From the map of gel morphologies of hydrogels prepared in water (Fig. 4.7), morphology of the final material changed from homogeneous through intermediate and bicontinuous to particulate, as either initial water concentration or crosslinker concentration were increased.

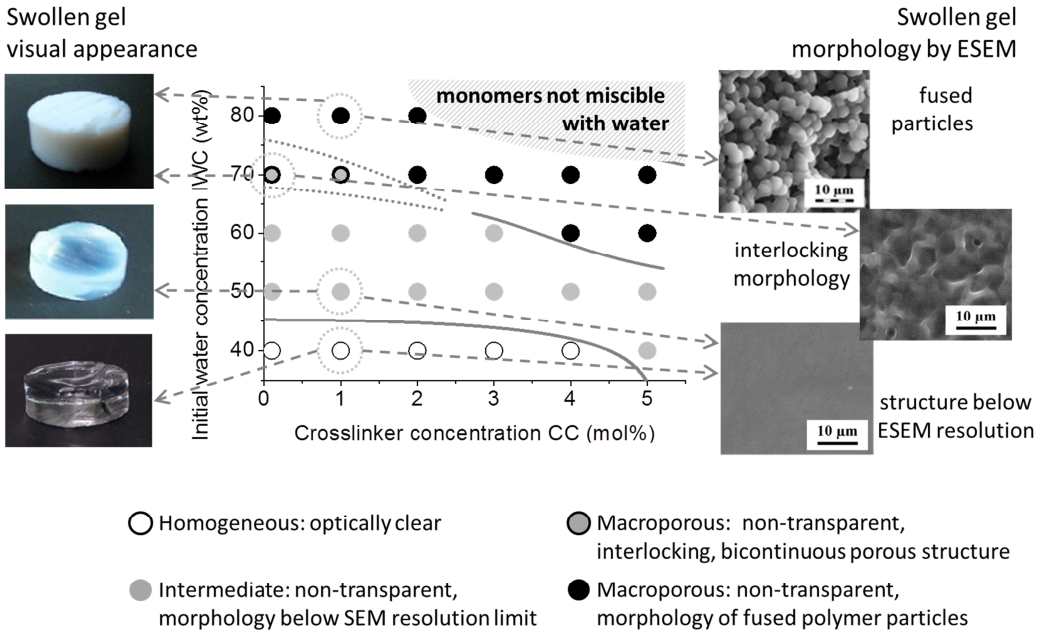

Figure 4.7 *Appearance and morphology of gels prepared with water as diluent, and swollen in water to equilibrium. Each point corresponds to a hydrogel prepared at certain initial dilution and crosslinker concentration.*

[1] The internal structure of intermediate gels is questionable: they may contain either droplets of swelling medium too small to be visualized under a microscope, or areas with different polymer concentration. The issue of intermediate gels morphology will be addressed later taking into account results from supplementary techniques (differential scanning calorimetry, shear rheometry).

Detailed studies of macroporous samples (initial water content = 70 wt% and 80 wt%) revealed that increasing crosslinker concentration generally led to smaller particles forming the hydrogel (Fig. 4.8).

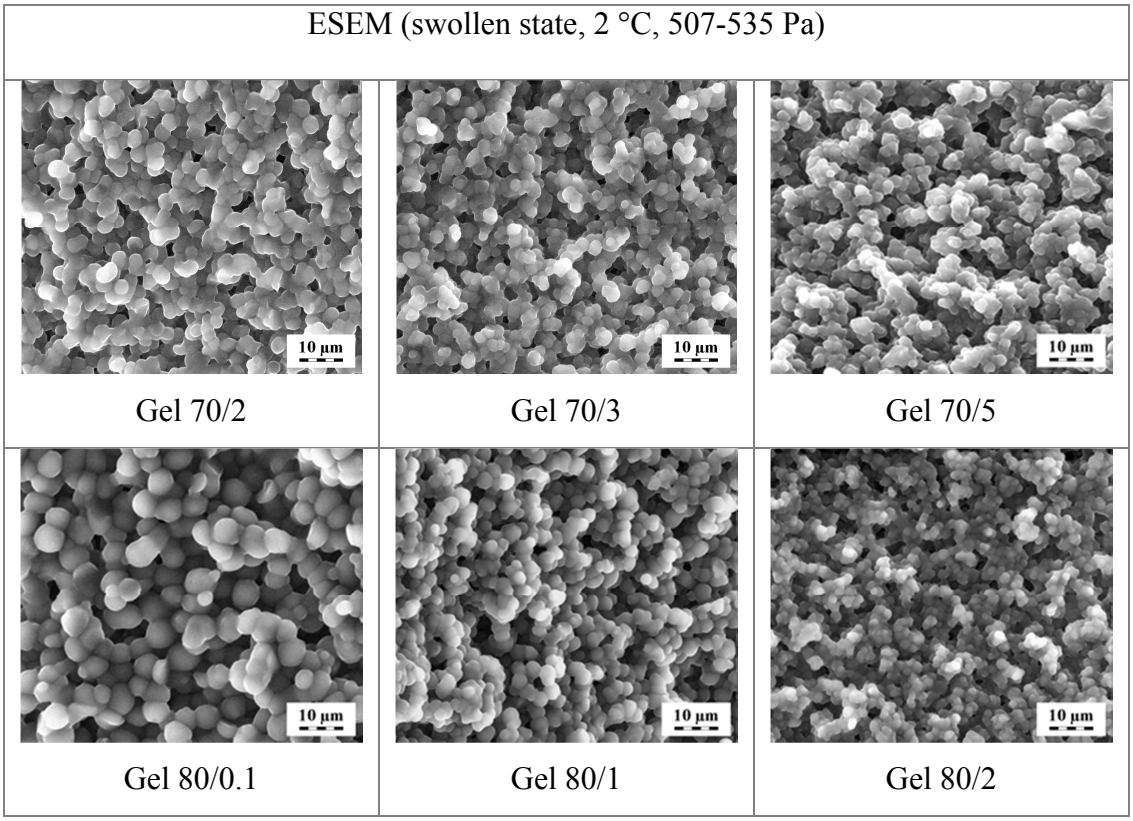

Figure 4.8 *ESEM pictures showing morphology of hydrogels prepared with 70 wt% and 80 wt% of water as diluent and various crosslinker concentrations, observed at equilibrium swollen state in water.*

In Fig 4.9 the effect of humidity controlled by chamber pressure during ESEM scanning on the revealed morphology is demonstrated (for hydrogel 60/5). This gel appeared as white (phase-separated) when swollen in water at laboratory conditions. However, it revealed completely homogeneous structure when examined by ESEM at 2ºC and chamber pressure above 520 Pa. At 440 Pa some heterogeneities of undefined type appeared in the ESEM image, and at 340 Pa or below typical macroporous morphology was observed. Thus, to achieve accurate results, the appropriate range of conditions must be found.

Gel 60/5, ESEM (swollen state, 2°C)		
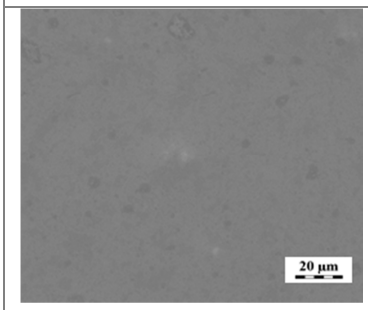	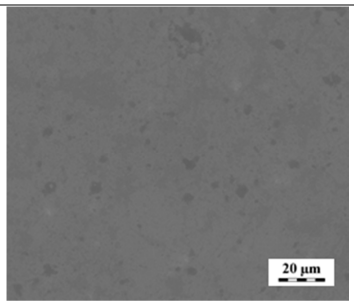	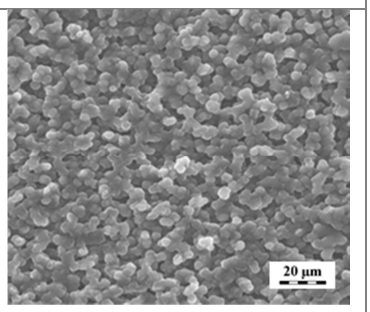
520 Pa	440 Pa	340 Pa

Figure 4.9 *ESEM images of the 60/5 hydrogel swollen in water. Chamber pressure is shown under corresponding pictures.*

Solvating power of diluent at gel preparation: effect on morphology. Thermodynamic quality of the diluent affects significantly the morphology of produced gel samples through miscibility changes. The effect of swelling medium solvating power was studied in detail in [**34**], where authors analyzed swelling of polyHEMA homogeneous gels in aqueous solutions of various inorganic salts. Ionic environment can cause „salting-in“ or „salting-out“ effects depending on the ions type. Salting-out solutions decreased the swelling medium solvating power, thus reducing swelling of gels; vice versa, salting-in compounds increased swelling of gels due to improved solvating power of the medium. Similar approach was used in [**70**] to increase porosity of hydrogels prepared for use as cell supports, by addition of a salting-out additive.

In this work, two ionic additives were used: salting-out sodium chloride and salting-in magnesium perchlorate. Increasing the solvating power of diluent by introducing $Mg(ClO_4)_2$ suppressed the phase separation, and homogeneous hydrogels could be formed at compositions corresponding to phase separation region in pure water (Fig. 4.10). Vice versa, introducing NaCl to polymerizing mixture enhanced the phase separation, and heterogeneous hydrogels were formed at compositions leading to homogeneous gels in pure water (Fig. 4.11).

Gel composition 70/2; SEM (frozen water-swollen sample)	
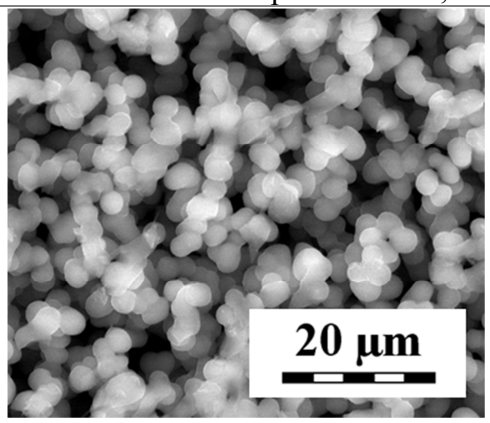 Preparation diluent: water	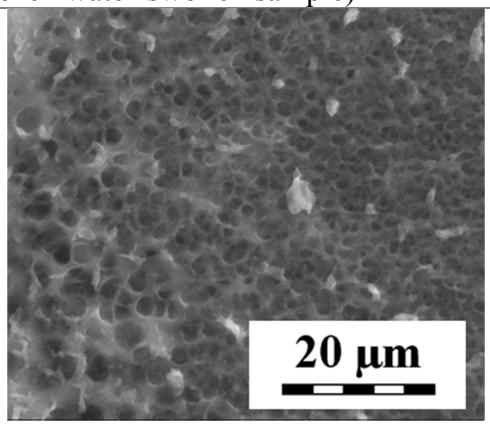 Preparation diluent: 0.05 M $Mg(ClO_4)_2$ in water
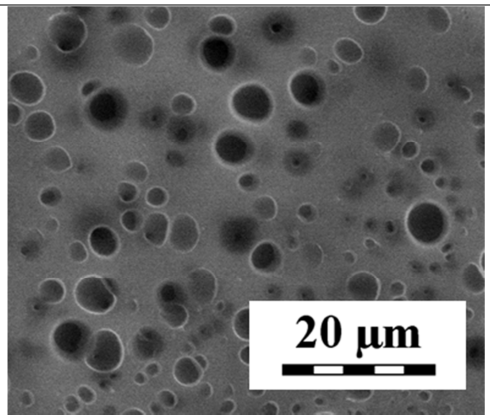 Preparation diluent: 0.2 M $Mg(ClO_4)_2$ in water	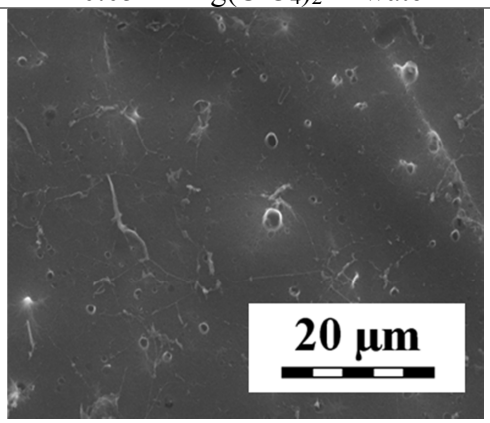 Preparation diluent: 0.3 M $Mg(ClO_4)_2$ in water

Figure 4.10 *Morphology by SEM of 70/2 gels prepared with aqueous $Mg(ClO_4)_2$ of varied concentration as diluent, and swollen in water.*

Gel composition: 40/1		
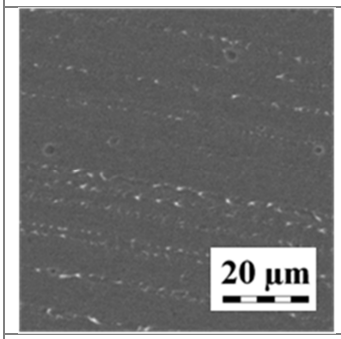	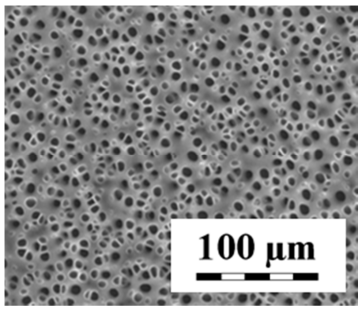	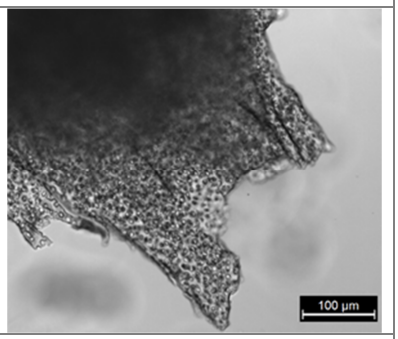
SEM (frozen water-swollen sample)		Light microscopy (water-swollen sample)
Preparation diluent: water	Preparation diluent: 0.6 M NaCl in water	

Figure 4.11 *SEM and light microscopy pictures of 40/1 hydrogels prepared with water or 0.6 M aqueous NaCl as diluent, and swollen in water.*

To observe the salting-out effect of NaCl on the macroporous structure, gels prepared with 70 wt% of water or aqueous NaCl, and 2 mol% of the crosslinker were studied (Fig. 4.12). Even with pure water as diluent, the 70/2 hydrogel consisted of relatively small, 1-3 μm in diameter, fused spherical particles. As expected, all hydrogels prepared at this composition with aqueous NaCl after reswelling in water were particulate. With addition of NaCl to 70/2 mixture, a fraction of smaller particles appeared, that likely allowed for higher connectivity of the swollen polymer phase.

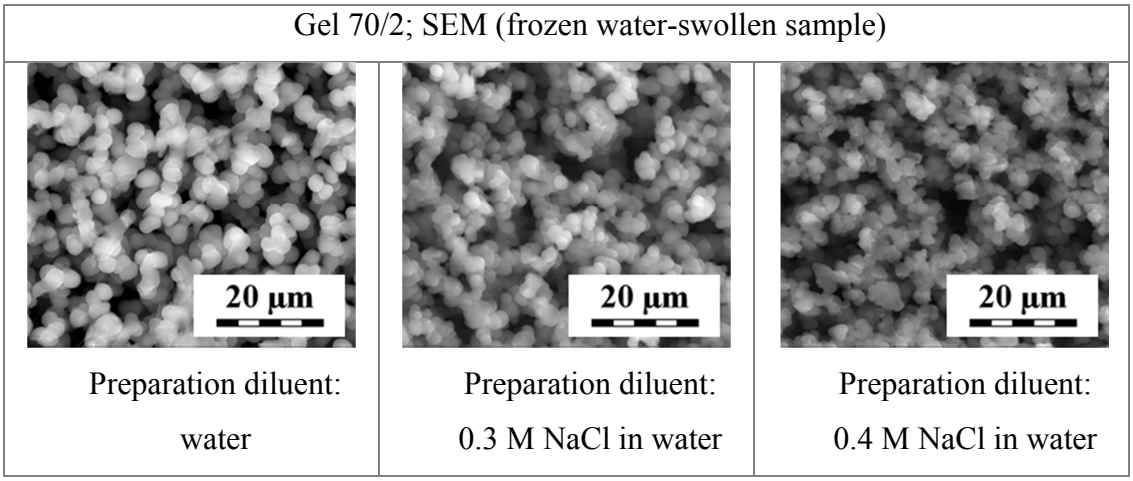

Figure 4.12 *Morphology by SEM of 70/2 gels prepared with aqueous NaCl of varied concentration as diluent, and swollen in water.*

Fine increase of NaCl concentration in the polymerizing mixtures containing 60 wt% of diluent and 1 mol% of the crosslinker allowed observation of transitional situations, visualizing structural outcome of stepwise enhancing phase separation (Fig. 4.13). With water as diluent, no heterogeneities are observed in SEM picture of a visually non-transparent 60/1 sample (Fig. 4.13a), thus, 60/1 is a typical "**intermediate**" sample. With 0.2 M of NaCl in the diluent at preparation, phase-separated diluent droplets appeared visible in SEM (Fig. 4.13b), and as NaCl concentration in the diluent increased to 0.4-0.425 M, the morphology type changed to **bicontinuous** (Fig. 4.13c-d). With even more NaCl in the diluent (0.45-0.5 M, Fig. 4.13e-g), the material morphology was still bicontinuous but the swollen polymer walls became thicker and porous, and they coexisted with spherical polymer particles fused to their edges. With 0.525 M (or more) NaCl in the diluent (Fig. 4.13h-i), the material morphology changed to **particulate**.

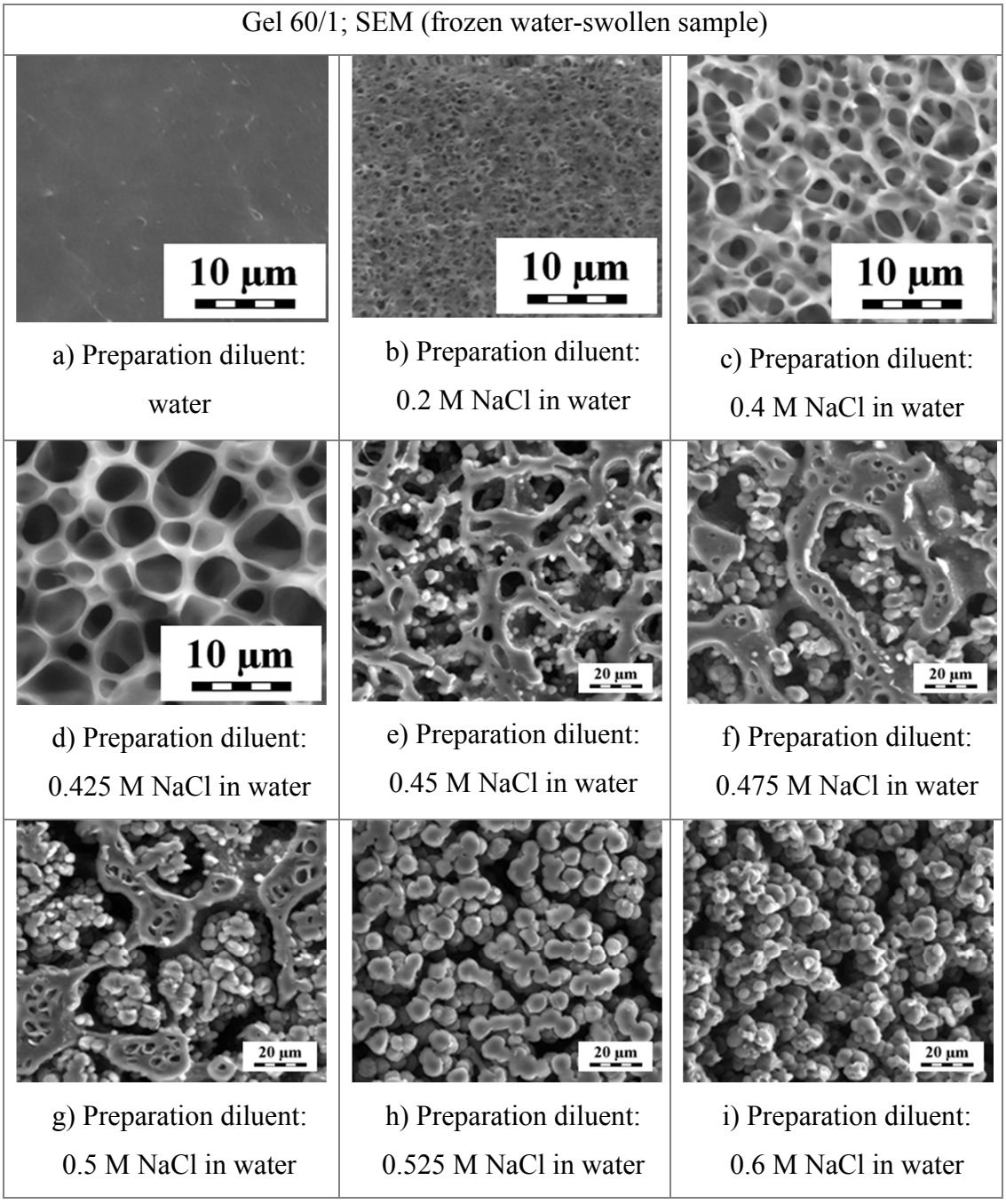

Figure 4.13 *Morphology by SEM of 60/1 hydrogel samples prepared with aqueous NaCl of varied concentration as diluent, and reswollen in water.*

Overall influence of the solvating power of diluent used for gel preparation on the final product morphology is summarized in Fig. 4.14-4.15.

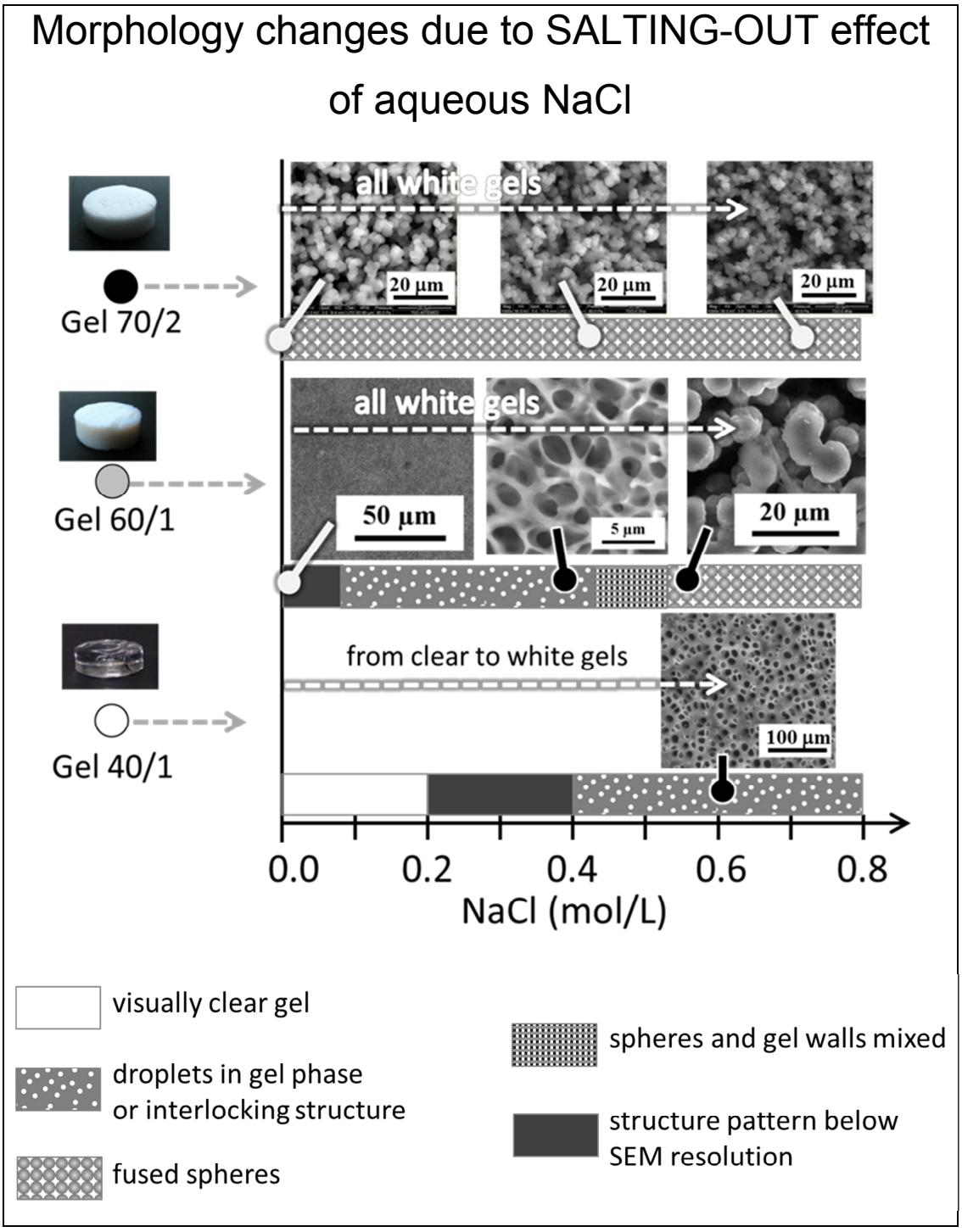

Figure 4.14 *Scheme of gel morphologies (SEM) prepared in diluent of decreasing solvating power, and reswollen in water. The schematic is self-explanatory.*

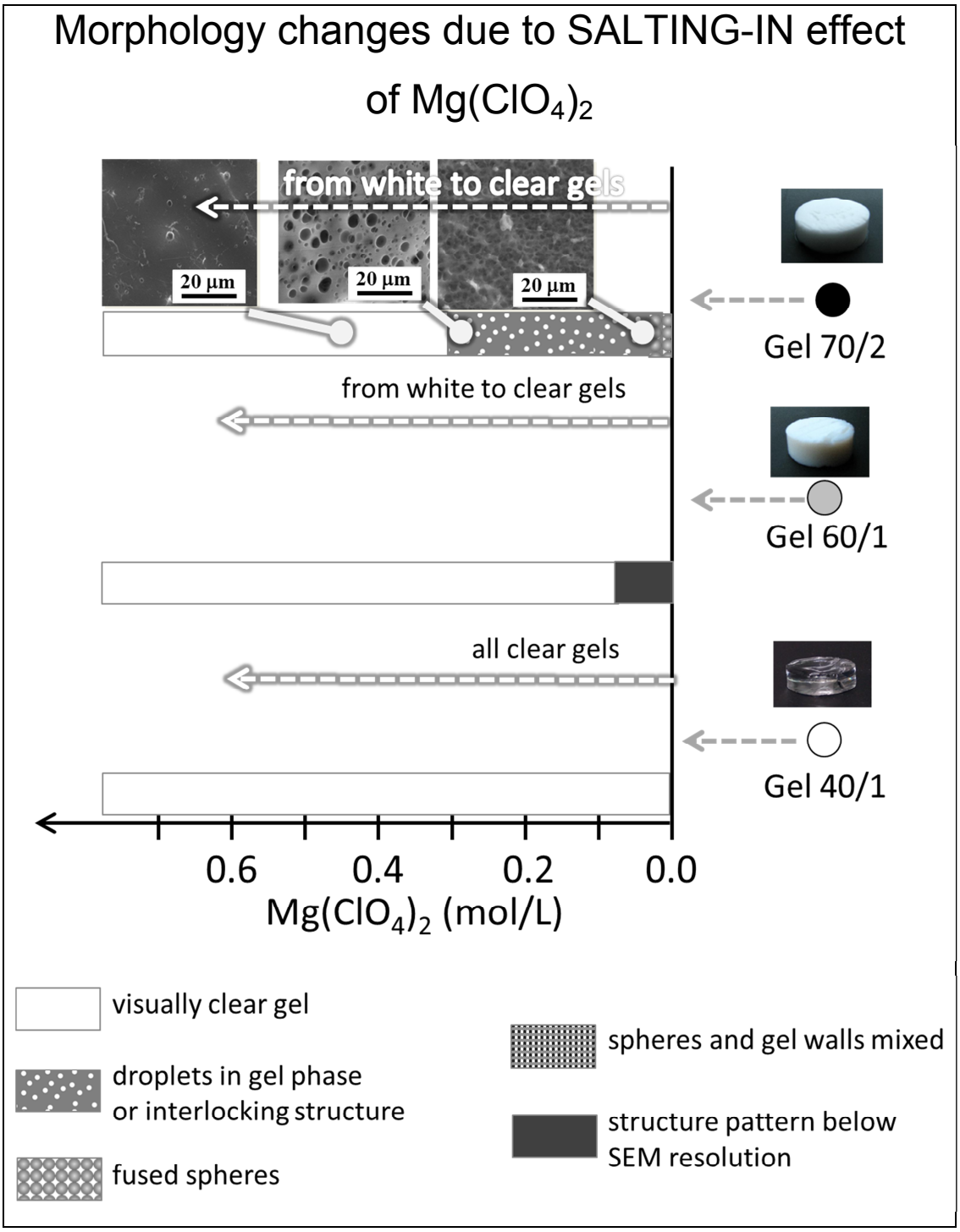

Figure 4.15 *Scheme of gel morphologies (SEM) prepared in diluent of increasing solvating power, and reswollen in water. The schematic is self-explanatory.*

4.3 Swelling of gels

Hydrogels typically serve in application in their highly swollen state. Especially in case of polyHEMA certain content of swelling liquid is necessary for the material to attain its rubbery (soft) state – as dry polyHEMA at room temperature appears in its vitrified state[2]. When these polymers are swollen in water to equilibrium, their glassy region moves well below the room temperature depending on exact polymer preparation conditions. This issue is addressed in discussion of swollen gels T_g measurement (Section 4.4.2, p. 85-86).

The quantitative data on swelling of model gels served in case of homogenous gels for estimating their crosslink density (concentration of elastically active network chains, ν_e). In case of heterogeneous gels, the total swelling included solvent in swollen matrix phase and solvent in voids. Reasoning based on the volume and weight balance was performed in order to estimate the volume fraction of (macro)pores in swollen gel which then was applied to correct the measured modulus of swollen gels [**113**]. Swelling in a very good solvent for polyHEMA, e.g. dimethylsulfoxide (Tab. 4.2) suppressed the physical interactions acting in the hydrophobic associates, and thus the gel network was hold together only by chemical crosslinks (Section 4.4.1, p. 78-80). The equilibrium swelling of gels was defined as weight of swelling medium per weight of the swollen gel, in g/g.

Swelling in water of gels prepared with water as diluent. A special feature of polyHEMA-water system is that uncrosslinked polyHEMA and polyHEMA homogeneous crosslinked gels do not swell to more than equilibrium water content ≈0.35-0.40 g water per g of swollen hydrogel (slightly depending on the crosslink density). At the initial dilutions lower than 40 wt% of water at preparation, the hydrogels equilibrium swelling was practically independent of initial dilution. Above this limit, the equilibrium swelling of final gel grew with increasing initial dilution (Fig. 4.16) due to phase separation.

[2] Tg of dry polyHEMA networks prepared with 1 mol% of crosslinker DEGDMA was determined in this work by DSC measurements: 97 to 117 °C.

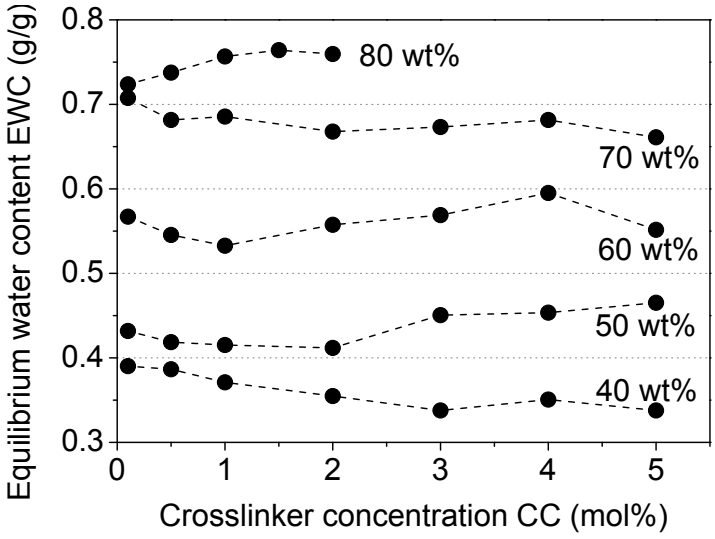

Figure 4.16 *Equilibrium water content in swollen hydrogels as a function of crosslinker concentration. Numbers at curves show the corresponding initial water content (wt%). Plotted data are given in numbers in Tab. 4.1.*

Table 4.1 *Equilibrium water content in swollen hydrogels prepared with water as diluent. The same data plotted in Fig. 4.16.*

Equilibrium water content, g water per g of swollen hydrogel							
Initial water content, IWC [wt%]	Crosslinker concentration, mol%						
	0.1	0.5	1	2	3	4	5
40	0.390	0.387	0.371	0.355	0.338	0.351	0.338
50	0.432	0.419	0.415	0.412	0.451	0.454	0.465
60	0.567	0.545	0.533	0.558	0.569	0.595	0.552
70	0.708	0.682	0.686	0.668	0.673	0.682	0.661
80	0.724	0.738	0.757	0.760	-	-	-

The equilibrium swelling EWC as a function of crosslinker concentration CC (Fig. 4.16) showed a complex trend revealing EWC dependence on sample structure. For instance, for gels prepared at initial dilution IWC = 60 wt% water, as CC increased from 0.1 to 1 mol%, EWC decreased due to increasing of elastically active crosslinks density. Then, with CC increasing from 1 to 4 mol% of the crosslinker, EWC increased. This was due to appearance and progress of phase separation. Finally, at CC = 4-5 mol%, EWC decreased again – due to increasing of crosslink density in particles of phase-separated gel or due to sparser packing of particles.

For different levels of IWC this trend could be observed only partially. For example, within series with IWC = 40-50 wt% no decrease of EWC in phase-separated materials was observed because relevant CC was not reached. Increase of EWC with increasing CC for particulate hydrogels with IWC = 80 wt% might be accounted for sparser packing of particles (Fig. 4.8). The same trend of swelling was observed in [**65**].

Alternatively, swelling data could be interpreted if replotted as the reciprocal volume fraction of polymer in swollen hydrogel, $1/\phi_2$, *vs* $1/\phi_2^0$, the reciprocal volume fraction of the monomer in the initial mixture (Fig. 4.17). The density of dry polymer was used in calculations instead of monomer density to account for contraction of the monomer during polymerization.

In this plot, the dotted 1-1 line represents the situation of equal initial and equilibrium water contents, that is, absence of any volume changes during polymerization and sol fraction extraction. Data at the 1-1 line would mean that the excess water in heterogeneous gel was separated only by microsyneresis (scheme in Fig. 1.1, p. 13). In the absence of sol (this was true for the discussed systems, Fig. 4.6), the data points below this line ($1/\phi_2 < 1/\phi_2^0$) mean shrinkage of the samples during or after polymerization and expulsion of a part of initially present diluent out of the sample – i.e., combined micro- and macrosyneresis. Data above the straight line would mean swelling to a volume higher than was the initial sum of volumes[3].

Inspection of the plots in Fig. 4.17 shows that for the studied systems microsyneresis was accompanied by weak macrosyneresis, which got stronger at highest dilution (initial water content 80 wt%). At the same time, crosslinker concentration had minor effect of the macrosyneresis.

[3] This could happen when no phase separation occurred, or water in the separated liquid phase – an aqueous solution – had activity lower than pure water (other additives used). Also, such data could point to a seemingly paradoxical situation when the volume of the gel swollen in the diluent which had been expelled from the sample (water) was larger after the gel had been made free of the constraints of the mold. Such situation (inverse syneresis) might arise when the gel phase imbibed during polymerization monomers from the liquid phase and expanded [**114**]. These special cases were not observed for the series discussed in this section.

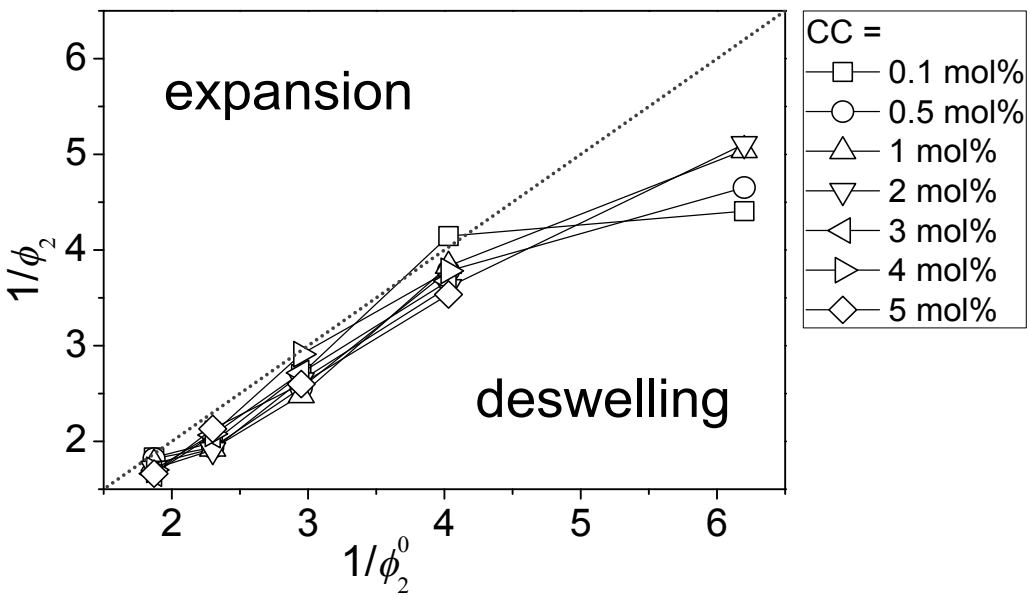

Figure 4.17 *Equilibrium volume of swollen gel per volume of the dry polymer vs. the reciprocal volume fraction of the monomer in the initial mixture corrected for polymerization contraction.*

Swelling in water of gels prepared with diluents of varied solvating power. If thermodynamic quality of the diluent at preparation was varied, the induced changes in the final gel morphology resulted in corresponding changes of the hydrogels swelling capacity.

For example, adding salting-out NaCl to the 40/1 mixture (giving homogeneous gel when water was used as diluent) led to promoting phase separation (Fig. 4.11) and the increase of equilibrium swelling in water (Fig. 4.18). Vice versa, adding salting-in $Mg(ClO_4)_2$ to the 70/2 mixture (macroporous gel when water was used as diluent) led to suppressing phase separation (Fig. 4.10) and the decrease of equilibrium swelling in water (Fig. 4.18).

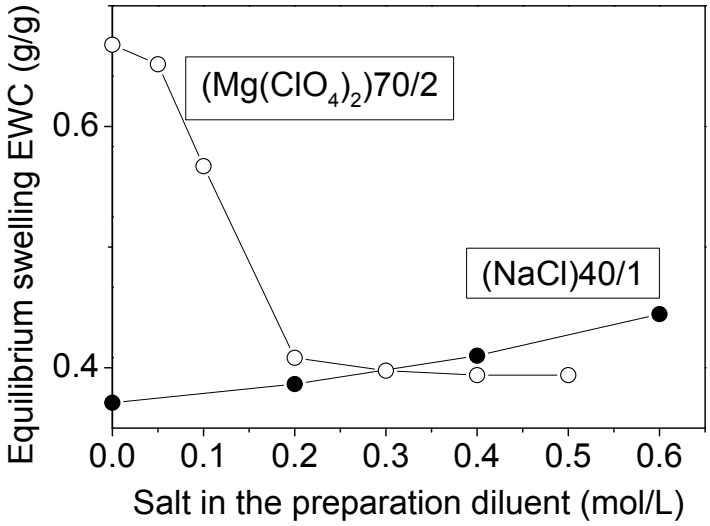

Figure 4.18 *Equilibrium swelling of hydrogels in water. Sample compositions: 40/1 prepared with aqueous NaCl as diluent, and 70/2 prepared with aqueous $Mg(ClO_4)_2$ as diluent.*

For a series of intermediate morphologies, transitional between homogeneous and macroporous ones (Fig. 4.13), prepared by adding NaCl to the polymerizing mixtures of the 60/1 composition, an unusual trend of equilibrium swelling was observed (Fig. 4.19). Below critical concentration of 0.4 M NaCl in the diluent, EWC grew with enhancing phase separation, but further increase of NaCl concentration led to lower swelling of the hydrogel. This result is in line with the samples morphology established by SEM. Indeed, at 0-0.4 M NaCl in diluent developing porosity led to increase of material swelling, further drop down was ascribed to more compact morphology of the interlocking bicontinuous type.

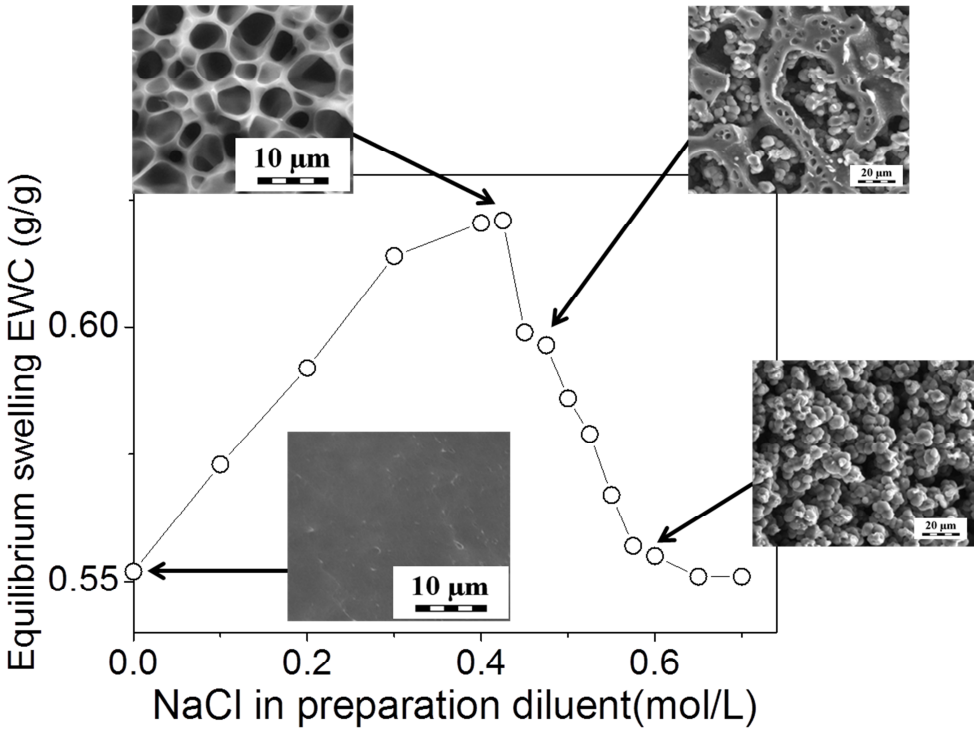

Figure 4.19 *Equilibrium swelling in water. Sample composition 60/1 prepared with aqueous NaCl as diluent. Inserts illustrate morphology type of final gel at corresponding diluent quality.*

Swelling in solvents other than water. When hydrogels were reswollen in solvents other than water, the equilibrium swelling degree changed according to swelling medium thermodynamic quality. For example, in dimethylsulfoxide DMSO (better solvent for polyHEMA than water) the corresponding gels swelled more, while addition of NaCl worsened thermodynamic quality of the swelling medium, and the gels swelled less. Data on the selected samples swelling in different media is collected in Tab. 4.2.

Table 4.2 *Swelling of selected gels prepared with water as diluent: re-swollen to equilibrium in water, dimethylsulfoxide DMSO and 3M aqueous NaCl.*

Sample composition	Equilibrium swelling in various media [g/g], 25 °C		
	water	DMSO	3 M aqueous NaCl
40/1	0.37	0.83	0.22
50/1	0.42	0.85	
60/1	0.53	0.88	0.39
70/1	0.69	0.92	
80/1	0.76	0.95	0.71

To conclude, the swelling ability of covalently crosslinked polyHEMA gels depends on a number of factors. First, the thermodynamic quality of the swelling medium determines the swelling capacity, influencing both the equilibrium swelling of the gel matrix, and the overall porosity (in case of porous samples). Then, increasing the crosslink density of the network generally decreases the amount of solvent absorbed at equilibrium. Finally, appearance and development of porous morphology increases the swelling capacity of polyHEMA due to fraction of swelling medium filling the pores.

As for porous crosslinked gels the factors of crosslink density and porosity acted simultaneously, a simple experimental feature of equilibrium swelling was not easy to be interpreted, and it should be analyzed in combination with other data, for example, mechanical behavior of the swollen gel.

4.4 Dynamic mechanical responses of gels

In this chapter, at first, the general precautions taken to determine dynamic shear mechanical properties of soft swollen gels will be discussed. Then, typical experimental curves will be presented to illustrate representative behavior of different swollen gel samples. Finally, the mechanical responses of gels will be discussed in connection with preparation and observation conditions.

General precautions during rheometry of swollen gels.

- The samples were examined in their fully relaxed state. This implied equilibration of the sample after loading to the measurement cell, after each change the measuring gap between rheometer plates, and after each change of temperature. To ensure this, the mechanical response of a sample to forced stress oscillations at 1 Hz was tracked in time under new conditions, and the measurement was not started before this preliminary test showed stationary properties for at least 20 minutes.
- The samples were examined in their equilibrium swollen state – fully immersed in the swelling medium in specially manufactures solvent shallow cup. Additional experiments proved that the additional friction of rheometer parts in the swelling medium was negligible, and did not affect the results.
- The shear properties were measured in the linear viscoelastic region as determined in amplitude sweep preliminary test.
- The measurement gap was selected so that the sample was in full contact with the rheometer parts, but the structure change due to compression was negligible (Section 10.1).

At low frequency end of an isothermal measurement, there was practically no frequency limit besides total experiment time (minimum frequency of 0.05 Hz was found reasonable). At high frequency end, the limit was set by resonance between the measuring system and the sample (depending on the sample dimensions and stiffness, typically 10-80 Hz). A special hardware attachment, Piezoelectric Rotary Vibrator (PRV) enabled direct measurement of viscoelastic response at higher frequency, practically up to 2000 Hz. However, this technique was limitedly applied. The sample thickness required for successful PRV measurement was 100-200 μm, comparable to the range of pores size in the studied gels.

In order to extend the frequency limits, a semi-empirical time-temperature superposition method was applied. Results presented in Section 10.2 confirm that in

the case of swollen polyHEMA gels, whose swelling degree showed only slight temperature dependence, this method gave reliable results and enabled to access the viscoelastic properties of the gels at 10^{-3} to 10^{3} Hz.

Dynamic mechanical analysis of swollen gels. Representative examples. A typical example of the dynamic mechanical spectra for a homogeneous covalently crosslinked polyHEMA gel swollen in water to equilibrium is presented in Fig. 4.20.

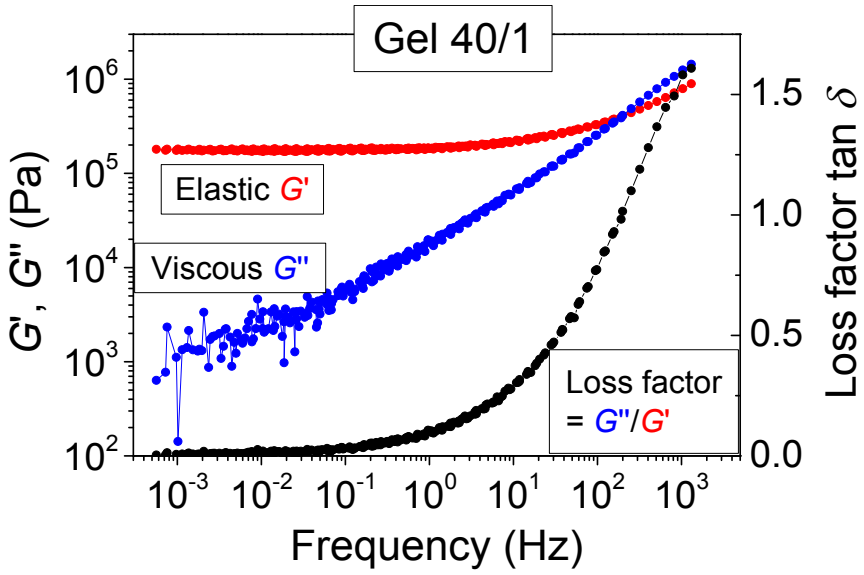

Figure 4.20 *Elastic and viscous shear moduli, and loss factor tan δ for water-swollen homogeneous gel 40/1. Equilibrium swelling of the sample was 0.371.*

For the 40/1 hydrogel, a traditional material in soft contact lenses applications, at frequency below 1 Hz, elastic shear modulus *G*' was practically independent of frequency, and was 1-2 orders of magnitude higher than the viscous shear modulus *G*''. In this range of frequencies, the 40/1 hydrogel is in its rubbery state. The loss factor was close to zero and frequency-independent, typically for chemically crosslinked polymer network. The *G*' value at such conditions is close to the equilibrium one, and may be used for calculation of the elastically active network chains concentration (crosslink density). Also, elastic modulus at the elasticity plateau (180 kPa for the 40/1 hydrogel) characterizes the overall gel strength.

G' started growing with frequency above 1 Hz, marking the onset of the main transition region (also referred to as α-relaxation or mechanical vitrification). *G*'' grew even faster, and at certain frequency (200 Hz) a crossover of elastic and viscous

moduli occurred. Increased losses (also documented by the loss factor tan δ = G''/G') are typical of samples entering the transition region.

Depending on the sample preparation conditions, and thus on its morphology, and/or observation conditions, the dynamic mechanical spectra significantly changed. These effects, discussed in detail in the subsequent sections, are documented in Figs. 4.21-4.24.

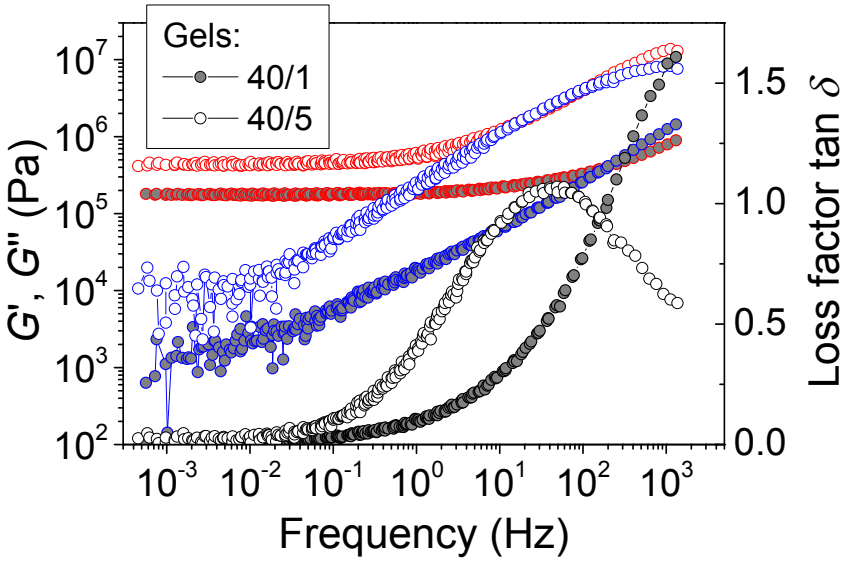

Figure 4.21 *Elastic and viscous shear moduli, and loss factor tan δ for water-swollen homogeneous gel 40/1 and water-swollen intermediate gel 40/5. Equilibrium swelling was: 0.371 (40/1) and 0.338 (40/5).*

Increase of the crosslinker concentration (Fig. 4.21) led to formation of stronger hydrogel, due to more of elastically active network chains per sample volume, this was reflected in the increase of shear moduli of the 40/5 hydrogel (430 kPa at 0.1 Hz) as compared to the 40/1 (180 kPa at 0.1 Hz). Moreover, as network chains of the 40/5 were shorter and more rigid, this sample showed onset of the glassy region st lower frequency (the crossover frequency was reduced to 10 Hz for the 40/5 sample as compared with 200 Hz for the 40/1).

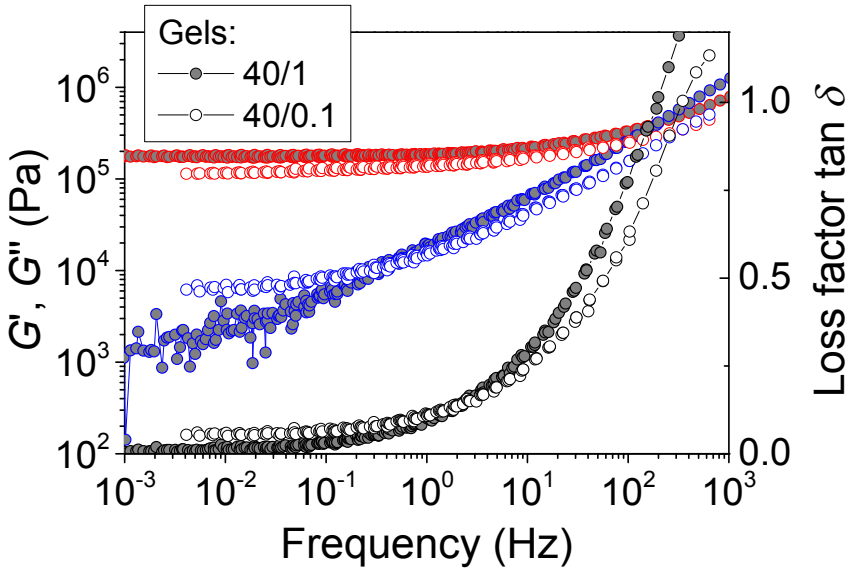

Figure 4.22 *Elastic and viscous shear moduli, and loss factor tan δ for water-swollen homogeneous gels 40/1 and 40/0.1. Equilibrium swelling was: 0.371 (40/1) and 0.390 (40/0.1).*

Decrease of the crosslinker concentration (viscoelastic responses of samples 40/1 and 40/0.1 are compared in Fig. 4.22) led to slight decrease of the elastic modulus due to less of elastically active chains per sample volume (115 kPa *vs* 180 kPa). Viscous modulus of the 40/0.1 hydrogel as a function of frequency showed a complex trend: with decreasing crosslinker content, *G*'' increased at lower frequency range (below 0.1 Hz) compared to the 40/1 sample, indicating higher mechanical losses, nearly frequency-independent. However, above 1 Hz viscous modulus of the 40/0.1 sample was lower than that of the 40/1 sample. Overall, this led to shift of vitrification to higher frequency (crossover of G' and G'' for the 40/0.1 sample occurred at 300 Hz).

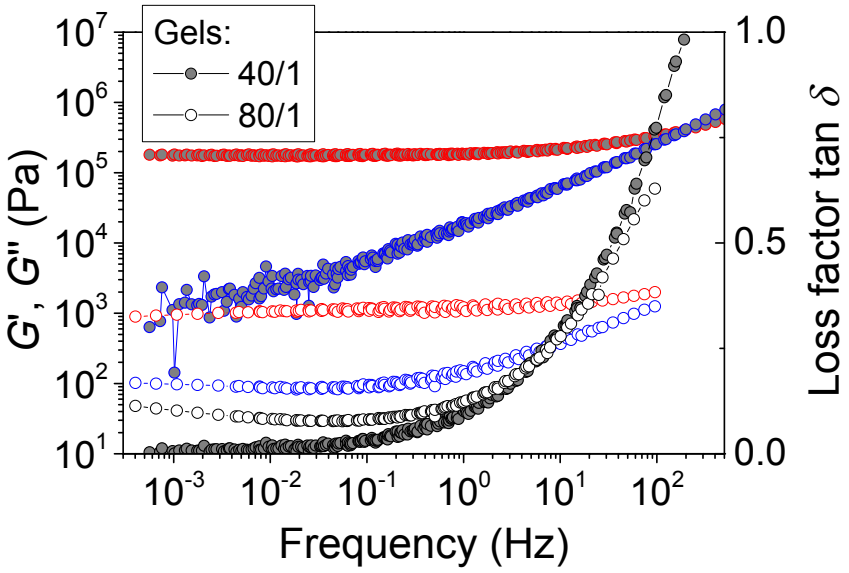

Figure 4.23 *Elastic and viscous shear moduli, and loss factor tan δ for water-swollen homogeneous gel 40/1 and water-swollen particulate gel 80/1. Equilibrium swelling was: 0.371 (40/1) and 0.724 (80/1).*

Morphology of fused spheres was reflected in an abrupt decrease of shear moduli (1 kPa *vs* 180 kPa in the plateau region, Fig. 4.23). The main transition onset was observed in roughly the same frequency range. The loss factor tan δ of the particulate 80/1 gel was higher than for the homogeneous 40/1 below ~1 Hz. The onset of secondary relaxation process was observed at very low frequency (~10^{-3} Hz) for the gel constructed of swollen polymer particles, fused together.

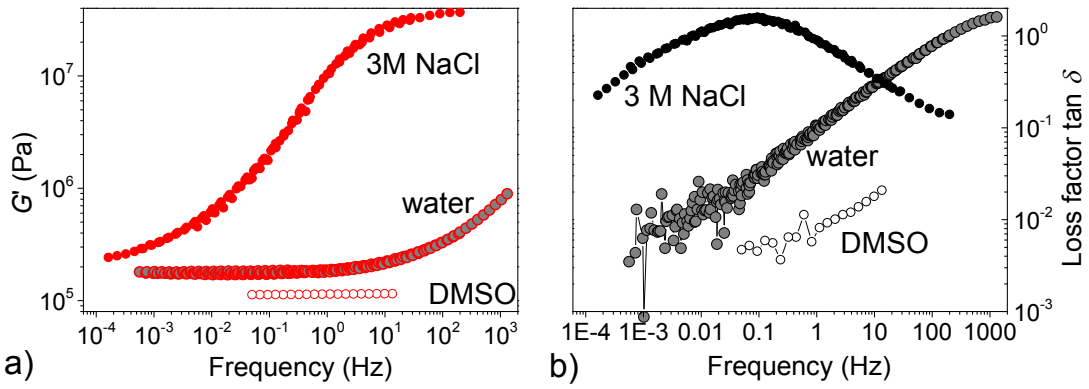

Figure 4.24 *(a) Elastic shear modulus and (b) loss factor tan δ for homogeneous gel 40/1 swollen in water, DMSO or 3M aqueous NaCl.*

Fig. 4.24 shows the effect of swelling medium on mechanical spectra of the homogeneous 40/1 gel, important properties are also tabulated in Tab. 4.3. In the medium of greater solvating power than water (DMSO), the elastic modulus was lower due to less polymer material per unit volume of swollen gel. The loss factor was much lower for the DMSO-swollen sample, the onset of α-relaxation was barely seen. Vice versa, swelling in less solvating medium (aqueous 3 M NaCl) led to shift of the α-relaxation to much lower frequency (crossover frequency for the 40/1 gel swollen in 3M NaCl was ~10^{-3} Hz vs 200 Hz for the water-swollen 40/1 gel). Therefore, the elastic modulus was significantly increased over the whole range of frequency, which is typical of a material in glassy state.

Data in Tab. 4.3 and in Fig. 4.24 demonstrate the importance of dynamic mechanical analysis in a broad range of frequencies. Whereas in the plateau region *G'* values for DMSO- and NaCl-swollen gels is 2.75 times, at 1 Hz the difference is 2 orders of magnitude, due to different vitrification behavior.

Table 4.3. *Equilibrium swelling and dynamic mechanical properties for the 40/1 gel swollen in different media.*

Swelling medium	Equilibrium swelling, g/g	*G'* (10^{-3} Hz), kPa	*G'* (1 Hz), kPa	tan δ (0.1 Hz)	mid-region of vitrification, Hz
water	0.371	180	187	0.031	1500
DMSO	0.832	115[a]	115	0.005	n/a
3M NaCl	0.219	317	10540	1.54	0.09

[a] estimate under assumption of frequency independence of *G'* in plateau region

4.4.1 Equilibrium elastic properties of gels

Gels prepared with water as diluent and swollen in water. Change of morphology from homogeneous or intermediate to particulate type was accompanied by an abrupt drop of the elastic shear modulus in the region of elasticity plateau. In Fig. 4.25, for a series of swollen hydrogels prepared with 2 mol% of the crosslinker, elastic shear modulus slightly decreased with initial dilution (40-60 wt% of water at preparation), and change of morphology to fused particles type caused a decrease of

G' by an order of magnitude, further increase of initial water content led to even lower modulus of the final hydrogel.

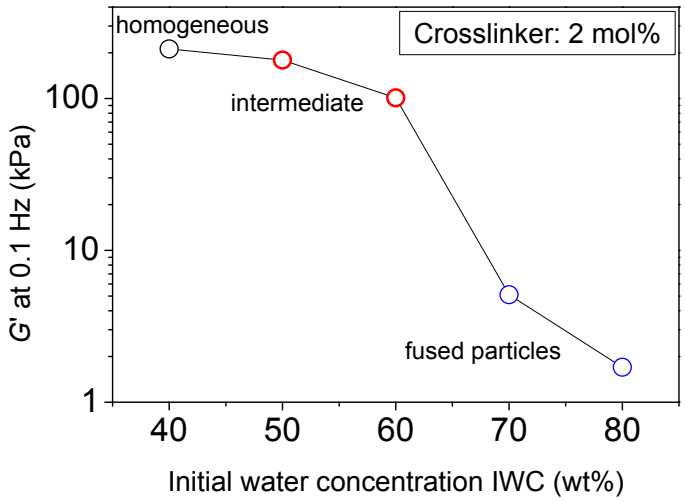

Figure 4.25 *Elastic shear modulus at 0.1 Hz (close to equilibrium) for hydrogels prepared with 2 mol% of the crosslinker and varied dilution, and swollen in water to equilibrium. Black symbol: homogeneous gel, red symbols: intermediate gels, blue symbols: fused particles morphology.*

In the same way, gels prepared at other crosslinker concentrations were tested, and results are collected in Fig. 4.26.

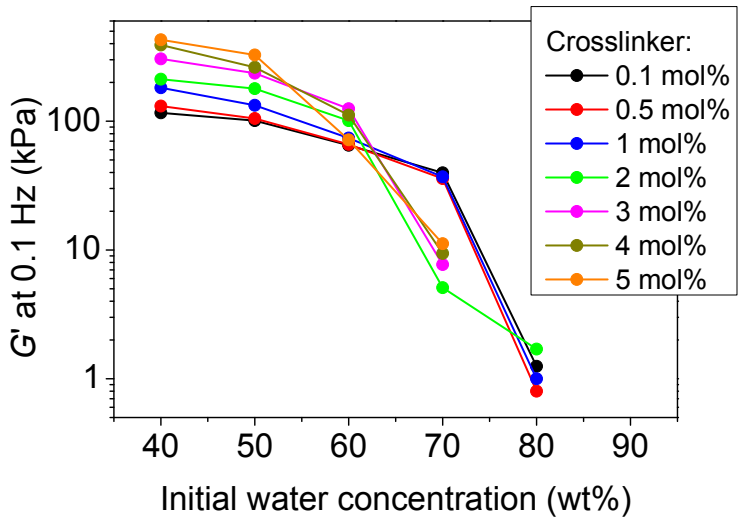

Figure 4.26 *Elastic shear modulus at 0.1 Hz (close to equilibrium) for hydrogels prepared with varied concentration of water and crosslinker, and swollen in water to equilibrium.*

To better visualize the crosslinker concentration effect, the data for hydrogel series prepared at constant initial dilution (70 wt% of water at preparation) and varied crosslinker concentration is plotted in Fig. 4.27.

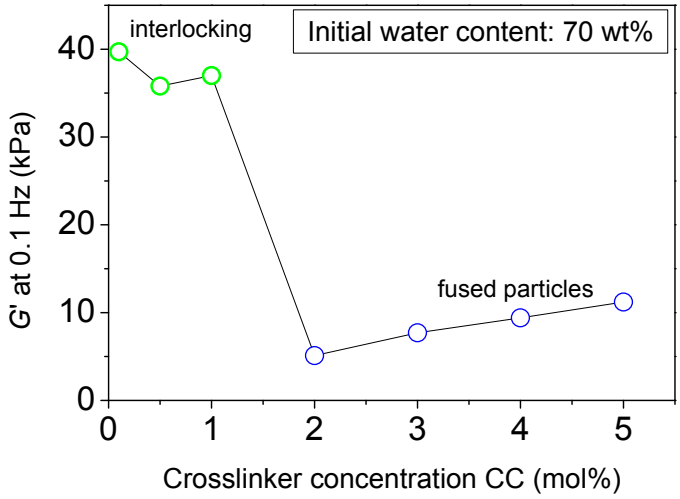

Figure 4.27 *Elastic shear modulus at 0.1 Hz (close to equilibrium) for hydrogels prepared with 70 wt% of water and varied crosslinker concentration, and swollen in water to equilibrium. Green symbols: interlocking morphology, blue symbols: fused particles morphology.*

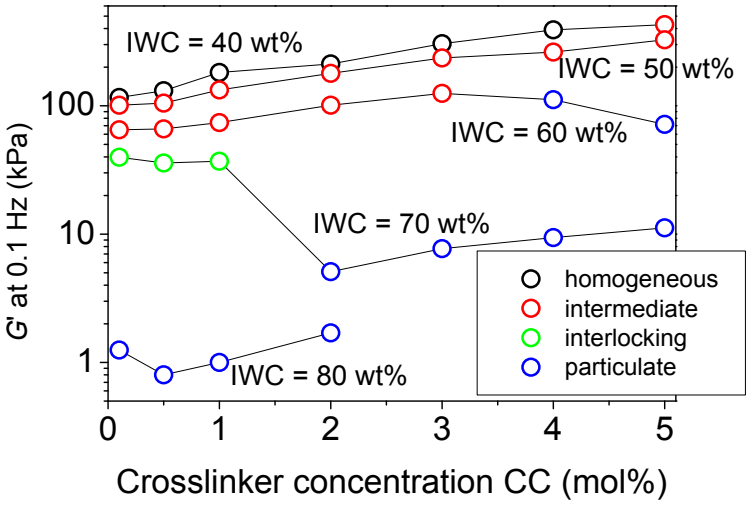

Figure 4.28 *Storage shear modulus at 0.1 Hz as a function of crosslinker concentration for hydrogels prepared with water as diluent and swollen in water. Numbers at curves show initial water content (wt%) for corresponding series. Black: homogeneous, red: intermediate, green: interlocking, blue: particulate gels.*

Equilibrium elastic shear moduli for all studied hydrogels polymerized in water and swollen in water to equilibrium are collected in Fig. 4.28.

- The materials showed strikingly different equilibrium shear modulus, in the range between 0.8 and 430 kPa.
- At constant crosslinker concentration, equilibrium shear elastic modulus always decreased with initial dilution (Fig. 4.26).
- Change of morphology to fused particles type was reflected in decrease of equilibrium elastic shear modulus, significantly steeper than that caused by the change of dilution for homogeneous and intermediate gels. The initial dilution corresponding to abrupt decrease of elastic shear modulus was shifted to lower water concentration with more crosslinker in the gel.
- Outside the border between particulate and intermediate hydrogels, at constant initial dilution, equilibrium shear modulus increased with concentration of crosslinker.
- However, when the change of morphology was caused by increasing crosslinker concentration, corresponding decrease of *G*' might be masked by the crosslinker effect (compare moduli in pairs 70/1, 70/2 and 60/3, 60/4, Fig. 4.28).

Effect of polymerization diluent on equilibrium elastic properties of hydrogels. In order to study the effect of the solvating power of diluent at preparation on the structure and elastic properties of final hydrogels, ionic compounds with salting-in ($Mg(ClO_4)_2$) or salting-out (NaCl) effect were used. PolyHEMA gels were polymerized in aqueous solutions of one of these salts, and the effect of the salt concentration on the elastic shear modulus was studied after reswelling of prepared samples in water. Results are reported in Fig. 4.29 along with the equilibrium swelling of corresponding hydrogels.

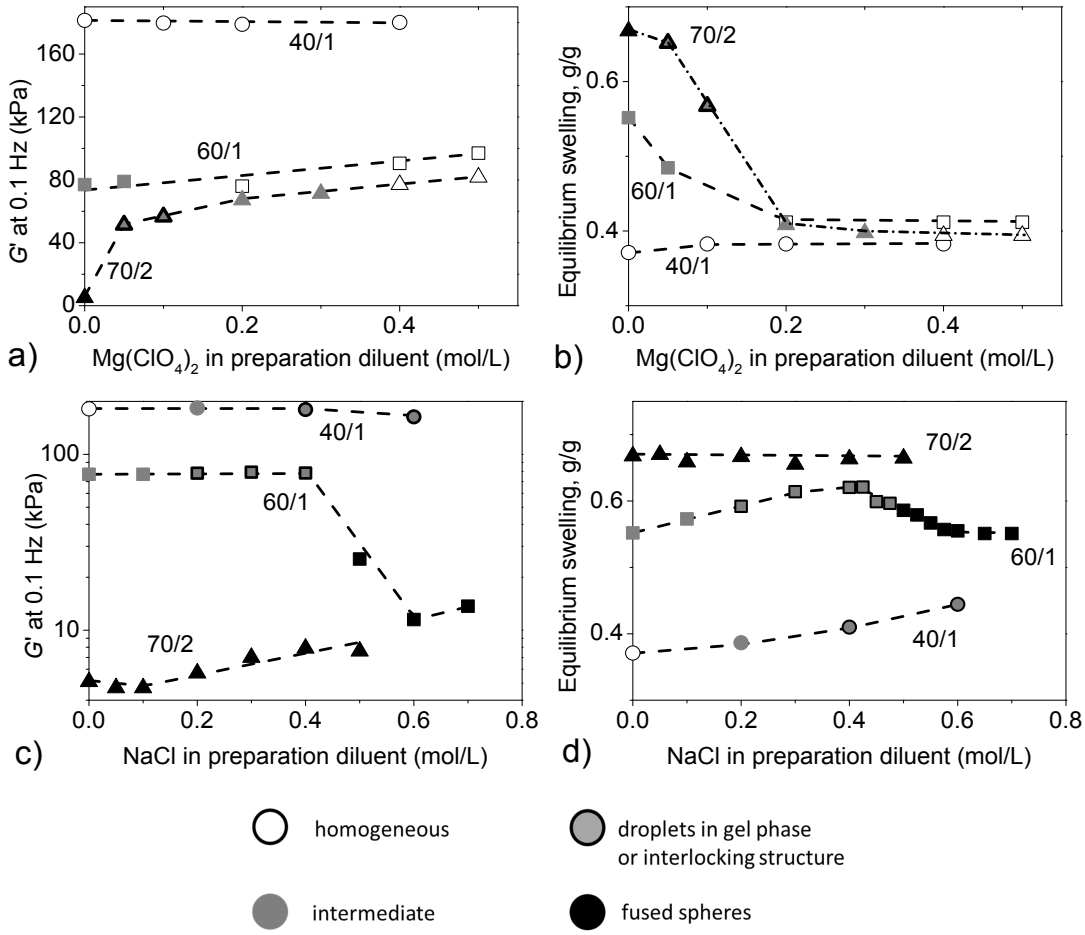

Figure 4.29 *(a, c) Elastic shear modulus at 0.1 Hz and (b) equilibrium swelling in water for hydrogels 40/1, 60/1, 70/2 prepared with aqueous (a, b) $Mg(ClO_4)_2$ or (c, d) NaCl of varied concentration as diluent, and reswollen in water. Samples composition is indicated by code near the curve. Symbol shape shows the hydrogel morphology.*

For compositions 60/1 and 70/2, addition of salting-in led to increase of the equilibrium elastic shear modulus, with hydrogels morphology changing to homogeneous (Fig. 4.29a). Constant value of *G'* was not reached for these compositions even at higher concentration of $Mg(ClO_4)_2$, 0.5 M[4].No effect of $Mg(ClO_4)_2$ addition was observed in case of 40/1 series, the final hydrogels were always optically clear, within this series.

[4] Study of hydrogels prepared with more than 0.5 M of $Mg(ClO_4)_2$ in the diluent was complicated – at such high concentration of perchlorate ions, some side reaction came into effect, and visible gas bubbles (also documented in SEM pictures) appeared in the hydrogels.

From Fig. 4.29b, homogeneous hydrogels prepared with showed similar equilibrium swelling in water (0.37-0.42 g/g) independently of the mixture composition. Still, the equilibrium modulus was different (between 70 kPa for the 70/2 gel at 0.4 M $Mg(ClO_4)_2$ and 180 kPa for 40/1 gels). Thus, introduction of a salting-in additive is an easy way to produce homogeneous hydrogels softer than could be manufactured with pure water as diluent at any initial dilution/crosslinker content combination.

As expected, the effect of salting-out NaCl was opposite (Fig. 4.29c, d). With decreasing solvating power of the diluent the phase separation was enhanced, and at some point the morphology of final hydrogel was changed to that of particulate type, which was reflected in abrupt drop of the elastic modulus.

For particulate hydrogels, further increase of NaCl concentration in polymerizing mixture led to increase of the elastic shear modulus at practically constant equilibrium swelling. This increase of *G*' was weaker than that due to suppressing phase separation. This effect could be explained by appearance of smaller particles fraction, leading to better connectivity of the swollen polymer phase and thus, higher elastic modulus.

Homogeneous gels. Elastically active network chains concentration. Concentration of elastically active network chains (EANC) can be calculated from the equilibrium elastic shear modulus G_e and equilibrium swelling data, according to Eq. 4.1:

$$G_e = RT\nu_e(\phi_2^0)^{2/3}(\phi_2)^{1/3} \quad (4.1)$$

where ν_e is the EANC concentration, in moles per dry unit volume of the network ϕ_2 is volume fraction of polymer in the gel swollen to equilibrium and ϕ_2^0 is volume fraction of polymerizable substances at preparation, R and T are the gas constant and absolute temperature, respectively.

In this section, results of such calculations for series of gels prepared with 40 wt% of water as diluent (40/X series) will be discussed. All this hydrogels are homogeneous, except for the 40/5 sample, which is intermediate. For majority of 40/X gels, the storage modulus is constant at frequency below 0.1 Hz, and can be considered equilibrium shear modulus, G_e. However, for gels with the lowest

crosslinker concentration 40/0[5] and 40/0.1 constant G' value was not reached even at 10^{-3} Hz. It was assumed that at frequency 10^{-3} Hz $G' \approx G_e$ with reasonable accuracy, and the concentration of elastically active network chains was determined taking this value for calculations. Since for homogeneous gels $\phi_2^0 = \phi_2$, Eq. 4.2 holds

$$G_e = RT\nu_e\phi_2^0 \tag{4.2}$$

Similar calculations were performed for the same 40/X gels reswollen in DMSO, swelling medium of greater solvating power than water. For polyHEMA gels swollen in DMSO, already at 0.1 Hz, G' reached its equilibrium value.

To conclude on the network structure, concentration of elastically active network chains ν_e should be compared with the ideal concentration of elastically active network chains, ν_{chem}. This quantity was calculated from the composition of polymerization mixture assuming that each consumed double bond of the crosslinker contributed to one EANC. The impact of the crosslinker DEGDMA present in commercial HEMA (0.07 wt% by gas chromatography) was also considered.

Results for water- and DMSO-swollen gels are summarized in Tab. 4.4 and in Fig. 4.30.

Table 4.4 *Equilibrium shear moduli and EANC concentration for gels prepared with 40 wt% water and varied crosslinker concentration, reswollen in water or DMSO.*

Sample	ideal [EANC] ν_{chem} [mol/L]	water		DMSO	
		G'(10^{-3} Hz) [Pa]	[EANC] ν_e [mol/L]	G'(0.1Hz) [Pa]	[EANC] ν_e [mol/L]
40/0	0.014	(1.10×10^5)[a]	(0.083)[a]	$4.25\cdot10^4$	0.049
40/0.1	0.034	$(1.15\cdot10^5)$[a]	(0.090)[a]	$4.40\cdot10^4$	0.057
40/0.5	0.113	$1.35\cdot10^5$	0.100	n/a	n/a
40/1	0.212	$1.80\cdot10^5$	0.130	$1.10\cdot10^5$	0.135
40/2	0.406	$2.10\cdot10^5$	0.147	n/a	n/a
40/3	0.596	$3.00\cdot10^5$	0.205	$2.50\cdot10^5$	0.271
40/4	0.786	$3.90\cdot10^5$	0.269	n/a	n/a
40/5	0.971	$4.30\cdot10^5$	0.289	$5.65\cdot10^5$	0.579

[a] equilibrium modulus might be not yet reached

[5] Crosslinker concentration at preparation CC = 0 mol% means that no crosslinker DEGDMA was added to the polymerizing mixture. However, there is some DEGGMA always present in commercial monomer HEMA. HEMA used in this work contained 0.07 wt% of HEMA, which was seemingly enough to produce covalently crosslinked bulk hydrogels.

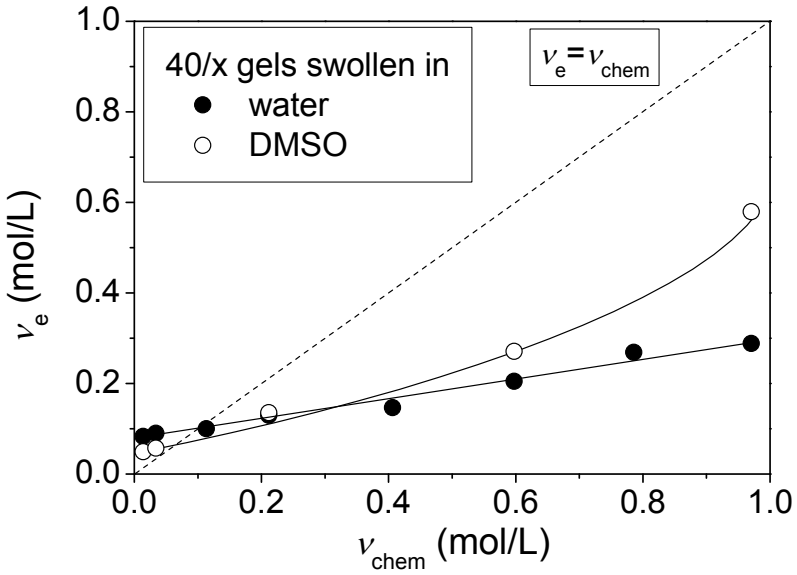

Figure 4.30 *Concentration of elastically active network chains determined experimentally and ideal concentration of elastically active network chains.*

The dependence of ν_e on ν_{chem} for water-swollen samples was close to linear with slope of 0.22 (due to incomplete utilization of crosslinker in forming EANCs). That slow relaxations caused likely by regrouping of hydrophobic clusters are still operative in case of water-swollen gels is documented by a relatively high value of tan δ for gels with lowest crosslinker content (e.g. Fig. 4.22).

Dependences for both water-swollen and DMSO-swollen 40/X series showed a positive intercept for $\nu_{chem} \rightarrow 0$ which could be due to still ongoing relaxations of hydrophobic clusters and/or permanent constraints (trapped entanglements). In DMSO, these hydrophobic clusters cannot exist, tan δ falls down to a very small value; thus, the positive intercept in case of DMSO-swollen samples is due to trapped entanglements.

In Fig. 4.30, another special feature for DMSO-swollen samples was observed: compared to water-swollen gels, the values of ν_e were considerably higher at higher crosslink densities, and the ν_e - ν_{chem} dependence was curved upward. This was seemingly caused by large stretching of the EANCs by swelling, over the Gaussian limit, and thus inapplicability of Eq. (4.2). The finite extensibility models of rubber elasticity are available [**115**], but at this stage the *G*' dependence on crosslink density for DMSO-swollen samples was not analyzed any further.

Phase-separated gels. Elastically active network chains concentration. Unlike the homogeneous hydrogels series 40/X, the porous samples contained voids

filled with swelling medium. When considering the elastic response of the matrix, it should be related to the amount of polymeric material. Assuming that swelling of the matrix equaled to swelling of homogeneous hydrogel with the same crosslink density (this will be discussed in Section 4.4.2), a trivial correction for the modulus was applied[6]: $G_e = G'\phi_2(40)/\phi_2(\mathrm{XX})$ with $\phi_2(40)$, volume fraction of polymer in the reference homogeneous sample and $\phi_2(\mathrm{XX})$, volume fraction of the porous gel counting also the solvent in pores. This corrected value of the modulus was used for calculating the concentration of elastically active network chains using Eq. (4.1) with $\phi_2^0 = \phi_2 = \phi_2(40)$.

Results of calculations are presented in Fig. 4.31. With increasing dilution (IWC = 40-60 wt%) EANC concentration and the slope of linear part of the curves steadily decreased, likely due to increasing impact of side reactions of cyclization. Developing of particulate hydrogel morphology caused a striking decrease of the EANC concentration calculated from experimental data.

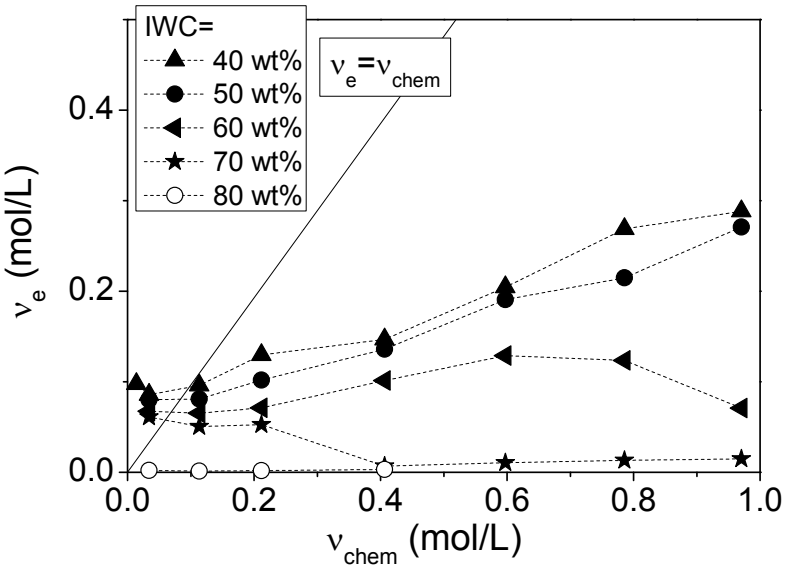

Figure 4.31 *Concentration of EANC determined experimentally for water-swollen gels and ideal concentration of EANC. Solid line shows equality of experimentally determined and calculated EANC concentrations.*

However, the values of ν_e for particulate gels should be called "fictive" because the trivial correction for the pores fraction was not sufficient for calculating

[6] Like in the 40/X series analysis, it was assumed that at frequency 10^{-3} Hz $G' \approx G_e$.

of the concentration of EANCs of the matrix in porous gels. Inhomogeneous stresses arising from varying thickness of the stressed macroporous material and participation of deformation modes other than shear counted among the other factors. Inhomogeneous stresses arisen from the fact that the force applied to the outer surface concentrated at a small fraction of the cross-section of the porous material. This situation is visualized by Fig. 4.32. The necks connecting the fused spheres are the effective load bearing parts of the macroporous material. The stress concentration is strongly enhanced by dangling structures, which means more material per the same cross-section of the neck. The stress concentration results in larger deformation and, therefore, in lower equilibrium modulus for the matrix compared to the true modulus of the matrix.

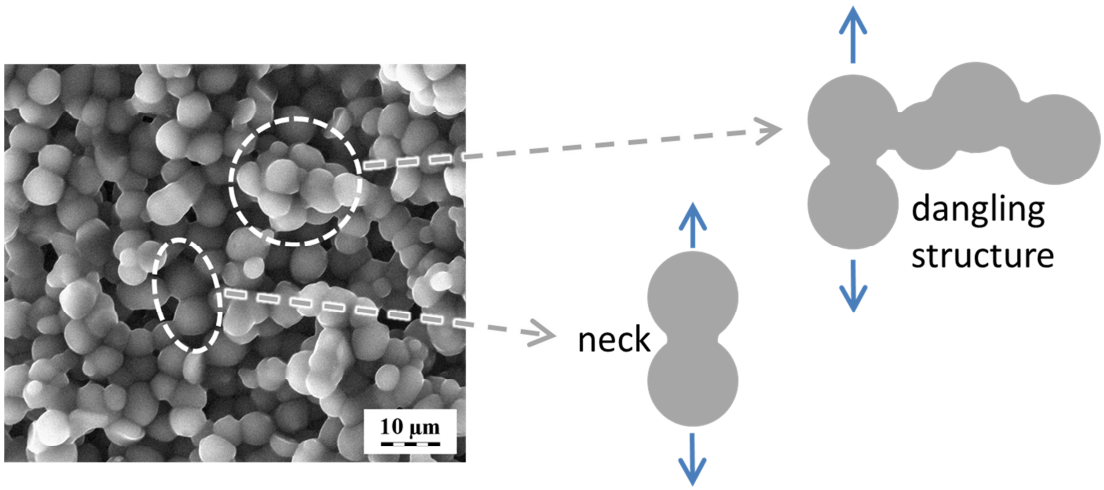

Figure 4.32 *SEM image of fused–sphere like macroporous gel (sample 80/0.1). Sketch visualizes necks connecting particles as loci of higher stress causing larger deformation, and large dangling structures.*

The magnitude of the stress concentration and, probably, different deformation geometries (bending, etc.) is difficult to estimate. The correct answer about the mechanical behavior of such heterogeneous swollen systems can be possibly obtained by applying the Finite Element Method. This was not analyzed any further at this stage.

4.4.2 Analysis of dynamic mechanical spectra to determine swollen gels morphology

Results presented in previous sections show that equilibrium properties of gels (swelling and shear elastic modulus) can reveal a special structural feature – presence of fused particles of swollen polymer surrounded by swelling medium. However, these properties in some cases led to incorrect conclusions. For instance, hydrogels prepared with 60-70 wt% of water and relatively high crosslinker concentration (4-5 mol%) showed quite high equilibrium elastic modulus and low swelling, typical of intermediate hydrogels, but are composed of fused polymer particles surrounded by water in the connected voids.

Examples presented in Figs. 4.21-4.24 demonstrate that analysis of **visco**elastic properties (particularly, loss factor tan δ behavior) in a range of frequencies adds to the information gained from the equilibrium properties. Same is concluded after factor analysis of results (Section 10.4).

Results of dynamic mechanical studies of gels prepared with water as diluent and swollen in water are collected in Fig. 4.33 (hydrogels prepared at a fixed crosslinker concentration and varied initial dilution) and Fig. 4.34 (hydrogels prepared at a fixed initial dilution and varied crosslinker concentration) in form of loss factor frequency dependences. Series of samples with different initial dilution or crosslinker content showed similar trends.

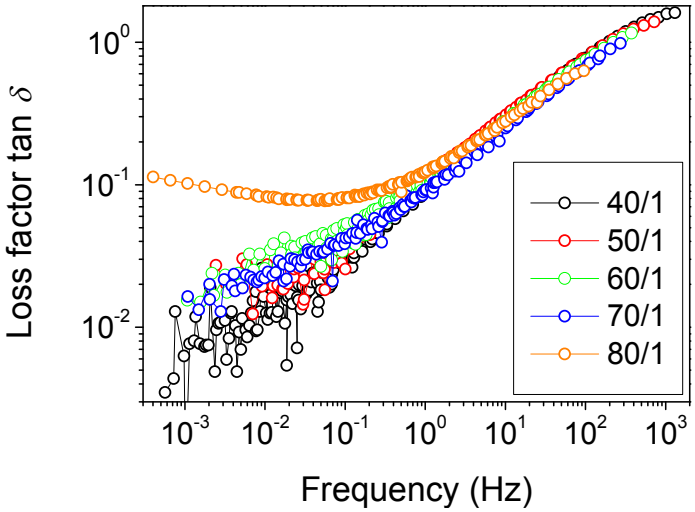

Figure 4.33 *Frequency dependences of loss factor for hydrogels prepared with 1 mol% of crosslinker and variable initial concentration of water as diluent, and swollen in water. Corresponding sample codes are shown near the curves.*

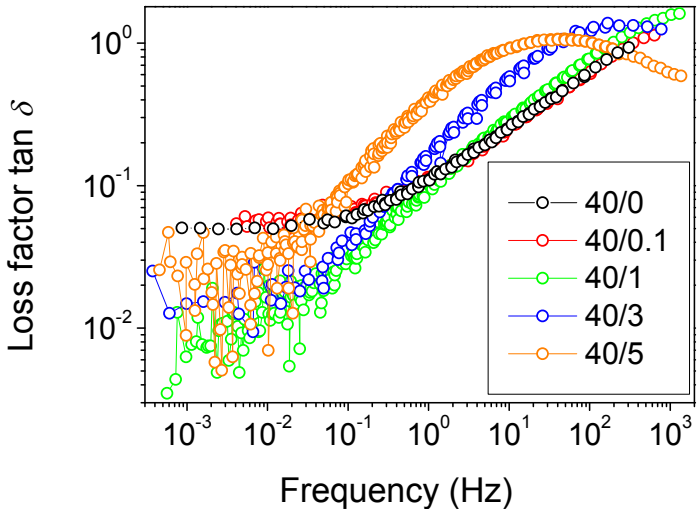

Figure 4.34 *Frequency dependences of loss factor for hydrogels prepared with 40 wt% of water as diluent and variable concentration of crosslinker, and swollen in water. Corresponding sample codes are shown near the curves.*

Within a series prepared with 1 mol% of crosslinker and variable initial water concentration (Fig. 4.33), the loss factor showed the onset of α-relaxation around 5 Hz for all the samples. Above 1 Hz the difference between the loss factors was negligible. Oppositely, increasing crosslinker concentration at constant initial dilution resulted in the shift of α-relaxation to lower frequencies (Fig. 4.34). Thus, IWC had minor effect on the high-frequency part of the loss factor profiles, corresponding to the α-relaxation process, whereas crosslinker content was one of major factors governing the α-relaxation onset frequency. The described trends are visualized also in Fig. 4.35a showing loss factors at 10 Hz.

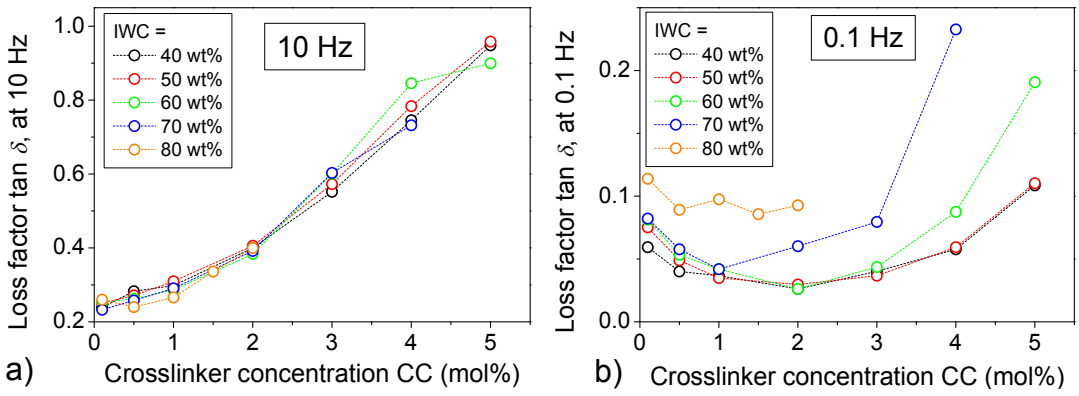

Figure 4.35 *Loss factor measured at 10 Hz (a) and at 0.1 Hz (b) as function of crosslinker concentration CC and initial water content IWC for hydrogels prepared with water as diluent and swollen in water.*

At lower frequencies, the effect of changing initial dilution IWC was more significant (loss factors at 0.1 Hz are shown in Fig. 4.35b). The loss factor dependence on crosslinker concentration showed a minimum at 1-2 mol% of DEGDMA. Loss factors for homogeneous, intermediate and interlocking hydrogels formed a single master curve, while loss factors for particulate samples were higher. The structural origin of these effects will be discussed in this section.

The trends revealed in mechanical behavior studies in the forced oscillation mode were in general confirmed by shear creep studies (results are shown in Section 10.3).

Influence of the swelling medium solvating power on dynamic mechanical properties of the gels is illustrated in Fig. 4.24.

Main transition (vitrification) of swollen hydrogels. The increase of loss factor with frequency above 0.1-1 Hz (Fig. 4.33-4.34) means that a swollen gel approaches the glass transition, possibly facilitated by hydrophobic aggregates or by reorganization of water molecules [**116**, **117**].

In the α-relaxation region, the loss factor was mainly governed by polymer chains segmental mobility: experimentally, the onset of main transition was shifted to lower frequency with increasing crosslinker concentration (Fig. 4.34).

That the change of main relaxation frequency with crosslinker content was indeed due to shift of the swollen network glass transition region, was confirmed by dynamic differential scanning calorimetry measurements (Fig. 4.36). In the DSC scans, multiple endotherms of ice melting around 0 °C were preceded by the polymer network glass transition. The glass transition of water-swollen 40/5 sample (-6° C) was found to be significantly higher than that for 40/1 and 40/0.5 samples (-32 to -14 °C). The glass transition multiplicity observed in case of 40/0.5 hydrogel is possibly due to heterogeneity of networks. For hydrogels prepared with more than 60 wt% water as diluent, the glass transition could not be observed in DSC because of overlapping with the intense broad peak of ice melting.

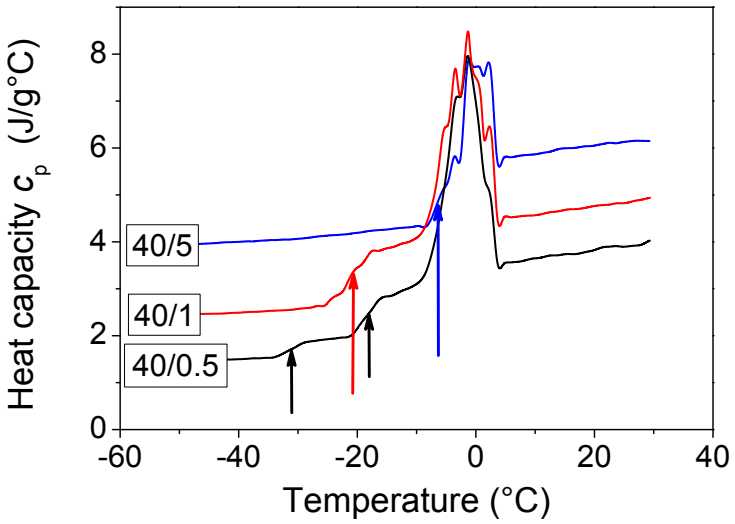

Figure 4.36 *The heat capacity of swollen polyHEMA gels (40/0.5, 40/1. 40/5) dependences on temperature. Arrows show polymer glass transition temperatures. Curves are shifted vertically for better representation. Sample codes are written next to the curves.*

The effect of swelling medium on the main transition process is documented in Fig. 4.24 for a homogeneous 40/1 gel. Trends for gels prepared at other initial dilutions and/or crosslinker concentrations (including particulate gels) were similar. In all cases, swelling of samples in medium of less solvating power (aqueous NaCl) shifted the main relaxation to lower frequencies (less than 10^{-2}-10^{-3} Hz), while medium of higher solvating power (DMSO) caused onset of frequency relaxation barely seen even at 1-10 Hz.

Thus, the main transition process of swollen polyHEMA gels was found to be very sensitive to concentration of the crosslinker used for network preparation (and associated change of chain segmental mobility), and to the solvating power of the swelling medium (in poor solvents the α-relaxation is facilitated by hydrophobic aggregation). Interestingly, the initial dilution showed negligible effect on the α-relaxation. Basing on this information, conclusion was made on the morphology of non-transparent hydrogels below the SEM resolution limit (intermediate gels).

Morphology of heterogeneous hydrogels with structure below SEM resolution. Intermediate hydrogels – non-transparent, heterogeneous samples with structure below electron microscopy resolution – were produced in a vast area of polymerizing mixture compositions (Fig. 4.7). In general, those gels can either incorporate very small solvent-filled droplets or microphases differing in the polymer

and/or crosslinker concentration. It was demonstrated [**118**] that non-porous hydrogels with inhomogeneous distribution of polymer material and crosslinker (semi-interpenetrating networks) possessed higher swelling degree and lower elastic modulus than hydrogels with same average concentration of crosslinker units, but evenly distributed. Thus, both morphology types described above would explain swelling and equilibrium elastic behavior of intermediate polyHEMA hydrogels.

The dynamic mechanical behavior on the main transition frequency range supported the morphology of solvent droplets within homogeneous polymer phase. Indeed, the main relaxation process occurred in the same frequency range in case of particulate (80/1), interlocking (70/1), intermediate (50/1, 60/1) and homogeneous (40/1) water-swollen samples at the same level of the crosslinker at preparation (Fig. 4.33). This is an indication that the matrix in phase-separated hydrogels had the same swelling properties in water as did homogeneous hydrogel of corresponding concentration of crosslinker[7]. The equality of the degrees of swelling in water of the matrix in porous gels and respective homogeneous gels might imply that also the network structure is the same. Such conclusion was corroborated by the closeness of α-relaxation maxima for gels of various morphologies reswollen in 3 M NaCl solution (Fig. 4.37).

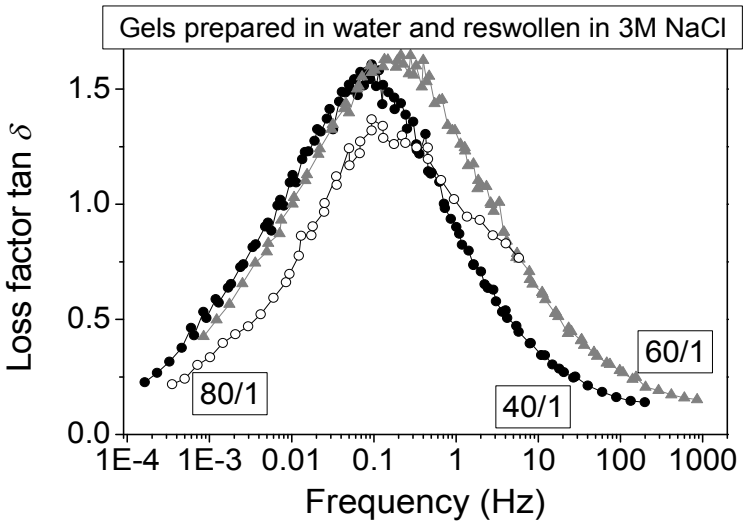

Figure 4.37 *Loss factor tan δ for hydrogels prepared at 1 mol% crosslinker and variable concentration of water, reswollen in 3M NaCl to equilibrium. Sample compositions are shown near the curves.*

[7] This assumption, now proved, was used previously for calculation of pore volume fraction in swollen porous gels, and correction of the equilibrium shear modulus for the fraction of pores in calculation of the elastically active network chains concentration.

That swollen polyHEMA matrix in an intermediate gel is the same as homogeneous gel with the same crosslinker concentration, implies that intermediate gels are most likely constituted of the continuous swollen polymer matrix incorporating small droplets of swelling medium. This conclusion was supported by differential scanning calorimetry of selected hydrogel samples (Fig. 4.38).

Water crystallization temperature T_c depends on the size of crystallization domain and on the nucleation mechanism [**119**]. If the characteristic size of water droplets exceeds 0.5 mm, the crystallization is usually off-set by the heterogeneous nucleation and crystallization temperature lays at -14 to -30 °C. If the size of droplet decreases below 100 μm, water crystallization starts by the homogeneous nucleation, and T_c decreases to below -40 °C. During the cooling stage of the swollen hydrogels one or several water crystallization exotherms were observed (Fig. 4.38). All hydrogels revealed an intense sharp exothermic peak at -13 to -23 °C ascribed to heterogeneous nucleation during bulk water crystallization. For hydrogels prepared with 40-50 wt% of water, in addition to this, one or several broad and weak exo peaks were observed at -50 to -37 °C. They were due to crystallization of water via homogeneous nucleation.

If this homogeneously nucleated water revealed for 40/1 and 50/1 samples was bound water, solvating polar polyHEMA groups, there would be no reason not to observe it in scans of 60/1 gel. Instead, this part of water must be contained within small, sub-micrometer size droplets that grow with enhancing phase separation, and finally a mixed nucleation mechanism observed for 40/1 and 50/1 hydrogels changes to purely heterogeneous one for 60/1 sample.

Low-frequency viscoelasticity reveals dangling chains in polyHEMA network and particulate morphology of hydrogels. The studied hydrogels are divided into three categories according to their low-frequency loss factor behavior. In case of non-particulate gels prepared with moderate to high (1-5 mol%) concentration of the crosslinker, tan δ dropped to very low values (below 0.01, equipment resolution limit) at 10^{-2}-10^{-3} Hz. The loss factor of water-swollen hydrogels prepared with concentration of the crosslinker below 1 mol% was significantly higher (0.04-0.08) at frequencies $<10^{-2}$ Hz, and was frequency-independent. Finally, particulate samples studied showed an onset of a broad and weak secondary relaxation maximum corresponding to $\sim10^{-4}$-10^{-5} Hz (at 25° C). These three types of behavior are illustrated in Fig. 4.39.

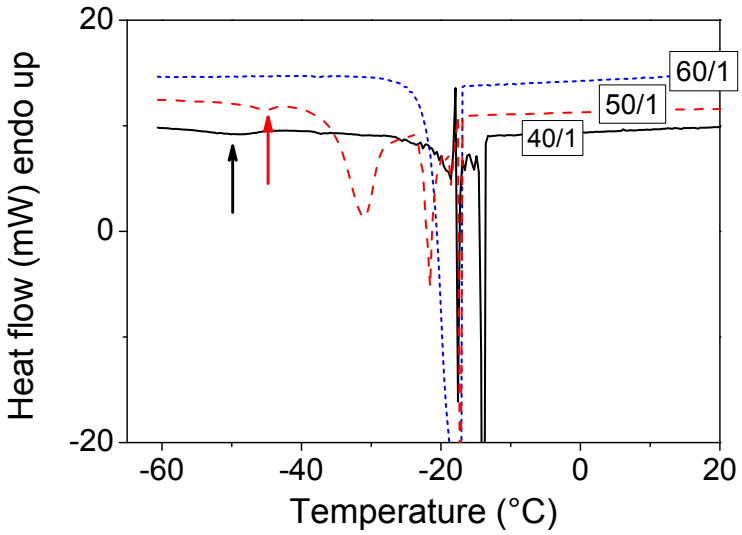

Figure 4.38 *The DSC (standard mode) traces of water crystallization in polyHEMA swollen gels 40/1, 50/1 and 60/1. Arrows show peaks of homogeneous water crystallization. Curves are shifted vertically for better representation, heterogeneous crystallization peaks are truncated. Sample codes are written near the curves.*

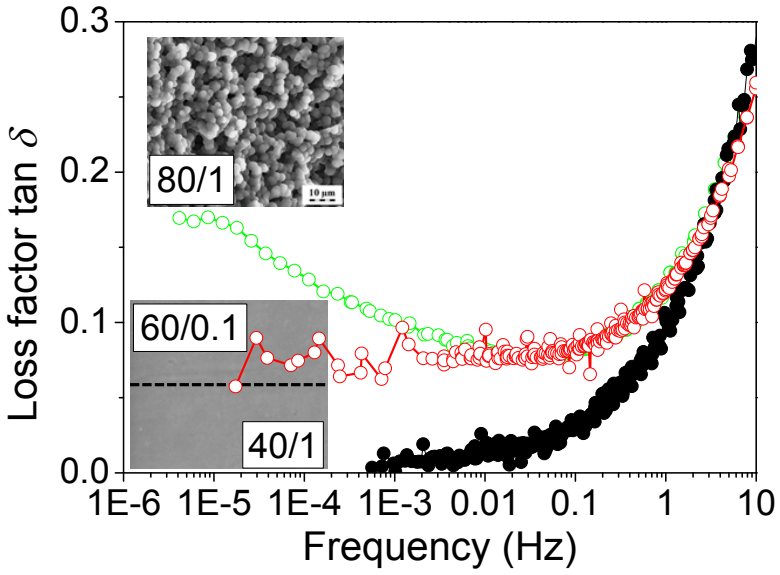

Figure 4.39 *Low-frequency loss factors for representative examples of particulate, lightly crosslinked and other hydrogels, swollen in water to equilibrium.*

The loss factor in a good solvent might be affected by removal (dissolution) of some clusters or associates that are present in poor solvent (water) due to physical interactions, but relaxations due to entanglements and dangling chains, if any, should not be influenced. After reswelling of hydrogels in DMSO, better solvent than water, the loss factors were at least an order of magnitude lower than for corresponding

water-swollen gels (representative example is shown in Fig. 4.24). As DMSO is known to disrupt hydrogen bonds present in water, hydrogen bonds between segments of readily available dangling chains are likely responsible for high losses at low frequencies for water-swollen lightly crosslinked gels.

The low-frequency tan δ behavior documented in Fig. 4.39 for the 80/1 sample was characteristic of all studied particulate hydrogels. Some examples are presented in Fig. 4.40. Apparently, the intensity of secondary relaxation increased with higher initial dilution of the polymerized mixture. At the same time, crosslink density had less impact on this secondary relaxation process/

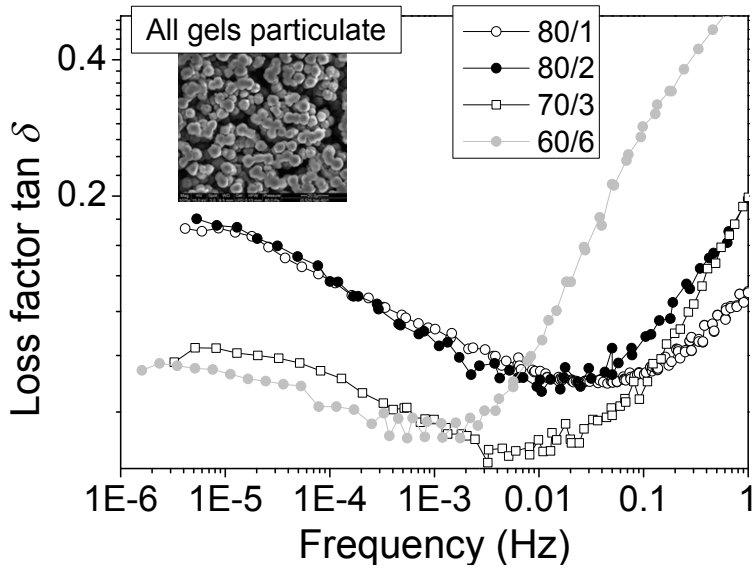

Figure 4.40 *Low frequency behavior of loss factor for fused-particles type hydrogels swollen in water to equilibrium.*

Same conclusion were made from analysis of low-frequency behavior of loss factors of hydrogels prepared with 1 mol% of crosslinker and 60 wt% of diluent of varied solvating power – pure water or aqueous NaCl solution. As seen from Fig. 4.41, the low frequency loss factors for hydrogels of intermediate and interlocking morphology were relatively low and almost identical. As the bicontinuous morphology was coexistent with fused spherical particles, the loss factor was increased, but still did not show the secondary relaxation onset. Only for particulate hydrogels the secondary relaxation was clearly seen.

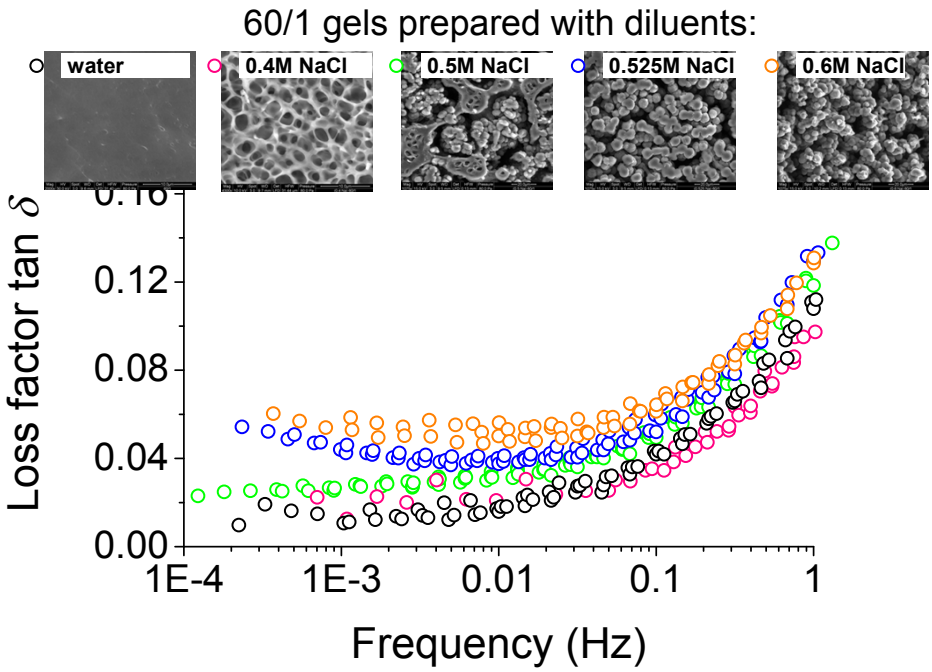

Figure 4.41 *Low frequency behavior of loss factor for hydrogels prepared with 60 wt% of diluent (aqueous NaCl of varied concentration) and 1 mol% of crosslinker, and swollen in water to equilibrium.*

Dangling chains were reported to be responsible for the low frequency relaxation in polyHEMA gels limitedly swollen with ethylene glycol [**102**], and that relaxation disappeared with increased swelling (in fact, shifted to higher frequencies and overlapped with the onset of the main relaxation). Similar approach was tested in this work: the samples prepared with water as diluent were swollen in much better solvent, DMSO, and tested in shear at low frequency. Indeed, the secondary relaxation maximum for sample 80/1 disappeared with increasing equilibrium swelling.

Although the consequence of swelling increase was the same in [**102**] and in this work, the mechanism behind seems to be different. In this work, the low-frequency relaxation maximum was observed only for particulate water-swollen gels, which contained fused polymer gel particles, surrounded by water. Disappearance of relaxation maximum after reswelling in DMSO might be connected with morphology changes at micrometer scale rather than with that at the level of chain segments. In the light microscopy pictures of water- and DMSO-swollen samples 80/1 (Fig. 4.42), with increase of overall swelling the particles became larger, and voids shrank.

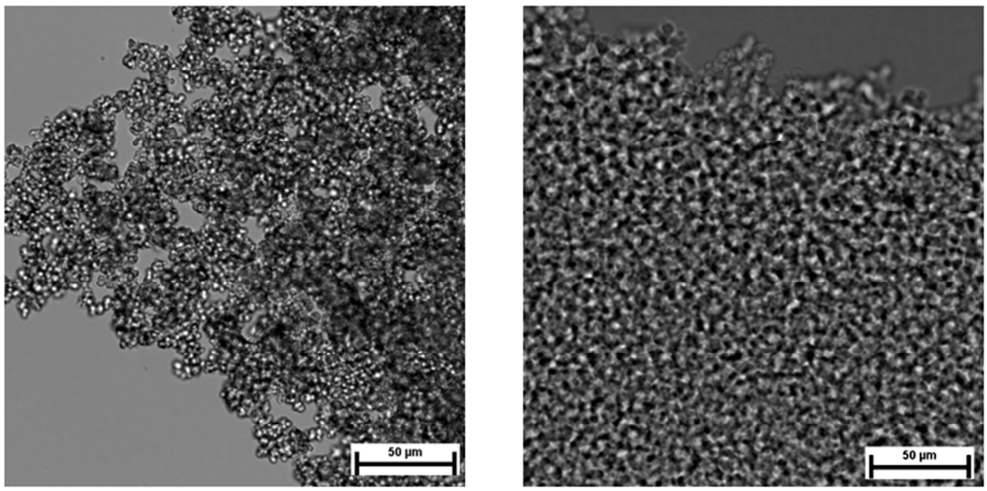

Figure 4.42 *Light microscopy pictures for water-swollen sample 80/1 (left, macropores and gel particles are observed) and DMSO-swollen sample 80/1 (particles are larger, and more collated).*

That the low-frequency relaxation maximum was only observed for particulate samples, suggests that long-range coordinated movements of substructures (dangling aggregates of collated polymer particles, Fig. 4.32) are responsible of it, and void (solvent-filled) space facilitates such movements. After swelling in better solvent, the movement of such aggregates is constrained due to either less void space or due to increase of the moving part weight (which should lead to relaxation at much lower frequency, not reached experimentally).

5 Conclusions

PolyHEMA hydrogels, including porous, have been intensively studied, and many publications about their morphology and properties are available. However, information about relationship of porous polyHEMA gels mechanical properties has been limited; this work adds some more knowledge on this.

Homogeneous and porous polyHEMA gels were prepared by cross-linking polymerization of HEMA in the presence of water at various dilutions and cross-linker contents. Large changes in morphology were achieved when water as diluent was replaced by salt solutions ($Mg(ClO_4)_2$ and NaCl) which improved or deteriorated, respectively, solvation power of the diluent. Varying of salt concentration made possible to fine tune the morphology and to control the passage from isolated droplets morphology to bicontinuous interlocking and fused-spheres like hydrogel structures.

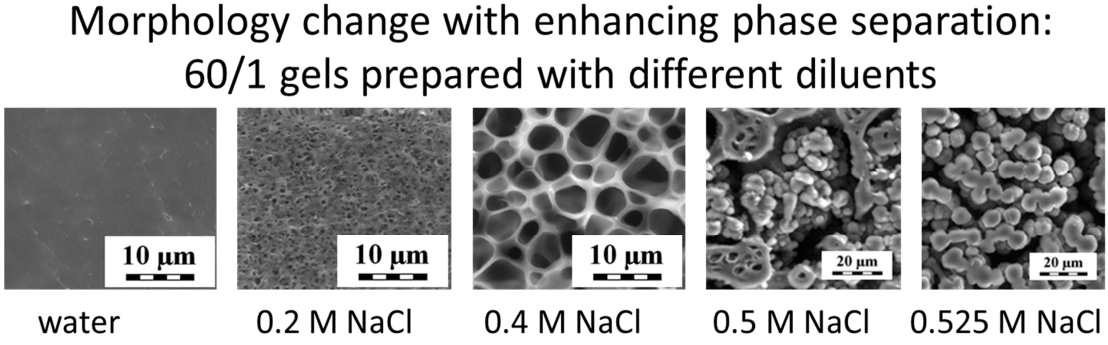

Swelling and mechanical behavior of hydrogels were investigated in relation to their morphology and matrix structure. The physical associates existing in water-swollen gels due to hydrophobic interactions limit the solubility of polyHEMA and swelling of polyHEMA gels. However, these associates were mobile enough to enable reaching mechanical equilibrium within the available frequency range (down to 10^{-3} Hz). This was valid except of gels of the lowest cross-link density and fused-spheres type hydrogels. Reswelling of the gels in a good solvent dissolved the associates and removed the slow relaxations.

From the elastic modulus in the rubbery region, concentration of the elastically active network chains was calculated. For homogeneous gels, its dependence on the crosslinker-to-HEMA ratio revealed that hydrophobic associates added to the crosslink density, acting as physical crosslinks. The impact of

permanent constraints (trapped entanglements) on the equilibrium elastic modulus was also noticeable.

The equilibrium elastic modulus of swollen hydrogels showed an abrupt decrease by about an order of magnitude when the sample morphology changed to fused-spheres type. However, even after correction for the pores fraction, the calculated values of elastically active network chains were unrealistically low, and should be called "fictive". Inhomogeneous stress fields caused stress concentration in engaged necks connecting a network of elastically active fused spheres. The stress concentration was strongly enhanced by dangling structures, which meant more material per the same cross-section of the neck. It resulted in larger deformation and, therefore, underestimation of true modulus of the matrix.

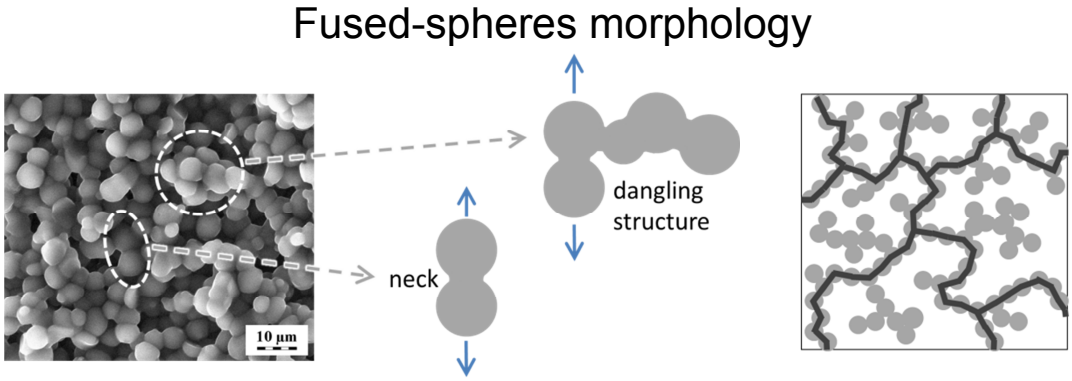

Dynamic mechanical spectroscopy results revealed that the high-frequency part of loss factor dependences (above 1 Hz), corresponding to the main transition region, was sensitive to the crosslinker-to-HEMA ratio, but not to diluent-to-HEMA ratio. In the low-frequency range viscoelastic properties (below 0.1 Hz), corresponding to the rubbery plateau, the loss factor depended on both initial dilution and crosslinker content.

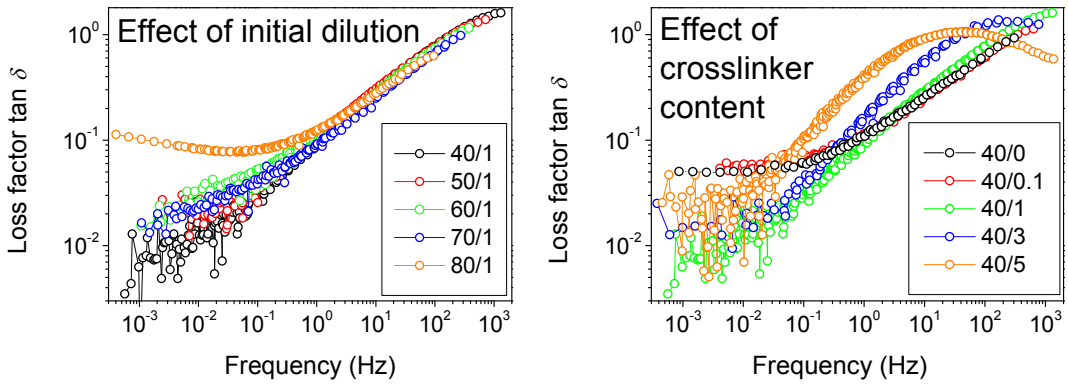

In the α-relaxation region, the frequency dependences of the loss factor for homogeneous and porous hydrogels prepared at constant crosslinker-to-HEMA ratio

merged into a single master curve which indicated that the porous hydrogel matrix was the same as homogeneous hydrogel of the same cross-link density.

The shift of vitrification region to lower frequencies with increasing of the crosslinker content was ascribed to shorter and more rigid network chains of the highly crosslinked samples. Similar trend was revealed by study of gels swollen in media other than water. Reswelling of gels in a better solvent caused dissociation of the physical associates and decreased the mechanical losses in the main transition region, thus moving onset of vitrification to higher frequency. On the contrary, reswelling of gels in the medium of less solvating power shifted the onset of main transition to much lower frequencies. This proved that physical associates assisted the vitrification of polyHEMA gels.

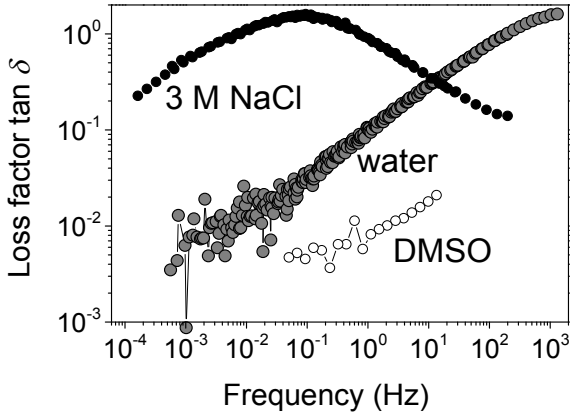

The effect of mobile physical associates on hydrogels mechanical response revealed in the main transition region was eliminated at lower frequency for majority of homogeneous and intermediate hydrogels. Only for gels of the lowest crosslink density, slow movements of larger associates causing relatively high mechanical losses were detected even at ~10^{-5} Hz. However, these physical associates were dissolved after reswelling in better solvent, and the loss factor dropped to very low values even in case of lightly crosslinked gels.

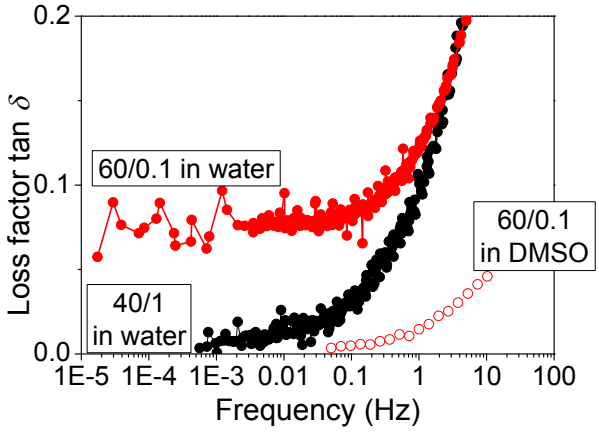

A special feature was observed in the low-frequency loss factor behavior of all studied hydrogels of fused-particles type morphology: an onset of secondary relaxation was revealed in their mechanical spectra. This relaxation disappeared after reswelling in better solvent, DMSO. It was neither observed in case of highly porous interlocking samples, which did not bear a network of fused particles.

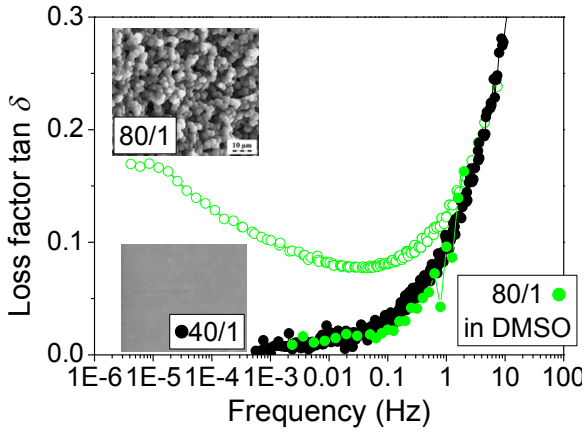

That the low-frequency relaxation maximum was only observed for particulate samples, suggested that long-range coordinated movements of substructures (dangling aggregates of collated polymer particles) were responsible for it, and void (solvent-filled) space facilitated such movements. After swelling in better solvent, the movement of such aggregates was constrained due to either less void space or due to increase of the moving part weight (which should lead to relaxation at much lower frequency, not reached experimentally).

It was found that conditions of measurement, in particular, gap between the measuring plates of rheometer, were crucial for correct measurement of mechanical response of soft hydrogels. Optimal measuring gap did not correspond exactly to the sample thickness as reaching the *no slippage* between sample and measuring geometry condition demanded certain small compression of the sample. However, too strong compression caused squeezing out water and thus incorrect measurement results. A special procedure to find the optimal value of compression from the measuring system response was developed and applied in this work. The gap settings significantly influenced the measured values. If the gap size was set with even 2% deviation from the optimal position (50 μm for the sample of 3 mm thickness), the deviation of measured modulus and loss factor from the correct values could be up to 25%, 100 μm deviation of the gap from the optimal position caused up to 2-fold error in measured values.

6 Bibliography

1. Jones RG. *Pure Appl Chem* 79:1801-1829 (2007)

2. Woodhouse JC. United States Patent 2129722, 09/13/1938.

3. Wichterle O, Lím D. *Nature* 185:117–118 (1960).

4. Voldrich Z, Tománek Z, Vacík J, Kopecek J. *J Biomed Mater Res* 9:675-685 (1975).

5. Chaterji S, Kwon IK, Park K. *Prog Polym Sci* 32 1083-1122 (2007).

6. Huo P, Zhou S, Liau C. United States Patent 6030416, 02/29/2000.

7. Weinschank J, Christ R. United States Patent 5331073, 07/19/1994.

8. Van Landuyt KL, Snauwaert J, De Munck J, Peumans M, Yoshida Y, Poitevin A, Coutinho E, Suzuki K, Lambrechts P, Van Meerbeek B. *Biomaterials* 28:3757-3785 (2007).

9. Šprincl L, Kopeček J, Lím D. *J Biomed Mater Res* 4:447-458 (1971).

10. Barvič M., Kliment K. Zavadil M. *J Biomed Mater Res* 1:313-323 (1967).

11. Cerný E, Chromeček A, Opletal A, Papoušek F, Otoupalová, J. *Scripta Med*, 43:63-75 (1970).

12. Šprincl L, Kopeček J, Lím D. *Calc Tiss Res* 13:63-72 (1973).

13. Winter GD, Simpson BJ. *Nature* 223:88-90 (1969).

14. Rubin RM, Marshall JL. *J Biomed Mater Res* 9:375-380 (1975).

15. Woerly S, Marchand R, Lavallee C. *Biomaterials* 11:97-107 (1990).

16. Ronel SH, D'Andrea MJ, Hashiguchi H, Klomp GF, Dobelle WH. *J Biomed Mater Res* 17:855-864 (1983).

17. Klomp GF, Hashiguchi H, Ursell PC, Takeda Y, Taguchi T, Dobelle WH. *J Biomed Res* 17:865-871 (1983).

18. Künzler JF. Hydrogels. In: Encyclopedia of Polymer science and Technology, vol. 2. New York: Wiley-Interscience, 2002. p. 691.

19. Flory PJ. *J Chem Phys* 9:660 (1941).

20. Huggins ML. *J Chem Phys* 9:440 (1941).

21. Koningsveld R, Stockmayer WH, Nies E. Polymer phase diagrams. Oxford: Oxford University Press, 2001. p. 212

22. Wiggins PM. *Prog Polym Sci* 20:1121-1163 (1995).

23. Ruiz J, Mantecon A, Cadiz V. *J Polym Sci Pol Phys* 41:1462-1467 (2003).

24. Müller-Plathe F. *Macromolecules* 31:6721-6723 (1998).

25. Ping ZH, Nguyen QT, Chen SH, Zhou JQ, Ding YD. *Polymer* 42:8461-8467 (2001).

26. Ghi PY, Hill DJT, Whittaker AK. *Biomacromolecules* 3:991-997 (2002).

27. Vackier MC, Hills BP, Rutledge DN. *J Magn Reson* 138:36-42 (1999).

28. Peschier LJC, Bouwstra JA, de Bleyser J, Junginger HE, Leyte JC. *Biomaterials* 14:945-952 (1993).

29. Roorda WE, Bouwstra JA, de Vries MA, Junginger HE. *Biomaterials* 9 494-499 (1988).

30. Pouchly J, Biros J, Benes S. *Macromol Chem* 180:745-760 (1979).

31. Dušek K, Janaček J. *Journal of Appl Polym Sci* 19:3061-3075 (1975).

32. Barcellos IO, Pires ATN, Katime I. *Polymer International* 49:825-830 (2000).

33. Canal T, Peppas NA. *J Biomed Mater Res* 23:1183-1193 (1989)

34. Dušek K, Bohdanecký M, Vošický V. *Collect Czech Chem C* 42:1599-1607 (1977).

35. Dušek K, Sedláček B. *Eur Polym J* 7:1275-1285 (1971).

36. Podgornik A, Štrancar A. Convective interaction media (CIM): Short layer monolithic chromatographic stationary phases. In: El-Gewely MR, editor. Biotechnology Annual Review. Amsterdam: Elsevier, 2005. pp. 281-333.

37. D. Horák, F. Lednický, V. Řehák, and F. Švec, *Journal of Applied Polymer Science*, 1993, **49**, 2041–2050.

38. Bandari R, Knolle W, Prager-Duschke A, Glasel HJ, Buchmeiser MR. *Macromol Chem Phys* 208:1428-1436 (2007).

39. Špánová A, Ritticha B, Horák D, Lenfeld J, Prodělalová J, Sučiková J, Štrumcová S. *J Chromatogr A*, 1009:215-221 (2003).

40. Lydon MD, Minett TW, Tighe BG. *Biomaterials* 6:396-402 (1985).

41. Shin H, Jo S, Mikos AG. *Biomaterials* 24:4353–64 (2003).

42. Kon M, de Visser A.C. *Plast Renconstr Surg* 67:288-294 *(*1981).

43. Bavaresco VP, Zavaglia CAC, Reis MC, Gomes JR. *Wear* 265:269-277 (2008).

44. Malmonge SM, Arruda AC. Artif Organs 24(3):174-178 (2000).

45. Schieker M, Seitz H, Drosse I, Seitz S, Mutschler W. *Eur J Trauma* 32:114–124 (2006).

46. Salgado AJ, Coutinho OP, Reis RL. *Macromol Biosci* 4:743–765 (2004).

47. Flynn L, Dalton PD, Shoichet MS *Biomaterials* 24 4265–4272 (2003).

48. Lesny P, Croos JD, Pradny M, Vacik J, Michalek J, Woerly S, Sykova E. *J Chem Neuroanatomy* 23:243–247 (2002).

49. Yu TT. Shoichet MS. *Biomaterials* 26:1507-1514 (2005).

50. Dixit V. *Artif Organs* 18(5):371-384, (2008).

51. LePage EB, Lane R, McKay D, Rozga J, Demetriou AA. *J Clinic Apheresis* 10:70-75 (1995).

52. Šprincl L, Vacik J, Kopeček J. *J Biomed Mater Res* 7:123-136 (1973).

53. Cima LG, Vacanti JP, Vacanti C, Ingber D, Mooney D, Langer R. *J Biomech Eng*; 113:143-51 1991.

54. Klawitter JJ, Hulbert SF. *J Biomed Mater Res Symp* 2:161–229 (1971).

55. Wake MC, Patrick CW, Mikos AG. *Cell Transplant* 3:339-43 (1994).

56. Mooney DJ, Baldwin DF, Suh NP, Vacanti JP, Langer R. *Biomaterials* 17:1417–1422 (1996).

57. Colton CK. *Cell Transplant* 4:415-436 (1995).

58. Přádný M, Šlouf M, Martinová L, Michálek J. *e-Polymer* no.043 (2005).

59. Strohalm J, Kopeček J. *Angew Makromolekul Chem* 70:109-118 (1978).

60. Kwok AY, Neo SA, Qiao GG, Solomon DH. *J Appl Polym Sci* 98:1462-1468 (2005).

61. Dušek K. *J Polym Sci Pol Lett* 16:1289-1299 (1967).

62. Kwok AY, Qiao GG, Solomon DH. *Polymer* 45:4017-4027 (2004).

63. Dusek K. Network formation in chain crosslinking (co)polymerization. In: Haward RN, editor. Developments in polymerization, vol. 3. London: Applied Science, 1982. pp. 143-206

64. Okay O. *Prog Polym Sci* 25:711–779 (2000).

65. Chirila TV, Chen YC, Griffin BJ, Constable IJ. *Polym Int* 32:221-232 (1993).

66. Danilatos GD. *Microsc Res Tech* 25:529-534 (1993).

67. Hasa J, Janaček J. *J Polym Sci Pol Lett* 16:317-328 (1967).

68. Kopeček J, Lim D. *J Polym Sci A1* 9:147-154 (1971).

69. Warren TC, Prins W. *Macromolecules* 5:506-512 (1972).

70. Liu Q, Hedberg EL, Liu Z, Bahulekar R, Meszlenyi RK, Mikos AG. *Biomaterials* 21:2163-2169 (2000).

71. Clayton AB, Chirila TV, Dalton PD. *Polym Int* 42:45-56 (1997).

72. Lou X, Dalton PD, Chirila TV. *J Mater-Sci Mater Med* 11:319-325 (2000).

73. Studenovská H, Vodiička P, Proks V,. Hlučilova J, Motlík J, Rypacek F. *J Tissue Eng Regen M* 4:454-463 (2010).

74. Krauch CH, Sanner A. *Naturwissenschaften* 55:539-540 (1968).

75. Oxley HR, Corkhill PH, Fitton JH, Tighe BJ. *Biomaterials* 14:1064-1072 (1993).

76. Přádný M, Lesný P, Fiala J, Vacík J, Šlouf M, Michálek J, Syková E. *Collect Czech Chem C* 68:812-822 (2003).

77. Přádný M, Lesný P, Smetana J, Vacík J, Šlouf M, Michálek J, Syková E. *J Mater-Sci Mater Med* 16:767-773 (2005).

78. Studenovská H, Šlouf M, Rypáček F. *J Mater Sci Mater Med* 19:615-621 (2008).

79. Vidaurre A, Cortazar IC, Ribelles JLG. *J Non-Cryst Solids* 353:1095-1100 (2007).

80. Lozinsky VI, Plieva FM, Galaev IY, Mattiasson B. *Bioseparation* 10:163-188 (2001).

81. Lozinsky VI. Russ Chem Rev 71:489–511 (2002)

82. Savina IN, Cnudde V, D'Hollander S, Hoorebeke LV, Mattiasson B, Galaev IY, Prez FD. Soft Matter 3:1176–1184 (2007).

83. Plieva FM, Ekstrom P, Galaev IY, Mattiasson B. *Soft Matter* 4:2418-2428 (2008).

84. Dainiak MB, Kumar A, Galaev IY, Mattiasson B. *Proc Natl Acad Sci* USA 103:849-54 (2006).

85. Plieva FM, Karlsson M, Aguilar MR, Gomez D, Mikhalovsky S, Galaev IY. *Soft Matter* 1:303–309 (2005).

86. Ozmen MM, Okay O. *Polymer* 46:8119–8127 (2005).

87. Saha K, Keung AJ, Irwin EF, Li Y, Little L, Schaffer DV, Healy KE. *Biophys J* 95:4426–4438 (2008).

88. Butler DL, Goldstein SA, Guilak F. *T Am Soc Mech Eng* 122:570-575 (2000).

89. ASTM Standard D7271, 2006, "Standard Test Method for Viscoelastic Properties of Paste Ink Vehicle Using an Oscillatory Rheometer", ASTM International, West Conshohocken, PA, 2006, DOI: 10.1520/D7271-06, www.astm.org

90. ASTM Standard D4440, 2008, "Standard Test Method for Plastics: Dynamic Mechanical Properties Melt Rheology", ASTM International, West Conshohocken, PA, 2008, DOI: 10.1520/D4440-08, www.astm.org

91. Wrolstad RE, editor. Current protocols in food analytical chemistry. New York: Wiley, 2007. Units H3.1-H3.3.

92. Lou X, van Coppenhagen C. *Polym Int* 50:319-325 (2001).

93. Clayton AB, Chirila TV, Lou X. *Polym Int* 44:201-207 (1997).

94. Chirila TV, Yu DY, Chen YC, Crawford GJ. *J Biomed Mater Res* 29:1029-1032 (1995).

95. Figura LO, Teixeira AA. Food physics. Physical properties – measurements and applications. Berlin: Springer-Verlag, 2007.

96. Bostan L, Trunfio-Sfarghiu AM, Verestiuc L, Popa MI, Munteanu F, Rieu JP, Berthier Y. *Tribology Int* 46:215-224 (2012).

97. Normand V, Ravey JC. *Rheol Acta* 36:610-617 (1997).

98. Zolzer U, Eicke HF *Rheol Acta* 32:104-107 (1993).

99. Ferry JD. Viscoelastic Properties of Polymers, 3rd edition. New York: John Wiley and Sons, 1980.

100. Kavanagh GM, Ross-Murphy SB. *Prog Polym Sci* 23:533-562 (1998).

101. Kopeček J, Lim D. *Collect Czech Chem C* 35:3394-3398 (1971).

102. Janáček J, Ferry JD. *Macromolecules* 2:370-378 (1969).

103. Janáček J, Ferry JD. *Macromolecules* 2:379-385 (1969).

104. Dušek K, Bohdanecký M, Prokopová E. *Eur Polym J* 10:239-247 (1974).

105. Janaček J. *J Macromol Sci Rev Macrormol Chem C* 9:147 (1973).

106. Gotoh T, Nakatani Y, Sakohara S. *J Appl Polym Sci* 69:895-906 (1998).

107. Lee WF, Lin YH. *J Appl Polym Sci* 102:5490-5499 (2006).

108. Perera DI, Shanks RA. *Polym Int* 39:121-127 (1996).

109. Lou X, Chirila TV, Clayton AB. *Eur J Polym Mater* 37:1-14 (1997).

110. http://www.malvern.com/labeng/products/bohlin/gemini/geminihr/geminihr.htm (accessed 01 October 2012)

111. Titze IR, Klemuk SA, Gray SD. *J Acoust Soc Am* 115: 392-401 (2004).

112. Kirschenmann L, Pechhold W. *Rheol Acta* 41:362–368 (2002).

113. Karpushkin E, Dušková-Smrčková M, Remmler T, Lapčíková M, Dušek K. *Polym Int* 61(2): 328-336 (2012).

114. Dušek K, Dušková-Smrčková M. *Prog Polym Sci* 25:1215-1260 (2000).

115. Treloar LRG. The physics of rubber elasticity. New York: Oxford University Press, 1975.

116. Pradas MM, Ribelle JLGs, Aroca AS, Ferrer GG, Antón JS, Pissis P. *Colloid Polym Sci* 279:323-330 (2001).

117. Pissis P, Kyritsi A, Konsta AA, Daoukaki D. *J Mol Struct* 479:163-175 (1999).

118. Puig LJ, Sanchez-Diaz JC, Villacampa M, Mendizabal E, Puig JE, Aguiar A, Katime I. *J Colloid Interf Sci* 235:278–282 (2001).

119. Franks F, editor. Water: A Comprehensive Treatise, vol. 7. New York and London: Plenum Press, 1982 (chapter 1).

120. Meyvis TKL, De Smedt SC, Demeester J, Hennink WE. *J Rheol* 43:933-950 (1999).

121. Jolliffe IT. Principal Component Analysis (Springer series in statistics). New York: Springer-Verlag, 2002.

122. Wold S, Esbessen K, Geladi P. *Chemometr Intell Lab* 2:37-52 (1987).

123. Abdi H, Williams LJ, *WIREs Comput Stat* 2:433-456 (2010).

7 List of Tables

8 List of Figures

4.5 IR spectra of HEMA/DEGDMA/water mixture, final swollen hydrogel, and their difference spectra (a). Conversion of C=C bonds in time followed by IR (b). Sample composition was 80/0.1.

4.6 Sol fraction in the hydrogels prepared from HEMA/DEGDMA/water mixtures, determined by extraction with water.

4.7 Appearance and morphology of gels prepared with water as diluent, and swollen in water to equilibrium.

4.8 ESEM pictures showing morphology of hydrogels prepared with 70 wt% and 80 wt% of water as diluent and various crosslinker concentrations, observed at equilibrium swollen state in water.

4.9 ESEM images of the 60/5 hydrogel swollen in water.

4.10 Morphology by SEM of 70/2 gels prepared with aqueous $Mg(ClO_4)_2$ of varied concentration as diluent, and swollen in water.

4.11 SEM and light microscopy pictures of 40/1 hydrogels prepared with water or 0.6 M aqueous NaCl as diluent, and swollen in water.

4.12 Morphology by SEM of 70/2 gels prepared with aqueous NaCl of varied concentration as diluent, and swollen in water.

4.13 Morphology by SEM of 60/1 hydrogel samples prepared with aqueous NaCl of varied concentration as diluent, and reswollen in water.

4.14 Scheme of gel morphologies (SEM) prepared in diluent of decreasing solvating power, and reswollen in water.

4.15 Scheme of gel morphologies (SEM) prepared in diluent of increasing solvating power, and reswollen in water.

4.16 Equilibrium water content in swollen hydrogels as a function of crosslinker concentration.

4.17 Equilibrium **v**olume of swollen gel per volume of the dry polymer vs. the reciprocal volume fraction of the monomer in the initial mixture corrected for polymerization contraction.

4.18 Equilibrium swelling of hydrogels in water. Sample compositions: 40/1 prepared with aqueous NaCl as diluent, and 70/2 prepared with aqueous $Mg(ClO_4)_2$ as diluent.

4.19 Equilibrium swelling in water. Sample composition 60/1 prepared with aqueous NaCl as diluent. Inserts illustrate morphology type of final gel at corresponding diluent quality.

4.20 Elastic and viscous shear moduli, and loss factor tan δ for water-swollen homogeneous gel 40/1. Equilibrium swelling of the sample was 0.371

4.21 Elastic and viscous shear moduli, and loss factor tan δ for water-swollen homogeneous gel 40/1 and water-swollen intermediate gel 40/5. Equilibrium swelling was: 0.371 (40/1) and 0.338 (40/5).

4.22 Elastic and viscous shear moduli, and loss factor tan δ for water-swollen homogeneous gels 40/1 and 40/0.1. Equilibrium swelling was: 0.371 (40/1) and 0.390 (40/0.1).

4.23 Elastic and viscous shear moduli, and loss factor tan δ for water-swollen homogeneous gel 40/1 and water-swollen particulate gel 80/1. Equilibrium swelling was: 0.371 (40/1) and 0.724 (80/1).

4.24 (a) Elastic shear modulus and (b) loss factor tan δ for homogeneous gel 40/1 swollen in water, DMSO or 3M aqueous NaCl.

4.25 Elastic shear modulus at 0.1 Hz (close to equilibrium) for hydrogels prepared with 2 mol% of the crosslinker and varied dilution, and swollen in water to equilibrium.

4.26 Elastic shear modulus at 0.1 Hz (close to equilibrium) for hydrogels prepared with varied concentration of water and crosslinker, and swollen in water to equilibrium.

4.27 Elastic shear modulus at 0.1 Hz (close to equilibrium) for hydrogels prepared with 70 wt% of water and varied crosslinker concentration, and swollen in water to equilibrium.

4.28 Storage shear modulus at 0.1 Hz as a function of crosslinker concentration for hydrogels prepared with water as diluent and swollen in water.

4.29 (a, c) Elastic shear modulus at 0.1 Hz and (b) equilibrium swelling in water for hydrogels 40/1, 60/1, 70/2 prepared with aqueous (a, b) $Mg(ClO_4)_2$ or (c, d) NaCl of varied concentration as diluent, and reswollen in water.

4.30 Concentration of elastically active network chains determined experimentally and ideal concentration of elastically active network chains.

4.31 Concentration of EANC determined experimentally for water-swollen gels and ideal concentration of EANC.

4.32 SEM image of fused–sphere like macroporous gel (sample 80/0.1). Sketch visualizes necks connecting particles as loci of higher stress causing larger deformation, and large dangling structures.

4.33 Frequency dependences of loss factor for hydrogels prepared with 1 mol% of crosslinker and variable initial concentration of water as diluent, and swollen in water.

4.34 Frequency dependences of loss factor for hydrogels prepared with 40 wt% of water as diluent and variable concentration of crosslinker, and swollen in water.

4.35 Loss factor measured at 10 Hz (a) and at 0.1 Hz (b) as function of crosslinker concentration CC and initial water content IWC for hydrogels prepared with water as diluent and swollen in water.

4.36 The heat capacity of swollen polyHEMA gels (40/0.5, 40/1. 40/5) dependences on temperature.

4.37 Loss factor tan δ for hydrogels prepared at 1 mol% crosslinker and variable concentration of water, reswollen in 3M NaCl to equilibrium.

4.38 The DSC (standard mode) traces of water crystallization in polyHEMA swollen gels 40/1, 50/1 and 60/1.

4.39 Low-frequency loss factors for representative examples of particulate, lightly crosslinked and other hydrogels, swollen in water to equilibrium.

4.40 Low frequency behavior of loss factor for fused-particles type hydrogels swollen in water to equilibrium.

4.41 Low frequency behavior of loss factor for hydrogels prepared with 60 wt% of diluent (aqueous NaCl of varied concentration) and 1 mol% of crosslinker, and swollen in water to equilibrium.

4.42 Light microscopy pictures for water-swollen sample 80/1 (left, macropores and gel particles are observed) and DMSO-swollen sample 80/1 (particles are larger, and more collated).

10.1 The complex shear modulus variation with increasing compression of the sample 40/1.0.

10.2 Frequency sweeps of G' (a) and G'' (b) at different normal compressions of sample 40/1.0: 0, 0.04 and 0.05.

10.3 Normal force and complex shear modulus dependences on sample 75/1.0 normal compression.

10.4 Amplitude sweep oscillatory shear test at different compressive deformations of sample 75/1.0 (heterogeneous).

10.5 Phase angle profiles at selected frequencies (indicated near the corresponding curves) for sample 75/1.0 at different compressive deformations (0.00 to 0.65).

10.6 Equilibrium swelling of selected hydrogels in water at different temperatures.

10.7 Elastic shear modulus (a), viscous shear modulus (b) and loss factor (c) for hydrogels prepared with 40 wt% of water as diluent and variable concentration of crosslinker, and swollen in water. Curves are result of time-temperature superpositions (measurements at 5-70 °C were shifted to a reference temperature of 25 °C).

10.8 Frequency dependences of loss factor for the gels 40/0 (a) and 80/1 (b) swollen in water to equilibrium. Open symbols are result of time-temperature superpositions (measurements at 5-70 °C were shifted to a reference temperature of 25 °C), full symbols are result of direct measurements at 25 °C in conventional mode (down to 10^{-4} Hz), or in PRV mode (up to 10^{3} Hz, 40/0 sample only).

10.9 Creep compliance curves for hydrogels prepared with various concentrations of water and crosslinker, sampled at 25 °C. Curves were referenced to the equilibrium creep compliance deduced from fitting according to Eq. 10.1.

10.10 Creep compliance curves from Fig. 10.9 colored according to classification (Tab 10.1).

10.11 Comparison of gel point and phase separation time.

10.12 Classification of hydrogels based on EWC.

10.13 Classification of hydrogels based on dynamic shear properties in forced oscillation mode.

10.14 Classification of hydrogels based on creep measurement.

10.15 Variance of the analyzed data matrix captured by subsequent principal components.

10.16 Loadings plots of 19 analyzed variables along PC1-PC2 (a) and PC1-PC3 (b).

10.17 Scores plot of the analyzed samples along PC1 and PC2. Scores along PC3 are shown in color mapping.

10.18 Classification of hydrogels based on PCA.

9 Abbreviations and symbols

9.1 Abbreviations

APS – ammonium persulfate
BDMA - 1,4-butanediol dimethacrylate
BHDMA - 2,3-dihydroxybutane 1,4-dimethacrylate
DEGDMA – di(ehyleneglycol) dimethacrylate
DSC – differential scanning calorimetry
DVG – 1,5-hexadiene-3,4-diol (divinyl glycol)
EANC – elastically active network chain
EDMA – ethylene glycol di(methacrylate)
ESEM – environmental scanning electron microscopy
EWC – equilibrium water content
HD – 1,5-hexadiene
HDMA – 1,6-hexanedimethacrylate (hexamethylene dimethacrylate)
HEMA - 2-hydroxyethyl methacrylate
LVR – linear viscoelastic region
NMR – nuclear magnetic resonance
PC – principal component
PC1 (PC2, PC3, …) – principal component 1 (2, 3, …)
PCA – principal component analysis
PRV – piezo-rotatory vibrator
SEM – environmental scanning electron microscopy
SMBS – sodium metabisulfite
TEMED – M,N,N',N'-tetramethylethylenediamine
UTS – ultimate tensile stress
WC (or WC*) – water content
polyHEMA - poly(2-hydroxyethyl methacrylate)

9.2 Symbols

ΔG_m - free (Gibbs) energy of mixing polymer with solvent
Δw – energy difference between polymer-solvent contact and mean of polymer-polymer and solvent-solvent contacts (Flory-Huggins model)
γ – shear strain
γ_0 – shear strain amplitude
δ – phase shift (angle)
ε – extension (compression) strain
ε_{comp} – compressive deformation in the normal direction
μ – chemical potential (partial Gibbs energy)
η – viscosity
ν_{chem} – ideal (theoretical) concentration of the elastically active network chains
ν_e – experimentally determined concentration of the elastically active network chains
σ – stress
σ_0 – initial stress (stress relaxation) or stress amplitude (forced oscillation)
σ_e – residual stress in the generalized Maxwell model
τ – relaxation time

ϕ - volume fraction
ϕ_2 – volume fraction of solvent (diluent)
ϕ_2^0 – volume fraction of solvent (diluent) at preparation state
χ - Flory interaction parameter (Flory-Huggins model)
ω - oscillation frequency
ω_0 - oscillation phase
A – creep fitting parameter
A_i – strain relaxation amplitude (creep fitting parameter)
B - creep fitting parameter
E – Young's modulus
$\boldsymbol{E}$ – residuals matrix in PCA model
G – shear modulus
G^* - complex shear modulus
G' – elastic (storage) shear modulus
G'' – viscous (loss) shear modulus
G_e – equilibrium shear modulus
J – compliance
J_∞ – equilibrium compliance
J_R – reduced creep compliance
$\boldsymbol{P}$ – loadings matrix in PCA model
R – gas constant
T – temperature
T_c – crystallization temperature
$\boldsymbol{T}$ – scores matrix in PCA model
$\boldsymbol{X}$ – data matrix in PCA model
a_T – horizontal shift factor (time-temperature superposition)
b_T – vertical shift factor (time-temperature superposition)
k – Boltzmann constant
m_s – weight of swollen sample
m_d – weight of dry sample
n – number of moles
t – time
t_c – gelation time
z – lattice coordinate number (Flory-Huggins model)

10 Attachments

10.1 Procedure to find a proper gap size for shear rheometry measurement

In simple application-oriented studies using basic rotational rheometry instruments, several types of forces can be imposed on testing material simultaneously and, therefore, stresses and strains are not easily defined. A universal procedure to get setup-independent mechanical properties under well-defined conditions is needed to understand relations between preparation conditions, sample structure, and its properties from the rheometry data.

According to our knowledge, there is no protocol for shear testing of soft non-flowing materials (chemically crosslinked swollen gels) among ASTM standards. The most complete descriptions of gels rheological testing is available in [**91**]. As stated there, two conditions are crucial for correct rheometry of gels: steady state and linear viscoelasticity of shear deformation. Under these conditions, it is possible to obtain a correct mechanical spectrum – a "fingerprint" of the sample. Another complication not mentioned in [**91**] is the choice of spacing between rotating and static rheometer plates (gap, see Fig. 3.1).

For soft solids, gap size determines sample normal deformation and normal force acting on it. This force must be high enough to prevent slippage of the sample and ensure perfect contact with rheometer plates; and sufficiently small not to affect the sample structure. That the sample is not fluid, makes impossible to remove the excess of material after setting a defined gap. The gap issue has been commented in [**120**] where the gap dependence of shear modulus was discussed for homogeneous dextran methacrylate hydrogels (and, to our knowledge, this is the only paper discussing this issue at all). Acceptable measurement conditions were found in [**120**] at compressions[8] $\varepsilon_{\mathrm{comp}} \approx 20\%$. From our results it follows that it is too much for some samples, especially for porous ones.

In the following section our method of finding a proper gap for testing soft solids in their intact state is described.

[8] Normal deformation that results from compressive stress on a sample was defined as the actual gap size related to the uncompressed state: $\varepsilon_{\mathrm{comp}} = (gap_0 - gap)/gap_0$ where gap_0 is the gap size at the initial contact of the sample with the rheometer plates.

10.1.1 Finding gap for homogeneous hydrogel (40/1)

The 40/1 gel sample was chosen as a typical representative of strong homogeneous polyHEMA hydrogel.

Thickness measurement with the digital micrometer at several locations (3.0±0.1 mm) was not reliable; mainly due to sample softness. At the gap of 3.1 mm the instrument showed zero normal force and highly distorted output signal, as the sample was not in contact with the rheometer upper plate. At the gap of 2.9 mm, the normal force was high (7 N or 22 kPa), indicating that the sample might be compressed too much.

Going down stepwise from 3.1 mm, gap_0 was found as a distance at which normal force exceeded the resolution limit of the instrument (0.05 N). At such low normal force, the slippage of the sample (indicated by output signal distortion in the forced oscillation mode) still caused incorrect results. Trials indicated that thrust of ≈ 0.1 N corresponding to the gap of 3.050 mm for the tested sample was enough to prevent sliding (signal harmonic distortion <1%). For comparison, in [**120**] values of 0.1 to 1 N are reported.

Further we analyzed compression-dependent shear moduli by changing the gap in small steps (Fig. 10.1).

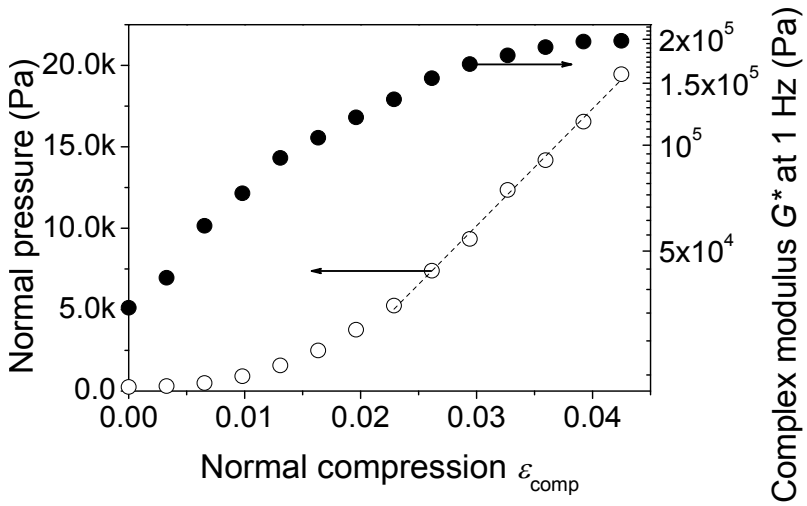

Figure 10.1 *The complex shear modulus variation with increasing compression of the sample 40/1.0. Zero compression was assigned to a gap at which the normal force was 0.05 N. Young's modulus was calculated from the linear part of the normal pressure curve; shear modulus was estimated as a leveled value of G* dependence.*

Starting from ε_{comp} of 2%, from the linear part of the normal force plot, Young's modulus was estimated (E=720±20 kPa). Complex shear modulus reached the constant value of G^*=200±10 kPa at ε_{comp} of 4-5%.

The reason for non-linear behavior under the incipient normal compression could be either structure change, or imperfect shape of the sample and surface defects. We attributed the behavior of the studied gels to the latter, as the tested deformation range were relatively small (up to 6%). The shape of the normal force curve was similar to that reported, for example, in [**71**]. The shear plateau modulus under increasing normal deformation was reported in [**120**]. In that work the authors also related their observations to the inhomogeneity of the sample surface.

In the frequency sweep tests in the linear viscoelastic region (LVR), Fig. 10.2, curves at ε_{comp} =0.04 and ε_{comp} =0.05) were essentially the same, but differed from that at ε_{comp} =0. Thus, at ε_{comp} ≈0.04 real material properties were measured, not the properties related to experimental setup. That the target ε_{comp} for correct measurement was not too high ensured that the measured values were as close to that of intact sample as possible.

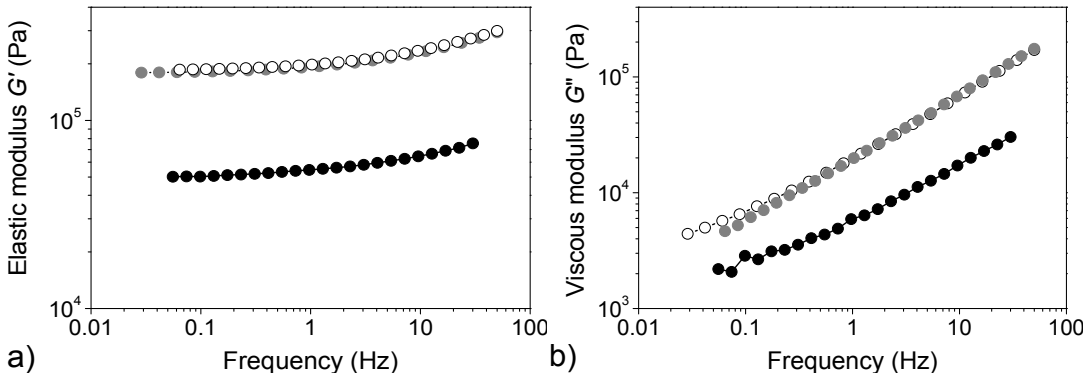

Figure 10.2 *Frequency sweeps of G' (a) and G'' (b) at different normal compressions of sample 40/1.0: 0 (black circles), 0.04 (grey circles) and 0.05 (open circles). Zero compression was assigned to a gap at which normal force was 0.05 N.*

The same ε_{comp} for correct measurement was found from analysis of the shear creep curves in the LVR. Again, at $\varepsilon_{comp} > 0.04$ creep compliance profiles overlapped. After removing the shear stress, creep angle decreased to zero, indicating absence of slippage.

Thus, the gap size should be selected in the "meaningful" region, where the full contact of geometry with the sample was achieved with minimum structure change. For the 40/1 sample, the arbitrary choice of the measurement gap size would result in complex shear modulus in the 5-200 kPa range (Fig. 10.1). Correct gap for rheological studies of macroscopically homogeneous hydrogel 40/1 corresponded to the least compressed state at which the shear modulus was independent of ε_{comp}.

In [**120**] similar conclusion was made but target gap size typically corresponded to 15-20% compression (sandpaper-modified rheometer plates were used, requiring higher normal force for perfect contact with the sample). We observe such "leveling off" at 4-5% of normal compression, and absence of slippage is proved in creep tests. In order to keep the sample structure as intact as possible, using the non-serrated plates that adhere to the tested material (steel for polyHEMA gels) is better than using sandpaper coverage or serrated plates.

10.1.2 Finding gap for particulate macroporous hydrogel (75/1)

Compression-dependent properties of the sample 75/1 were studied as an example of hydrogel containing communicating pores filled with water. It was not possible to reach gap-independent mechanical response in this case (compare Figs. 10.1, 10.3). Normal force increased nearly proportionally to normal compression only from ε_{comp} of 0.5. Shear modulus did not reach constant value up to ε_{comp} of 0.65. Evidently, normal force induced pushing out of water, thus changing the sample morphology (total pore volume) and affecting its mechanical properties.

To find the proper gap size, the balance should be found between achieving the best sample-plates contact and dewatering of the sample accompanied by pore volume and shape change.

At the amplitude sweeps at ε_{comp} in the range of 0 to 0.65 (Fig. 10.4), the *G'* steadily increased with compression, and the linear viscoelastic region was wider than at $\varepsilon_{comp} = 0$. Starting from $\varepsilon_{comp} = 0.17$, the LVR range of strains remained constant. We attributed the broadening of LVR to improving the sample-plates contact, while further modulus increase at constant upper limit of LVR was ascribed to sample dewatering. If so, gap size for correct measurement of shear properties corresponded to the lowest normal deformation at which the LVR reached the constant strain range. However, this method was very approximate and meticulous.

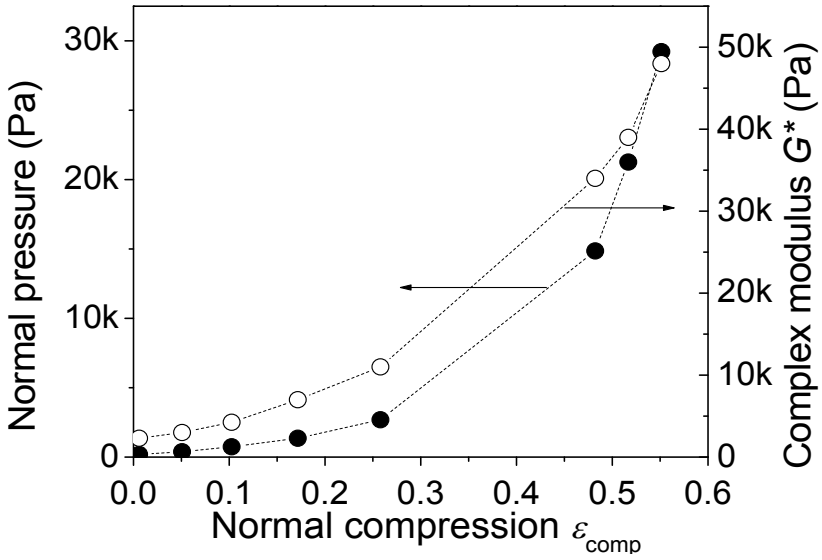

Figure 10.3 *Normal force and complex shear modulus dependences on sample 75/1.0 normal compression. Zero compression was assigned to a gap at which the normal pressure was 0.05 N.*

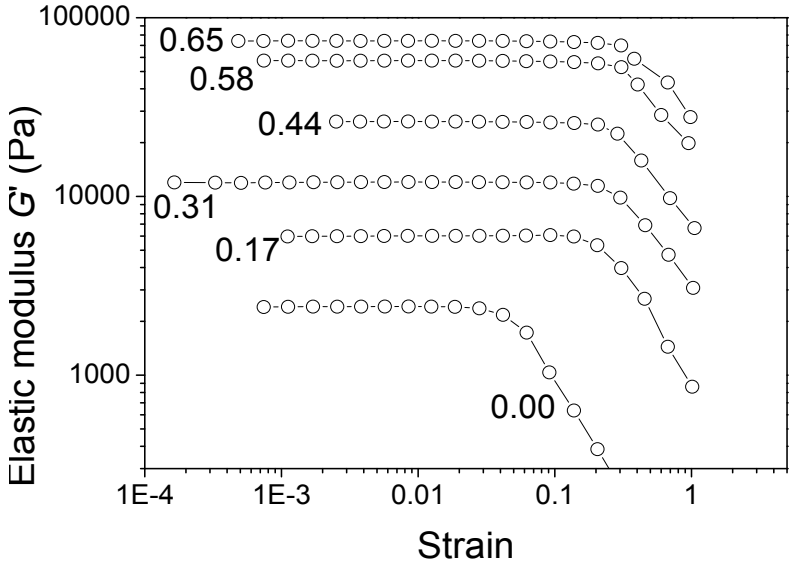

Figure 10.4 *Amplitude sweep oscillatory shear test at different compressive deformations of sample 75/1.0 (heterogeneous). Sample compressive deformation is indicated near the curve. Zero compression was assigned to a gap at which normal pressure was 0.05 N.*

Analysis of frequency sweeps at different ε_{comp} seemed more convenient. For particulate sample 75/1, the frequency sweep profiles were compression-dependent

over the whole range of studied normal deformations. The loss factors at the three selected frequencies are shown in the Fig. 10.5.

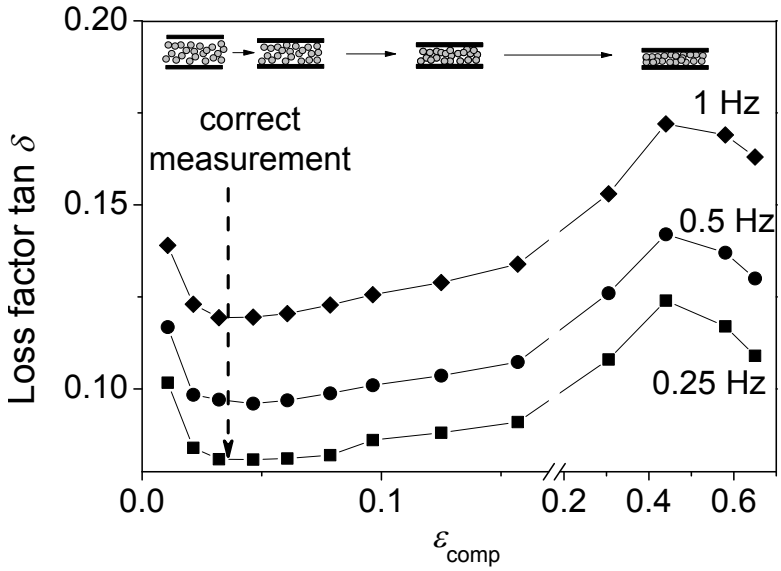

Figure 10.5 *Phase angle profiles at selected frequencies (indicated near the corresponding curves) for sample 75/1.0 at different compressive deformations (0.00 to 0.65). Zero compression was assigned to a gap at which normal pressure was 0.05 N.*

At ε_{comp} of 0.00 to 0.03-0.05, the phase angle decreased, due to improving contact of a sample with the rheometer plates and vanishing impact of direct contact with surrounding water. Then phase angle curves showed a plateau (at ε_{comp}=0.03-0.07), when the contact was very good, and the change of hydrogel morphology was negligible. At higher ε_{comp} (0.07 to 0.4), phase angle started to grow; this could be ascribed to pushing out of water. Further phase angle decrease should be ascribed to further morphology changes due to compression of sample with free water in voids practically pushed out.

10.1.3 Conclusion on gap size finding procedure

The procedures to determine proper gap are different for 40/1 (homogeneous) and 75/1 (heterogeneous, particulate) hydrogels. In both cases, the ultimate appeal is to find a balance between improving the contact between the sample and the rheometer plates, and sample dewatering and structure changing.

Correct gap for rheological studies of macroscopically homogeneous hydrogel 40/1 corresponds to the least compressed state at which the shear modulus was independent of ε_{comp}.

Correct gap for rheological studies of particulate sample with communicating pores is found at the least compressed state in the range of ε_{comp}. where phase angle is relatively independent of compression.

Noteworthy, for majority of the samples studied target gap corresponded to ε_{comp} of 3-4%, which (taking into account variety of samples morphology and similarity of preparation procedure) supported the assumption that compression dependence of measured rheological properties was due to sample shape and surface roughness.

10.2 Time-temperature superposition

Time temperature superposition (or time-frequency superposition, or method of reduced variables) is a procedure to expand the time or frequency range, at which a material properties are studied at a given temperature. This technique involves the use of temperature-dependent shift factors for measured material functions (vertical shift factor, b_T) and for time or frequency (horizontal shift factor, a_T). If time-temperature superposition is obeyed, the use of shift factor will yield a master curve showing viscoelastic behavior over a larger range of time scales than could be studied using a single-temperature measurement. For example, a master curve for the elastic shear modulus G' measured over a range of T is obtained by plotting $b_T G'(T)$ as a function of $a_T \omega$ using logarithmic scales on both axis.

According to [**99**], the time-temperature superposition is applicable when the various relaxation times related to a given relaxation process have the same temperature dependence which usually holds in terminal and plateau zones, and, to a fair extend, in the transition zone (but the temperature dependence of the shift factors may be different). In practice, the validity of time-temperature superposition may be judged about with several semi-qualitative criteria:

- accuracy of matching of adjacent curves measured at different temperatures, when superimposed;
- validity of the same shift factors for all viscoelastic functions;
- reasonable form (Arrhenius or Williams-Landell-Ferry) of the shift factors temperature dependence.

For the polyHEMA hydrogels change of swelling with temperature, and approaching to glass transition at the lower edge of temperatures investigated (5-10 °C) could potentially lead to incorrect time-temperature superposition result.

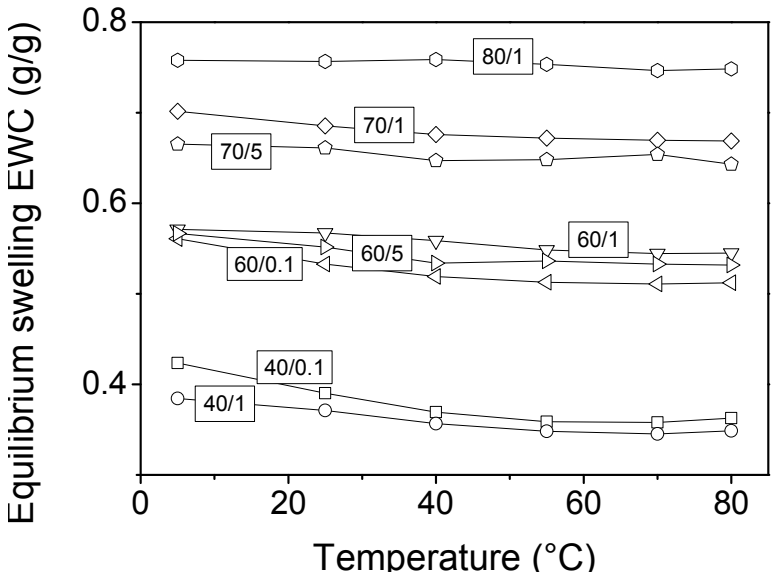

Figure 10.6 *Equilibrium swelling of selected hydrogels in water at different temperatures.*

According to EWC measured over a range of temperatures (Fig. 10.6), the change in swelling in comparison with the reference temperature (25 °C) did not exceed 5% (being the most pronounced for samples prepared at low dilution).

The results of automatic frequency-temperature superposition (only horizontal shift of the experimental curves, as described in Experimental part) compared with manual superposition (arbitrary vertical shifts applied to produce visually best match) showed no significant difference. Therefore, no vertical shift was applied in this work.

The horizontal shift factors calculated for G'' produced also reasonably smooth G' and tan δ master curves (see example in the Fig. 10.7 for series of samples prepared with IWC = 40 wt% and variable amount of the crosslinker)

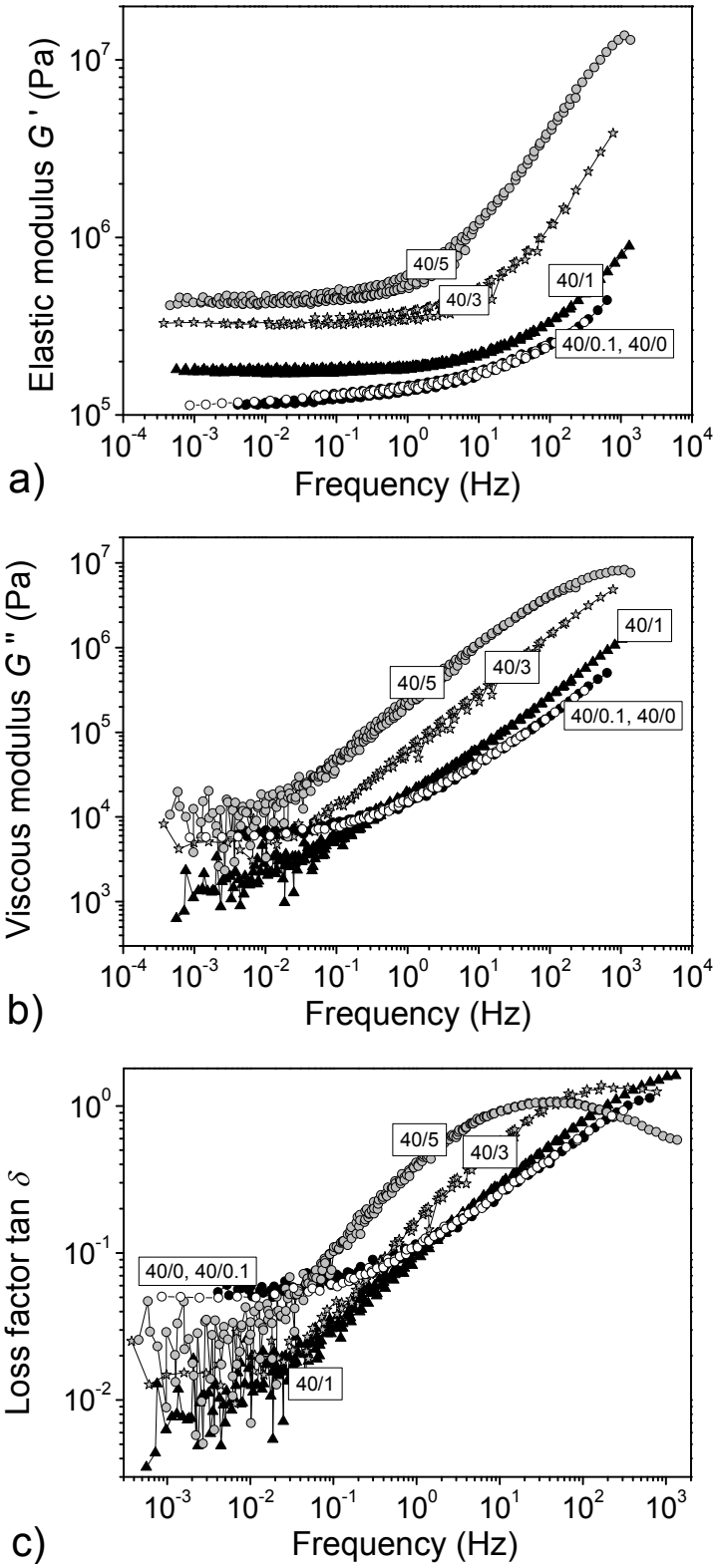

Figure 10.7 *Elastic shear modulus (a), viscous shear modulus (b) and loss factor (c) for hydrogels prepared with 40 wt% of water as diluent and variable concentration of crosslinker, and swollen in water. Curves are result of time-temperature superpositions (measurements at 5-70 °C were shifted to a reference temperature of 25 °C).*

Two characteristic samples – 40/0 homogeneous and 80/1 highly porous – were selected for comparison of the superimposed and directly measured loss factors. The behavior the 40/0 sample was characterized by low tan δ below 1 Hz and well developed increase of tan δ in the high-frequency region towards the glass transition. The 80/1 sample was characterized by larger losses in the low frequency region, with a pronounced increase at high frequency, similar to 40/0, and a weaker increase below 10^{-2} Hz (secondary relaxation).

In both cases (Fig. 10.8), the superimposed and directly measured dependences could not be distinguished from one another within the experimental accuracy. Thus, in this special case of swollen polyHEMA network, when the swelling changes were not of large magnitude the time-temperature superposition could be applied to achieve the enhanced range of shear oscillation frequencies within reasonable testing time.

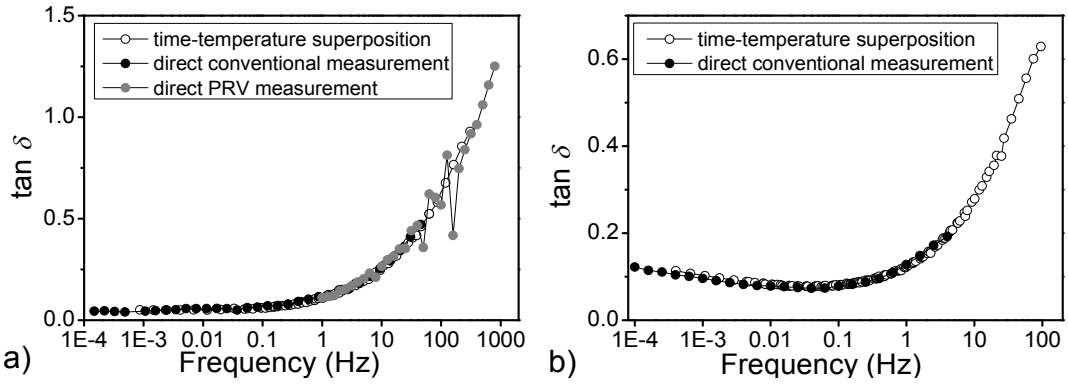

Figure 10.8 *Frequency dependences of loss factor for the gels 40/0 (a) and 80/1 (b) swollen in water to equilibrium. Open symbols are result of time-temperature superpositions (measurements at 5-70 °C were shifted to a reference temperature of 25 °C), full symbols are result of direct measurements at 25 °C in conventional mode (down to 10^{-4} Hz), or in PRV mode (up to 10^{3} Hz, 40/0 sample only).*

10.3 Shear creep measurements

For easier comparison, creep curves were subjected to some post-treatment. Each curve was first fitted with the Eq. 10.1[9]:

[9] The trials showed that biexponential form leads to poor approximation for some curves, while 4th exponent introduced did not increase fitting accuracy.

$$J = J_\infty + Ae^{-Bt}\sin(\omega t + \omega_0) - \sum_{i=1}^{3} A_i e^{-t/\tau_i} \quad (10.1)$$

In Eq. 10.1, τ_i and A_i are strain relaxation times and amplitudes, J_∞ is equilibrium creep compliance, A, B, ω and ω_0 are parameters describing free oscillations of strain [**98**, **99**].

After, the experimental curves were scaled to J_∞ and plotted as $J_R(t) = J(t)/J_\infty$. Plots for all the samples studied are collected in the Fig. 10.9.

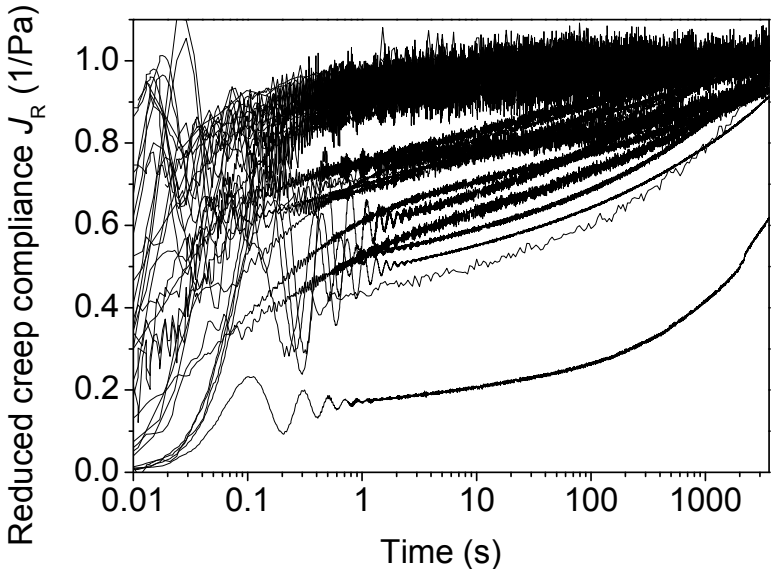

Figure 10.9 *Creep compliance curves for hydrogels prepared with various concentrations of water and crosslinker, sampled at 25 °C. Curves were referenced to the equilibrium creep compliance deduced from fitting according to Eq. 10.1.*

Inspection of the plot revealed characteristic times, creep compliance at which enabled for classification of the samples into 4 qualitatively different groups:

A: fast creep within the whole range of time scales;

B: slow creep at ultra-short time scale, then creep compliance grows very fast;

C: slow creep at short time scale, intermediate creep at longer time scale;

D: slow creep within the whole range of time scales.

Characteristic values of J_R are summarized in the Tab. 10.1, creep curves are colored in accordance with this classification in Fig. 10.10. Classification of the hydrogels into groups A-D according to their shear creep properties is consistent with the change of preparation conditions: initial water concentration IWC and crosslinker concentration CC (Fig. 10.14).

Table 10.1 *Classification of hydrogels prepared with water as diluent according to their shear creep behavior.*

Group code	Relative creep compliance J_R at time scale of		
	~0.05 s	~1 s	~10-100 s
A	fast ($J_R > 0.5$)	fast ($J_R > 0.8$)	fast ($J_R > 0.8$)
B	intermediate (J_R ~0.5)	fast ($J_R > 0.8$)	fast ($J_R > 0.8$)
C	intermediate (J_R ~0.5)	slow ($J_R < 0.8$)	intermediate ($0.7<J_R<0.8$)
D	slow ($J_R < 0.5$)	slow ($J_R < 0.8$)	slow ($J_R < 0.7$)

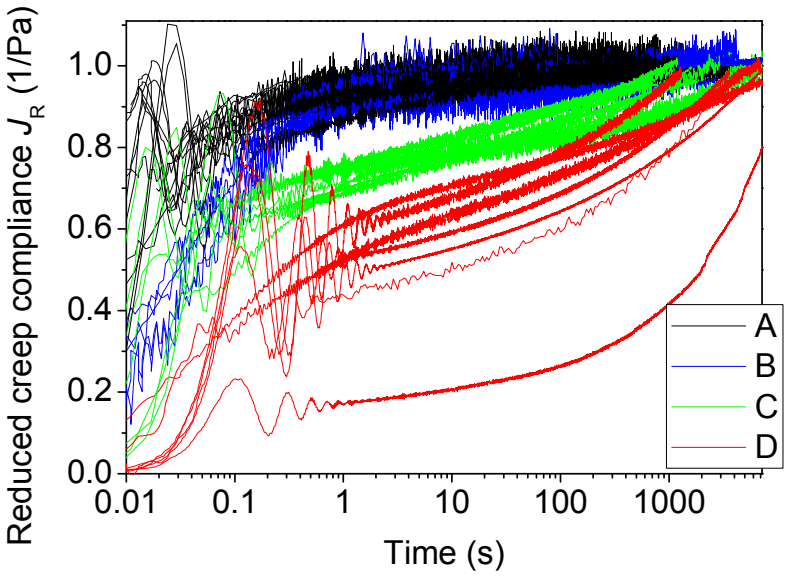

Figure 10.10 *Creep compliance curves from Fig. 10.9 colored according to classification (Tab 10.1).*

10.4 PCA

The idea of principal component analysis (PCA) is to reduce the dimensionality of a data set consisting of interrelated variables, retaining as much as possible of the valuable information. This is achieved by transforming to a new set of variables, the principal components (PCs), which are uncorrelated, and which are ordered so that the first few retain most of the variation present in the original variables.

The goals of PCA are

(1) to extract the most important information from the data table;

(2) to compress the size of the data set by keeping only this important information;

(3) to analyze the structure of the observations and the variables.

PCs are computed as linear combinations of the original variables. The first principal component PC1 is required to have the largest possible variance (therefore it will 'explain' or 'extract' the largest informative part of the data table). The second component PC2 is computed under the constraint of being orthogonal to PC1 and to have the largest possible inertia. The other components are computed likewise. The values of these new variables for the observations are called factor scores, and these scores can be interpreted geometrically as the projections of the observations onto the principal components.

Details of computations are described in a number of reviews [**121-123**]. Briefly, PCA starts from a decomposition of a source data matrix **X** (n×m, n samples in rows and m variables in columns) onto two complementary matrices: scores **T** (n×a) and loadings **P** (m×a) in accordance with

$$\mathbf{X} = \mathbf{T}\mathbf{P}^{\mathrm{T}} + \mathbf{E} = \sum_{i=1}^{a} \mathrm{t}_i \mathrm{p}_i^{\mathrm{T}} + \mathbf{E} \qquad (10.2)$$

where $a << n,m$ is the number of principle components (PCs); t_i (n×1) and p_i (m×1) are the orthogonal/orthonormal vectors, respectively, constituting the matrices **T** and **P.** The matrix product of **T** and $\mathbf{P}^{\mathrm{T}}$ reproduces the most important variance in **X**, leaving the noise (or error) in a residual matrix **E** (n×m). In fact, PCA performs a projection of the X-data onto a lower-, i.e. a-dimensional PC space, where it can be effectively presented and analyzed. The data dimensionality reduction is achieved due to correlations between the source variables in **X**. For this reason the method is specifically advantageous for the analysis of data with a large number of mutually correlated variables.

The matrices **T** and **P** provide valuable information on the internal data structure. Their interpretation is based on the fundamental fact that correlation between two variables or similarity of two samples correspond to the distance between them in the PC-space. Pair-wise scores plots $\mathrm{t}_i - \mathrm{t}_j$, in particular, $\mathrm{t}_1 - \mathrm{t}_2$ as capturing the main data variance, are often referred to as 'sample maps' revealing their grouping and outliers. Similarly, the loadings plots ('variable maps') show the variable correlations. The distance from the origin to a sample in the score or a variable in the loadings plot along a certain PC reflects their importance with regard to this PC. Comparison of respective score and loadings plots helps to find out interrelations between the samples and the variables. In the present work PCA scores have been used to investigate the grouping of samples with regard to their target

properties. Their relation to multiple variables, provided by the loadings, should reveal the effects of experimental factors and compare the efficiencies of analytical methods based on measured properties (Tab. 10.2).

In this work the PCA modeling was performed in the Unscrambler® software, version 9.7.

The following measured properties were used as input variables (see details of their measurement in corresponding sections):

Table 10.2 *Variables input to the Principal Component Analysis.*

Parameter (label in plots)	Description	Units	Range
IWC	Initial water concentration	wt%	[40..80]
CC	Crosslinker concentration	mol%	[0.1..5.0]
EWC	Equilibrium water content	g/g	[0.34; 0.76]
P	Porosity calculated from the EWC	-	[0..0.63]
G'-0.1	*G*' at 0.1 Hz	kPa	[0.82; 430]
G'-1	*G*' at 1.0 Hz	kPa	[0.92; 530]
G'-10	*G*' at 10.0 Hz	kPa	[1.1; 990]
G''-0.1	*G*'' at 0.1 Hz	kPa	[0.073; 47]
G''-1	*G*'' at 1.0 Hz	kPa	[0.12; 210]
G''-10	*G*'' at 10 Hz	kPa	[0.27; 940]
tg-0.1	Loss factor at 0.1 Hz	-	[0.026; 0.23]
tg-1	Loss factor at 1.0 Hz	-	[0.10; 0.48]
tg-10	Loss factor at 10.0 Hz	-	[0.24; 0.96]
J-0.04	J_R at 0.04 s	-	[0.16; 0.88]
J-0.1	J_R at 0.1 s	-	[0.16; 0.91]
J-1	J_R at 1 s	-	[0.17; 0.98]
J-10	J_R at 10 s	-	[0.21; 1.00]
J-100	J_R at 100 s	-	[0.26; 1.00]
CreepG	Equilibrium shear modulus, $1/J_\infty$	kPa	[0.33; 370]
Cr-tmin	Smallest of relaxation times deduced from creep	s	[0.01; 5.5]
Cr-tmax	Largest of relaxation times deduced from creep	s	[0.50; 6000]

As the variables ranges and units were different, before PCA procedure each variable was scaled by its standard deviation and centered (so that the mean across all samples is zero). The purpose of this transformation was to give all variables included in an analysis an equal chance to influence the model, regardless of their original variances.

10.4.1 Classification of hydrogels from different measurements

In this section classifications of gels prepared with water as diluent and swollen in water are presented. Depending on the used method and properties taken into account (gelation and phase separation time, equilibrium swelling, shear properties), analyzed samples have shown distinct areas in the initial dilution – crosslinker concentration maps, revealing groups of gels with similar properties.

Comparison of the **gel point time and phase separation time** for the polymerizing mixtures (Fig. 4.3) showed that at relatively low IWC and CC phase separation did not occur at all till polymerization is over. Increase of initial dilution and/or crosslinker concentration led to phase separation after the gel point, more diluent and/or crosslinker led to earlier phase separation, before formation of the network (Fig. 10.11).

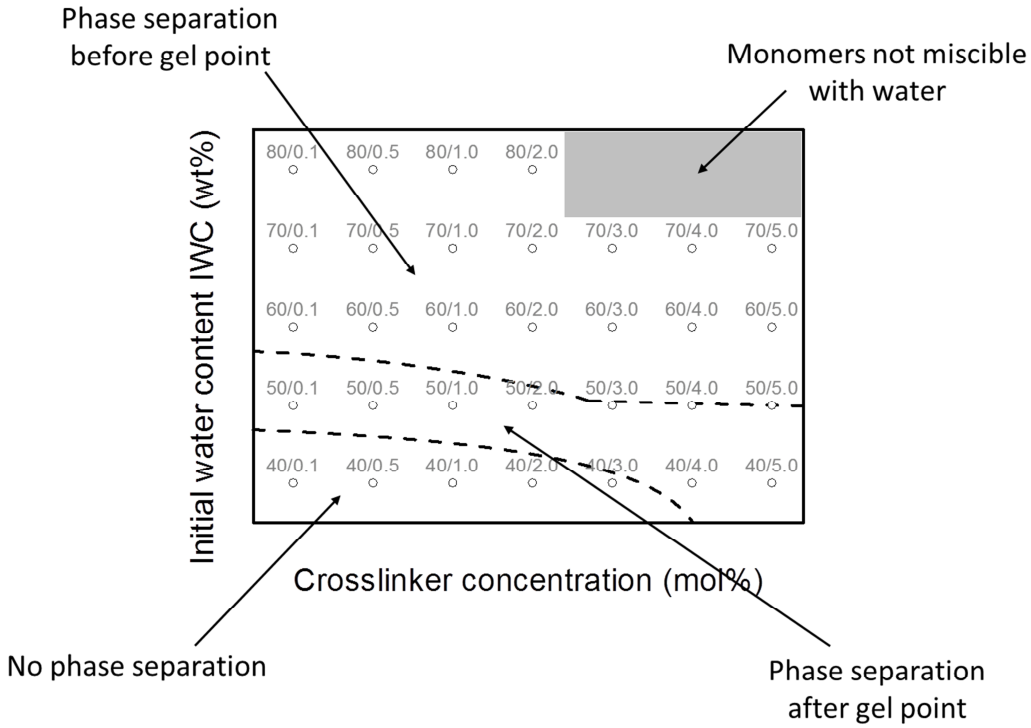

Figure 10.11 *Comparison of gel point and phase separation time. Fractions of water (IWC) and crosslinker DEGDMA (CC) at preparation are indicated in sample codes, IWC/CC.*

According to **swelling behavior** (Fig. 4.16), the samples could be classified into following groups (Fig. 10.12):

A. equilibrium swelling is comparatively low and decreases with increasing crosslinker concentration – behavior expected for gels with small fraction of pores, or non-porous;
B. equilibrium swelling increases with increasing crosslinker concentration – phase separation effect becomes comparable to that of crosslink density;
C. equilibrium swelling is relatively high and almost independent of crosslinker concentration – swelling is determined solely by phase separation, its effect dominates over the crosslink density.

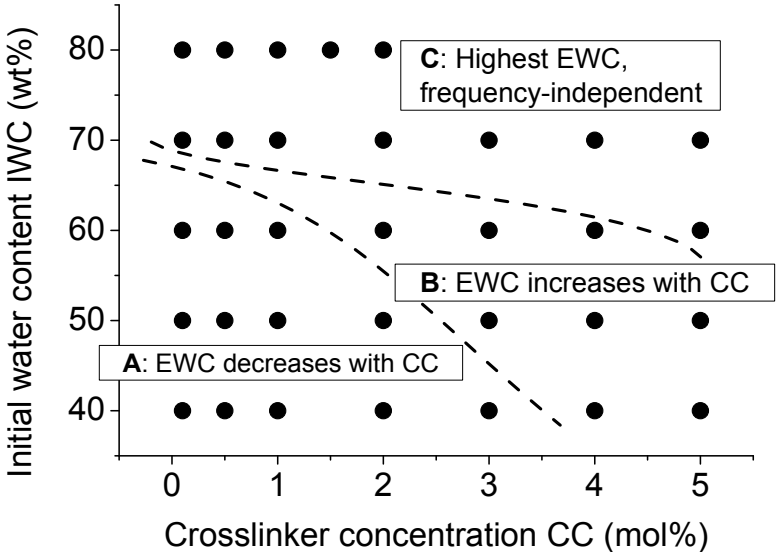

Figure 10.12 *Classification of hydrogels based on EWC. Each point corresponds to hydrogel prepared at given IWC and CC. Bottom line – onset of phase separation as revealed by EWC measurements, upper line divides macroporous and intermediate hydrogels.*

According to **shear properties in the plateau region** (0.1-1 Hz), the hydrogels could be classified as shown in Fig. 10.13. Here the solid line divides two well defined groups of samples. Those above this line possess low dynamic moduli and low-frequency loss factor higher than for homogeneous samples with the same crosslinker content. Dashed line divides the "high-modulus" hydrogels area (under the solid line) into samples with relatively low loss factor, tending to zero within experimental accuracy, and with relatively high loss factors showing plateau at the tan δ plots at lowest frequencies achieved. The trends revealed in mechanical behavior studies in the forced oscillation mode were in general confirmed by **shear creep** studies (Fig. 10.14). Fastest creep over the whole time scales range was

characteristic of samples prepared at intermediate crosslinker content and at low to moderate initial dilution (A). Increase of CC (B) led to significantly slower creep at ultra-short time scale. Most particulate gels (D) showed the slowest creep over the whole time scale. Group C samples with intermediate creep compliance laid in between groups A and D, or at very low crosslinker content area.

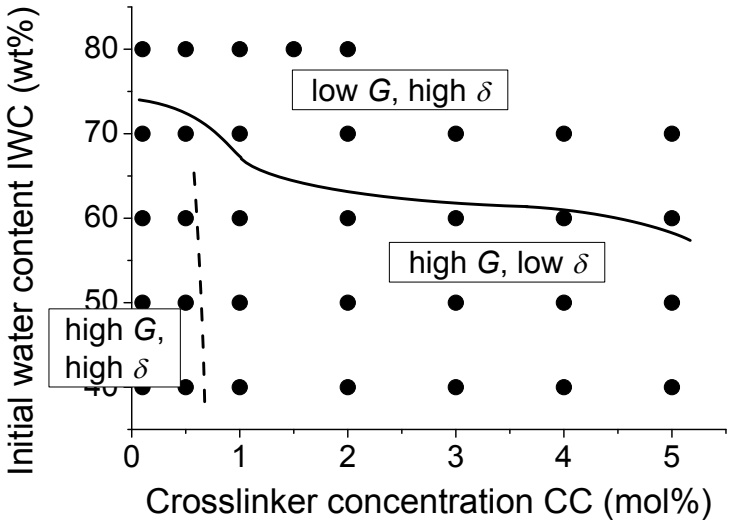

Figure 10.13 *Classification of hydrogels based on dynamic shear properties in forced oscillation mode. Each point corresponds to hydrogel prepared at given IWC and CC. Details are explained in the text.*

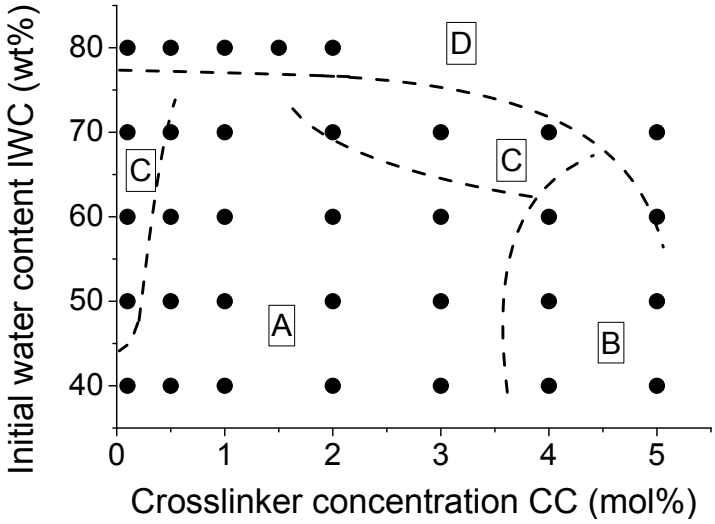

Figure 10.14 *Classification of hydrogels based on creep measurement. Each point corresponds to hydrogel prepared at given IWC and CC. Details are explained in the text.*

10.4.2 Unsupervised PCA

In the PCA model built for 33 samples (preparation with water as diluent and swollen in water) and 19 variables (of the variables listed in Tab 10.1, those related to preparation conditions, IWC and CC, were excluded), almost 93% of data variation was accumulated in first 3 principal components PC (Fig. 10.15). Residual variation was less than expected measurement accuracy, thus 3 first PCs were included into the PCA model for further analysis.

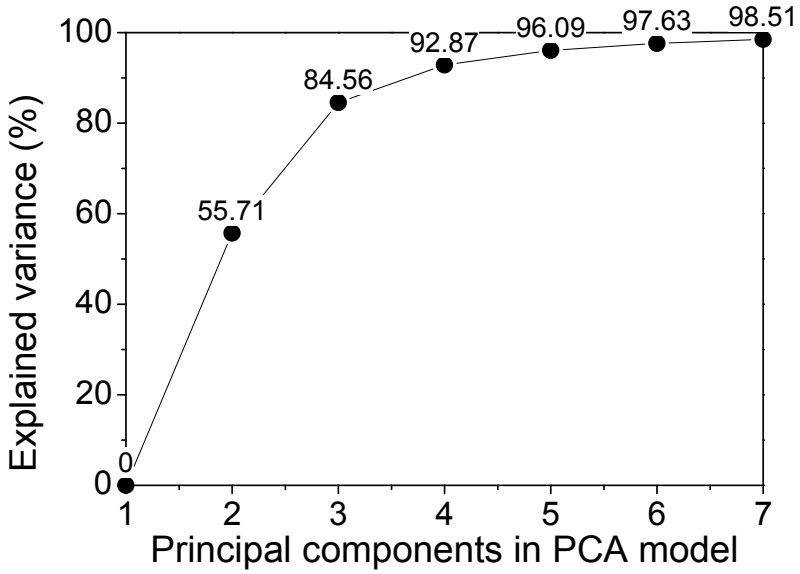

Figure 10.15 *Variance of the analyzed data matrix captured by subsequent principal components.*

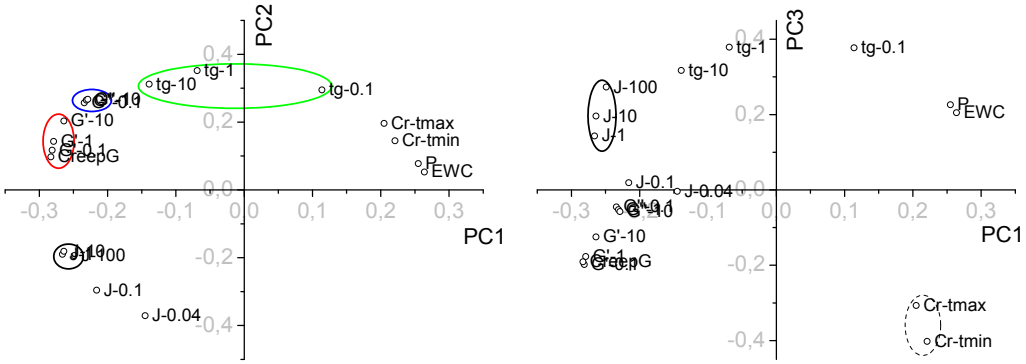

Figure 10.16 *Loadings plots of 19 analyzed variables along PC1-PC2 (a) and PC1-PC3 (b).*

Analysis of the loading plots (Fig. 10.16) assisted in proper choice of variables that were most informative to classify the hydrogels according to their properties. In the loadings plot PC1-PC2 groups of correlated (positively or

negatively) and non-correlated variables were revealed. For example, the elastic shear moduli (red circle) and viscous shear moduli (blue circle) over at least 2 decades of frequency were strongly correlated. Interestingly, their ratios (loss factors, encircled green) measured at 0.1 and 10 Hz were spread over PC1, which captured major part of the data variance. This showed the benefit of frequency sweep oscillation measurements as compared to single-frequency shear, and demonstrated that the loss factor was definitely among the most informative variables to analyse.

The overall porosity P was positively correlated with the EWC, and both were negatively correlated with shear moduli and creep compliance J_R. This was also in line with findings reported in Section 4: more swollen hydrogels were generally more porous, less mechanically strong, and showed slowest creep.

Creep compliance J_R at 1, 10 and 100 s were strongly correlated in the PC1-PC2 space, but showed noticeable difference along PC3 (Fig. 10.16b, black circle). Minimum and maximum creep relaxation times showed similar trend (Fig. 10.16b, dashed circle). This could possibly mean that PC3 captured difference in long-time creep behavior, not observed along PC1 and PC2.

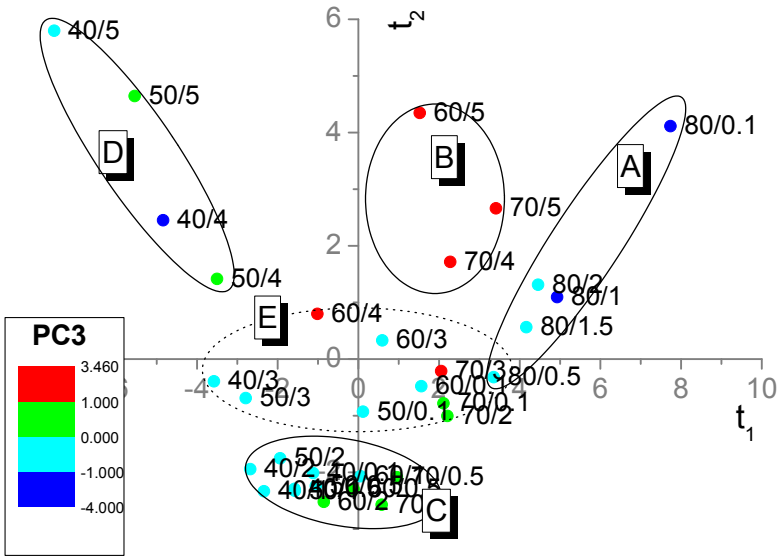

Figure 10.17 *Scores plot of the analyzed samples along PC1 and PC2. Scores along PC3 are shown in color mapping.*

The major result of PCA leading to samples classification according to complex of their properties is the scores plot (Fig. 10. 17). The samples in the scores plot were divided into several groups, consistent with the preparation conditions:

distribution along PC1 was mainly due to IWC, while PC2 was mainly responsible for changes related to CC.

Comparison of scores and loadings plots showed how changes in preparation conditions influenced the properties of final gels. Changing IWC affected mostly EWC and elastic shear modulus, while CC governed almost solely the loss factors at 1-10 Hz and creep compliance at ultra-short time scale. It should be noted that PCA brings no new information to the data set; it only extracts most important features and eliminates noisy (random) variance. Thus, conclusions about influence of preparation conditions on the properties deduced from loadings and scores plots were expected to be similar to those obtained from single-variables analysis, but presented in a convenient graphical form.

Novel information extracted from the PCA plots is that about correlations between variables. Correlated variables cannot be changed independently within the scope of the applied synthetic procedure. For instance it is unlikely to prepare samples with high swelling ability, but low loss factor at low frequencies, or relaxing fast in creep. On the other hand, uncorrelated variables can be changed independently, for example, shear moduli and creep rate at short time scale.

5 groups revealed in the scores plot (Fig. 10.17), and their properties from comparison of scores and loadings plots are listed in Tab. 10.3.

Table 10.3 *Classification of hydrogels prepared with water as diluent from the PCA*.

Group	Preparation conditions, porosity from ESEM	Characteristic properties (from loadings plot)
A	Particulate; prepared with highest IWC	High EWC, low shear moduli, slow creep, high mechanical losses at 0.1 Hz
B	Particulate; prepared with higher CC and lower IWC (compared to A)	High mechanical losses, slow creep
C	Homogeneous and intermediate; prepared with relatively low CC and IWC	Fast creep and low mechanical losses
D	Homogeneous and intermediate; prepared with higher CC (compared to C)	High shear moduli and mechanical losses at 1-10 Hz, low EWC
E	Intermediate composition	Grouping near the origin of PC1-PC2 space: average properties.

Location of group E around origin in PC1-PC2 space meant that they did not show any extreme properties characteristic of any of groups A-D, or these features were mutually compensated (PCA accounts for all the variables simultaneously, in complex). Very likely this corresponds to intermediate, transition situations. For example, samples 40/3 and 50/3 in between groups C and D corresponded to gradual transition from low-crosslinked to highly crosslinked non-porous samples, with properties transitional between those characteristic cases. Same was true for samples in between groups A and C. In this sense group E might represent a set of samples at the borders of distinct groups. On the other hand, pair of samples (60/4, 70/3) that were close to zero along PC1 and PC2 showed up unusually high PC3 scores, and should therefore be assigned to group B. For the same reason (unexpectedly low PC3 score) the 80/0.5 sample likely belonged to the group A

Taking into account these considerations, the classification showed in Fig. 10.18 might be deduced according to the PCA of the studied samples.

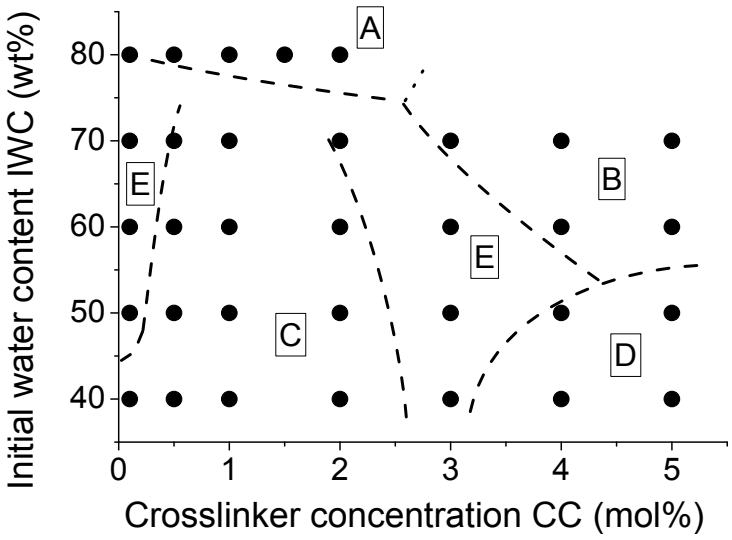

Figure 10.18 *Classification of hydrogels based on PCA. Each point corresponds to hydrogel prepared at given IWC and CC. Details are explained in the text.*

11 List of publications

Papers published in scope of the PhD work:

1. Karpushkin E., Dušková-Smrčková M., Remmler T., Lapčíková M., Dušek, K. Rheological properties of homogeneous and heterogeneous poly(2-hydroxyethyl methacrylate) hydrogels. // *Polymer International*, vol. 61(2), p. 328–336, 2012. DOI: 10.1002/pi.3194
2. Hobzova R., Duskova-Smrckova M., Michalek J., Karpushkin E., Gatenholm P. Methacrylate hydrogels reinforced with bacterial cellulose. *Polymer International*, vol. 61(7), p. 1193–1201, 2012. DOI: 10.1002/pi.4199
3. Karpushkin E., Dušková-Smrčková M., Dušek, K. Rheology and porosity control of poly(2-hydroxyethyl methacrylate) hydrogels (accepted for publication in *Polymer,* DOI: 10.1016/j.polymer.2012.11.055).

Conference abstracts published in scope of the PhD work:

1. Karpushkin E., Dušková-Smrčková M., Šlouf M. Rheological and morphological studies of HEMA hydrogels // 6th YoungChem 2008 International Congress of Young Chemists. Book of abstracts, p. 51. Cracow, Poland, October 15-19, 2008.
2. Karpushkin E., Dušková-Smrčková M., Lapčíková M., Dušek K. Rheological behaviour of swollen hydrogels // New frontiers in macromolecular science. 73th PMM, book of abstracts, p. 148. Prague, 5-9 July 2009.
3. Karpushkin E., Dušková-Smrčková M., Přadný M., Hobzová R., Dušek K. Hydrogel scaffolds: link between mechanical response and hydrogel microstructure // Baltic Polymer Symposium 2009. Book of abstracts, p. 10. Ventspils, Latvia, 22-25 September 2009.
4. Karpushkin E., Dušková-Smrčková M., Michálek J. Mechanical properties of hydrogel-nanofibers constructs for use in tissue engineering // 7th International Congress of Young Chemists YoungChem2009. Book of abstracts, p. 50. Warsaw, Poland, 14-18 October 2009.
5. Hobzová R., Karpushkin E., Kotek J., Dušková-Smrčková M., Michálek J., Gatenholm P. Příprava a charakterizace mechanických vlastností kompozitů bakteriální celulóza-hydrogel. 6. Česko-slovenská konference POLYMERY 2010. 04. -07.10.2010, Liblice. Programová brožura konference. s. 114-115.

6. Karpushkin E., Dušková-Smrčková M., Přádný M., Hobzová R., Dušek K. Peculiarities of rheological behavior of network polymer hydrogels: chemometrical analysis // 5th All-Russian Kargin conference "Polymery-2010" Book of abstracts, p. 236. Moscow, Russia, 21-25 June 2010.
7. Duskova-Smrckova M., Karpushkin E., Michalek J., Dusek K. Morphology and Rheological Properties of Porous Hydrogels for Tissue Engineering. Polychar 19. Katmandu, Nepal, 20-24 March 2011. Book of abstracts. P. 18.
8. Karpushkin E., Dušková-Smrčková M., Michálek J., Dušek K. Rheological studies of poly(2-hydroxyethyl methacrylate) hydrogels in shear. III conference of young scientists "Rheology and physical-chemical mechanics of heterophase systems". Book of abstracts, P. 78. Suzdal, Russia, 10-15 May 2011.
9. Hobzová R., Dušková-Smrčková M., Karpushkin E., Michálek J., Gatenholm P. Kompozitní materiály na bázi syntetického hydrogelu a bakteriální celulózy. 63. Zjazd chemikov. 05.-09.09.2011, Tatranské Matliare. ChemZi, Roč. 7, č. 13 (2011), s. 216-217.
10. Dušková-Smrčková M., Dušek K., Karpushkin E. Polymer (hydro)gels in laboratory and life. How they form, look and perform. 1st International Workshop of CoE PoliMaT. Contributions to the Working Session with the International Scientific Council. Ljubljana PoliMat, 2011, p. 9-11.
11. Karpushkin E., DuškováSmrčkováM., Dušek K. High and low frequency mechanical responses of heterogeneous hydrogels. 7th International Conference on Nanostructured Polymers and Nanocomposites, 24-27.04.2012, Prague. Book of Abstracts, p. 345.

Other papers published during PhD study (October 2008 - present):

1. Karpushkin E.A., Zezin S.B., Zezin A.B. Intergel interpolyelectrolyte reaction and synthesis of hybrid composites based on charged microgels and inorganic nanocrystals. *Polymer Science Series B*, 2009, vol. 51(1-2), p. 33-37, DOI: 10.1134/S1560090409010059.
2. Karpushkin E.A. University education in the field of natural science in Czech Republic and in Russia. *Russian Journal of Chemistry*, 2011, vol. 55(4), p. 110-113 (in Russian). Reprinted from: Natural sciences education: trends in

Russia and in the world. Moscow State University, 2001. P. 115-124 (in Russian).

3. Berkovich A.K., Chebotaeva G.S., Karpushkin E.A., Kislenkov V.E., Artemov M.V. Influence of multiwall carbon nanotubes on the rheological behavior of polyacrylonitrile solution in DMSO. XIX All-Russian conference „Structure and dynamics of molecular systems". May-El Republic, Russia, 25-30 June 2012. (Conference Proceedings, vol. 2, p. 158-160).

Other conference abstracts published during PhD study (October 2008 - present):

1. Chebotaeva G.S., Artemov M.V., Kislenkov V.E., Karpushkin E.A., Berkovich A.K., Sergeev V.G. Influence of multiwall carbon nanotubes on the rheological behavior of polyacrylonitrile solution in DMSO. XIX All-Russian conference „Structure and dynamics of molecular systems". Book of abstracts, P. 191. May-El Republic, Russia, 25-30 June 2012.
2. Berkovich A.K., Karpushkin E.A., Sergeev V.G. Rheological studies of components interaction and structure formation in PAN/CNT/DMSO dispersions. 26 Symposium on rheology, 10-15 September, Tver, Russia. Book of abstracts, p. 44.